Empirical and theoretical modelling of solar shading factor

Chalotte B. Henriksen
&
Mathias Villumsen

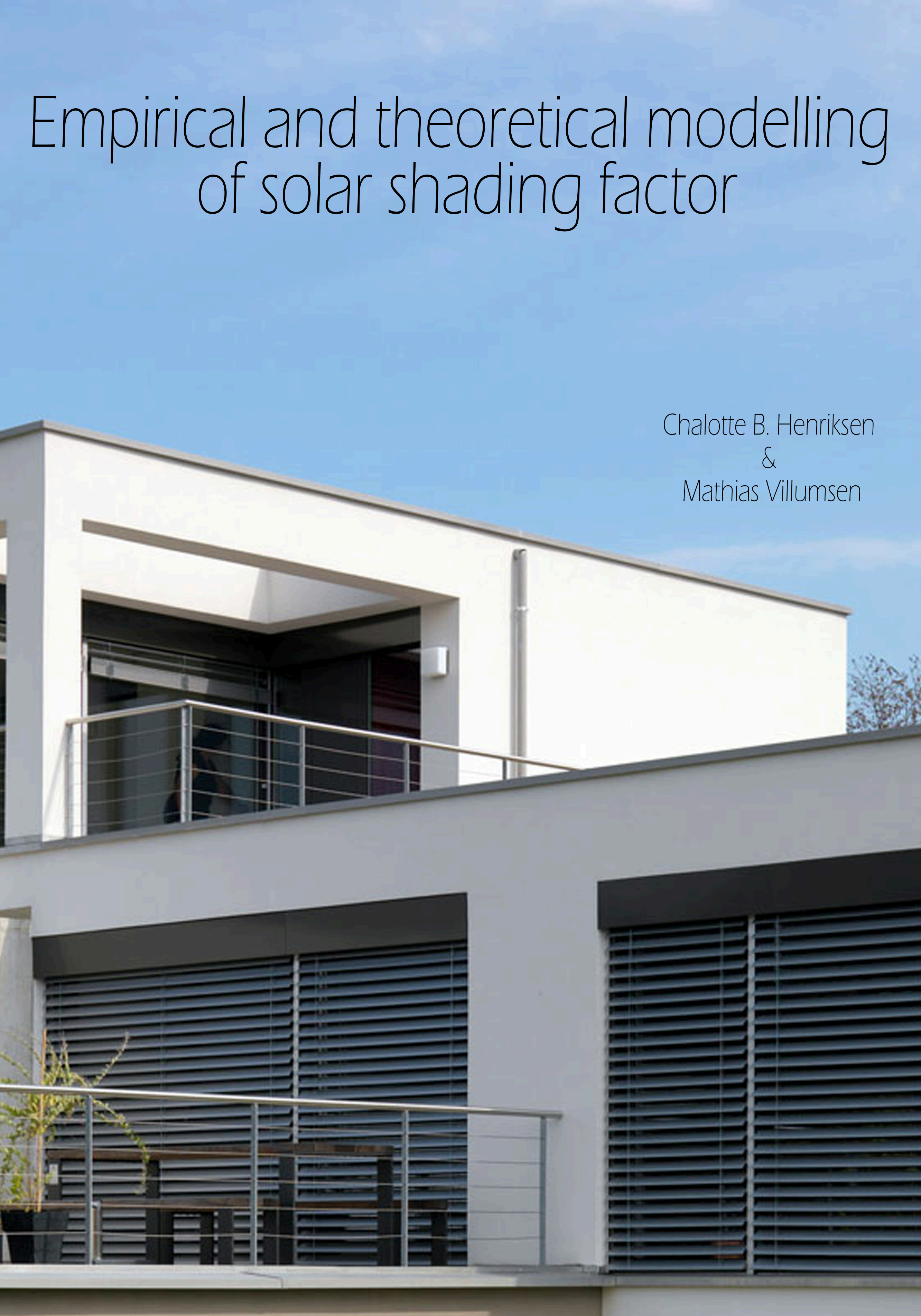

AALBORG UNIVERSITY

Students' report

The School of Engineering and Science
Study Board of Civil Engineering
Sohngårdsholmsvej 57
9000 Aalborg
http://www.ses.aau.dk

Title:
Empirical and theoretical modelling of solar shading factor

Project:
Master's thesis
Indoor Environmental Engineering

Project period:
September 2011 - June 2012

Project group:
B119b

Participants:

Chalotte Bach Henriksen

Mathias Villumsen

Supervisors:

Per K. Heiselberg

Frederik V. Winther

Editions: 5
Report pages: 126
Appendix pages: 76
Completed: June 14th, 2012

Synopsis:

The scope of the project is to develop a model for calculation of the g-value of a glazing system including Venetian blinds. This is done through present available literature and experiments.
Two main parameters are investigated. This includes the shading factor of the Venetian blinds and the exterior heat transfer coefficient on the outside of the glazing due to a change in airflow compared to glazings with no use of shading. Through experiments only the slat angle is varying while the theoretical models are varying dependent on both radiation angle and slat angle.
The velocity profile in the cavity is measured to study the type of air flow. The solar radiation through the window, both with and without shading, is measured for calculation of the shading factor of the Venetian blind.
The theoretical models are evaluated and compared with measurements done in a laboratory.

DANISH SUMMARY

Dette afgangsprojekt ved kandidatuddannelsen inden for Indeklima og Energi på Aalborg Universitet omhandler empirisk og teoretisk modellering af solafskærmningsfaktoren for udvendige persienner. Dette indebærer bestemmelsen af U-værdien for en rude og bestemmelsen af g-værdien for ruden samt ruden inklusive persienner, hvorunder en energimæssig betragtning af den udvendige konvektive og strålingsmæssige varmeoverføringsevne, som funktion af persiennen er relevant. Udviklede teoretiske modeller sammenholdes med forsøgsresultater.

Rapporten er opdelt i fire hovedkategorier, som hver især beskæftiger sig med hovedessenserne af projektet, hvoraf der som start gives en kort gennemgang af de fundamentale emner, som projektet har beskæftiget sig.

Hernæst præsenteres en gennemgang af to adskilte litteraturstudier, der omhandler en gennemgang af henholdsvis tidligere udviklede teoretiske modeller til bestemmelse af solafskærmningsfaktoren for et glas system indeholdende persienner, samt et studie der omhandler eksperimentelle opstillinger til bestemmelse af solafskærmningsfaktoren. Disse litteraturstudier bruges, som inspiration til udviklingen af egne modeller og enkelte sammenholdes med opnåede resultater.

Der er udviklet teoretiske modeller på baggrund af *DS/EN 673: Glass in building - Determination of thermal transmittance (U-value) - Calculation method* [Standard, 2011c] samt *DS/EN 410: Glass in building - Determination of luminous and solar characteristics of glazing* [Standard, 2011b], som har dannet grundlag for bestemmelsen af henholdsvis U-værdien samt g-værdien for en tolags rude. Ud fra ray-tracing teknikker er der udviklet en model, der har fået navnet ***optimal-surface model***, da denne modsat mange andre modeller der er blevet studeret gennem litteraturstudiet, bruger det nødvendige antal overflade af solafskærmningen. Modellen har til formål at bestemme solafskærmningsfaktoren for persiennen ud fra den mængde strålingsenergi, der fra solen kommer igennem persiennerne, enten som blivende direkte transmitteret samt spejlende og diffust reflekteret. Den udvendige overgangsisolans for ruden med tilhørende persienner er bestemt ud fra antagelser om, at flowet i hulrummet, mellem rude og persienner, sker ved fri konvektion. At dette er tilfældet, er til dels eftervist gennem forsøg, men den litteratur der på nuværende tidspunkt er til rådighed, har vist sig ikke at være tilstrækkelig inden for dette emne.

Der er i klima-laboratoriet på Aalborg Universitet udført en række forsøg til sammenligning med den teoretiske del af projektet. Der er udført forsøg af rudens direkte solenergitransmittans, da det ikke var muligt at måle rudens egentlige g-værdi idet en hot box ikke var til rådighed. Den direkte solenergitransmittans har derfor dannet grundlag for

bestemmelse af solafskærmningsfaktoren, idet transmittansen er målt for ruden og for ruden inklusive persienner. Forsøgene er blevet udført ved lamelvinklerne 0°, 15°, 30°, 45°, 60° og 70°. Gennem forsøgene er der ligeledes indsamlet data til bestemmelse af den udvendige overgangsisolans, som ud fra en varmebalance opstillet for rudens udvendige overflade er blevet beregnet. Endvidere er der blevet set på solafskærmningens effekt på varme kontra lys, hvilket der ikke kunne konkluderes noget endeligt ud fra idet målingerne lå inden for måleudstyrets usikkerheder. Flowet i hulrummet, mellem persienner og rude, er blevet undersøgt igennem målinger af hastighedsprofilet. Dette er gjort i flere højder og flowet har vist sig at være en blanding af både fri og tvungen konvektion. Dette fordi flowet har karakteristika der minder om fri konvektion, idet hastigheden stiger som funktion af højde, men samtidig kan hastighedsprofilet ikke sammenlignes fuldt ud med et forventet profil for fri konvektion. På trods af dette er sammenlignelige beregninger lavet ud fra en antagelse om, at flowet sker ved fri konvektion. Dette er gjort i mangel på litteratur der dækker emnet.

Rapporten afsluttes med en sammenholdning af teori og praksis. Denne viser, at beregningerne af den direkte solenergitransmittans for ruden stemmer overens med målingerne. Ses der på solafskærmningsfaktoren som funktion af lamelvinkel er tendensen for målinger og beregninger den samme, dog uden de matcher hinanden helt. De teoretiske beregninger regner for højt for små lamelvinkler hvilket skyldes at der bag ***optimal-surface modellen*** ligger en antagelse om, at lamellerne er uendeligt tynde og ikke er kurvede. Den udvendige overgangsisolans er ifølge forsøgene lavere end hvad beregninger viser. Dette skyldes at den anvendte litteratur til beregningerne ikke er ment til situationen med en persienne foran en rude, hvorfor det kan konkluderes at der mangler viden / litteratur inden for dette emne.

Preface

This report is a Master's thesis on the Master Programme in Indoor Environmental Engineering at Aalborg University spring 2012. The report is written by group B119b.

Reading guide

The project consists of a main report and an appendix report, together with an annex DVD in the back of the main report. When referring to an appendix it will for instance be written as appendix A. On the DVD there will be attached files which are used in the project and these are divided into the relevant chapters used in the report. To be able to read some of the files it is necessary to have these programs; MATLAB and Excel. In some of the attached annex's there might have been used full stop and in others decimal comma, this is because not all programs are using the Danish punctuation.

Through the main report there will be references to sources which are collected in the literature list in the back of the report. The Harvard method is used for references which mean that the sources are stated [Last name, year]. The references are referring to the list of literature. If the sources are placed before a full stop, they are referring to the concerned sentence and if the sources are placed just after a full stop they refer to the previous section. Figures, tables and equations are numbered regarding the chapter, e.g. the first figure in chapter 2 will be figure 2.1, the next figure 2.2 etc. The figures made by members of the group will not have a source reference.

CONTENTS

Nomenclature

Symbols

a	Slope of a line	$[-]$
A	Area	$[\mathrm{m}^2]$
A	Constant	$[-]$
b	Intersection with y-axis	$[-]$
C_d	Discharge coefficient	$[-]$
c_p	Specific heat capacity	$[\mathrm{J}/\mathrm{kgK}]$
d	Thickness of material layer	$[\mathrm{m}]$
E	Solar radiation	$[\mathrm{W}/\mathrm{m}^2]$
E_{ref}	Energy balance	$[\mathrm{kWh}/\mathrm{m}^2]$
F	Beam/diffuse split factor	$[-]$
g	Total solar energy transmittance	$[-]$
g	Gravitational acceleration	$[\mathrm{m}/\mathrm{s}^2]$
h	height	$[\mathrm{m}]$
h	Time	$[\mathrm{h}]$
H	Height of specific opening	$[\mathrm{m}]$
H_0	Neutral plane	$[\mathrm{m}]$
h_c	Internal convective heat transfer coefficient	$[\mathrm{W}/\mathrm{m}^2\mathrm{K}]$
h_e	External heat transfer coefficient	$[\mathrm{W}/\mathrm{m}^2\mathrm{K}]$
h_i	Internal heat transfer coefficient	$[\mathrm{W}/\mathrm{m}^2\mathrm{K}]$
h_r	Internal radiative heat transfer coefficient	$[\mathrm{W}/\mathrm{m}^2\mathrm{K}]$
h_s	Thermal conductance of each gas space	$[\mathrm{W}/\mathrm{m}^2\mathrm{K}]$
h_{sun}	Altitude angle of the sun	$[^\circ]$
h_t	Thermal conductance of the glazing	$[\mathrm{W}/\mathrm{m}^2\mathrm{K}]$
i	Angle of incidence	$[^\circ]$
I	Incident solar radiation	$[\mathrm{W}/\mathrm{m}^2]$
K	Extinction coefficient	$[\mathrm{m}^{-1}]$
l	Characteristic length	$[\mathrm{m}]$
L	Pane spacing	$[\mathrm{m}]$
L	Thickness of glass pane	$[\mathrm{m}]$

LT	Light transmittance	$[-]$
n	Exponent	$[-]$
n	Refractive index	$[-]$
p	Angle dependent parameter	$[-]$
p	Profile angle	$[^\circ]$
p_t	Pressure difference	[Pa]
q	Air flow rate	$[\mathrm{m^3/s}]$
q''	Heat flux	[W]
q_e	Secondary heat transfer factor towards the outside	$[-]$
q_i	Secondary heat transfer factor towards the inside	$[-]$
r	Reflection of radiation	$[-]$
R	Thermal resistance	$[\mathrm{m^2K/W}]$
r_c	Slat curvature	$[-]$
s	Distance between slats	[m]
s	Width of gas space	[m]
S_λ	Relative spectral distribution of the solar radiation	$[-]$
s_f	Solar shading factor	$[-]$
s_{LT}	Shading factor due to light	$[-]$
t	Temperature	$[^\circ\mathrm{C}]$
T	Absolute temperature	[K]
T_{ref}	Absolute mean temperature	[K]
T_m	Absolute mean temperature	[K]
U	Thermal transmittance	$[\mathrm{W/m^2K}]$
v	Slat width	[m]
v	Velocity	$[\mathrm{m/s}]$
V	Slat length	[m]
w	Width of subsurfaces on the slat	[m]
w_{window}	Window width	[m]
W	Directly radiated height of the glazing	[m]
α_c	Heat transfer coefficient due to convection	$[\mathrm{W/m^2K}]$
α_e	Absorptance	$[-]$
α_r	Heat transfer coefficient due to radiation	$[\mathrm{W/m^2K}]$
β	Expansion coefficient	$[\mathrm{K^{-1}}]$
β_{sur}	Slope of the surface	$[^\circ]$
Δ	Difference	$[-]$

ϵ_b	Emissivity, back	$[-]$
ϵ_f	Emissivity, front	$[-]$
γ_{sun}	Azimuth angle of the sun	$[°]$
γ_{sur}	Azimuth angle of the surface	$[°]$
λ	Thermal conductivity	$[\mathrm{W/mK}]$
Λ	Thermal conductance	$[\mathrm{W/m^2K}]$
μ	Dynamic viscosity	$[\mathrm{kg/ms}]$
Ω	Radiation angle	$[°]$
ϕ	Slat angle	$[°]$
Φ	Heat flow	$[\mathrm{W}]$
ψ	View factor	$[-]$
ρ	Density	$[\mathrm{kg/m^3}]$
ρ_{bb}	Beam-beam reflectance	$[-]$
ρ_{bd}	Beam-diffuse reflectance	$[-]$
ρ_{dd}	Diffuse-diffuse reflectance	$[-]$
ρ_{beam}	Beam reflectance	$[-]$
ρ_e	Reflectance	$[-]$
σ	Stefan Boltzmanns constant	$[\mathrm{W/m^2K^4}]$
τ_e	Solar direct transmittance	$[-]$
θ	Refraction angle	$[°]$
υ	Kinematic viscosity	$[\mathrm{m^2/s}]$
$\perp$	Perpendicular components	$[-]$
$\parallel$	Parallel components	$[-]$

MODEL NUMBERS

Gr	Grashof's number	$[-]$
Nu	Nusselt's number	$[-]$
Pr	Prandtl's number	$[-]$
Ra	Rayleigh's number	$[-]$
Re	Reynolds' number	$[-]$

Part 1

Fundamentals

- Introduction
- Solar characteristics
- Window
- Solar shading
- Energy balance

CHAPTER 1

INTRODUCTION

As the trend of building move towards well insulated houses and offices with little or no need for heating the important question of design goes from *"how do we keep the energy from leaving the building envelope"* to *"how do we keep the energy from entering the building envelope"*.

The facades of offices are typically dominated by windows while the same goes for south oriented facades for houses. This leaves big open areas in which solar radiation can enter the building envelope. As a result of this overheating can occur. Overheating has become a hot topic in modern building as more and more face problems with indoor temperatures as high as 30 °C [Larsen, 2010]. Due to this, solar shading has become an important parameter in todays building designs. Static solar shading has been a known design parameter since ancient time [WebEcoist, 2012], but as overheating can occur all over the year due to nowadays building designs, the need for dynamic solutions have increased massively. This leads to ways of controlling the solar gains in terms of shading devices. The most common, but one of the least investigated shading types is the Ventian blinds. They are widely used but theoretical model developing of their performance are on an early stage [Wright et al., 2007]. Proper knowledge of Venetian blinds performance is crucial in the design of dynamic control strategies to ensure thermal comfort within buildings.

This project will contain a suggestion on how the theoretical performance of glazing systems including Venetian blinds can be handled.

1.1 RESEARCH QUESTION

How is it possible to perform a detailed model for determining the energy characteristics of a glazing system mounted with a solar shading in form of a Venetian blind with varying slat angles?

1.2 PROBLEM DELIMITATION

Throughout this project only the external heat transfer coefficient h_e have been investigated, i.e. the internal heat transfer coefficient h_i is not investigated.

Some simplifications are made to the model of the energy characteristics in case of a glazing system with a Venetian blind as solar shading. Those are:

- The slats are flat and not curved
- The slats have no thickness
- The slats are opaque
- The reflections from the glazing are not taken into considerations
- The number of specular reflections between the surfaces on the slats are set to ten
- The number of diffuse reflections between the slats are set to five, and they are only considered in case of diffuse reflection from the radiated surface on the slat
- The properties of the solar shading is assumed to be independent on wavelength
- Only the direct solar radiation is taken into account, i.e. the diffuse reflection from the sky is not considered

CHAPTER 2

SOLAR CHARACTERISTICS

This small chapter about the sun is meant as a guidance in understanding which parameters and what knowledge that have been useful for this project when looking at angular dependent glazing characteristics. It will not contain any formulas on how to calculate the solar altitude angle, the incident angle or any alike, just a description on how these are defined. Furthermore short- and longwave radiation will be addressed.

2.1 SUN CHART

In order to create a model to calculate the properties of a glazing system for various situations, the angle of incidence needs to be defined. The angle of incidence is varying throughout the day as the sun is following its path across the sky. This path have been calculated for the location of Copenhagen and is shown in figure 2.1 for the 21st in every month of the year. The calculation is seen in annex 1 on DVD.

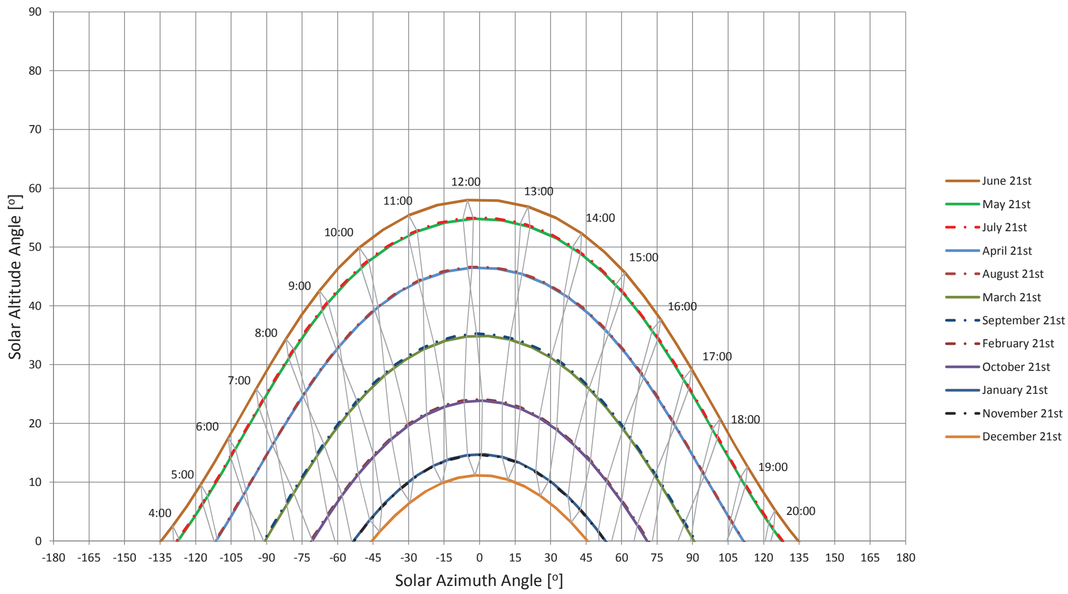

Figure 2.1: *Sun chart at the location of Copenhagen.*

The sun chart shown in figure 2.1 is based on the solar azimuth angle and the solar altitude angle as shown in figure 2.2. These two parameters along with the orientation and slope of the window are used for determination of the angle of incidence.

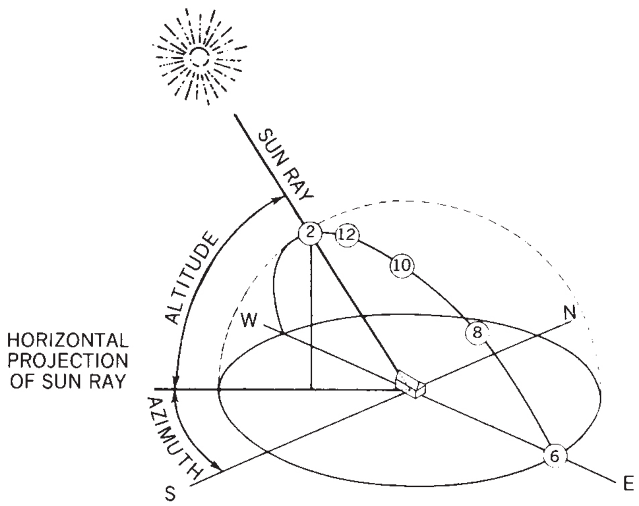

Figure 2.2: *Solar azimuth and altitude angle. [Heiselberg, 2008]*

2.2 DETERMINATION OF THE ANGLE OF RADIATION

This section deals with the description of two ways of calculating the angle of the radiation Ω; angle of incidence and profile angle. Both methods are commonly used but produce different results. When dealing with solar shading the profile angle method has shown to give the most accurate results, why this will be used in the later calculations [Yahoda and Wright, 2004]. Despite of this, both methods is described in the following.

2.2.1 ANGLE OF INCIDENCE

When the solar azimuth angle and the solar altitude angle shown in figure 2.2 is calculated, the angle of incidence can be determined. The angle of incidence is defined as the angle between the beam radiation on a surface and the normal to that surface. [Duffie and Beckman, 2006] This is illustrated in figure 2.3.

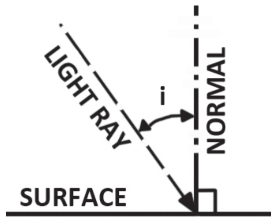

Figure 2.3: *Illustration of the angle of incidence, **i**.*

The angle of incidence is calculated from equation 2.1[Stampe et al., 2006].

$$cos(i) = cos(\gamma_{sun} - \gamma_{sur}) \cdot cos(h_{sun}) \cdot sin(\beta_{sur}) + sin(h_{sun}) \cdot cos(\beta_{sur}) \tag{2.1}$$

where:

h_{sun}	*Altitude angle of the sun* [°]
i	*Angle of incidence* [°]
β_{sur}	*Slope of the surface* [°]
γ_{sun}	*Azimuth angle of the sun* [°]
γ_{sur}	*Azimuth angle of the surface* [°]

The angle of incidence calculated at azimuth and altitude angles from -90 to +90° on a vertical surface is given in figure 2.4.

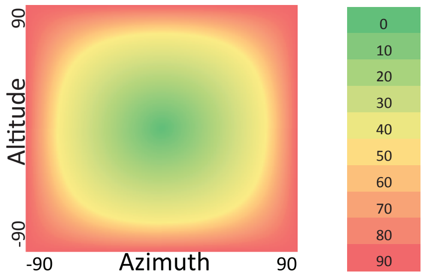

Figure 2.4: *The angle of incidence as function of azimuth angle on the x-axis and altitude angle on the y-axis.*

2.2.2 PROFILE ANGLE

The profile angle is given from equation 2.2.

$$tan(p) = \frac{tan(h_{sun})}{cos(\gamma_{sun} - \gamma_{sur})} \tag{2.2}$$

where:

p	*Profile angle* [°]

In a similar way as for the calculation of the angle of incidence, the profile angle is given at azimuth and altitude angles from -90 to +90° for a vertical surface in figure 2.5.

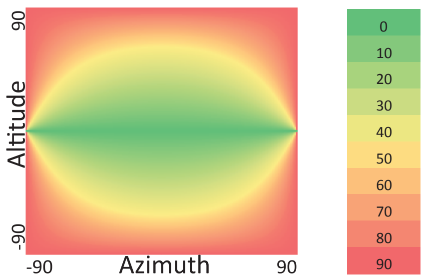

Figure 2.5: *Profile angle as function of azimuth angle on the x-axis and altitude angle on the y-axis.*

As can be seen by comparing figures 2.4 and 2.5, the profile angle method is less dependent on the azimuth angle of the sun.

2.3 LONGWAVE AND SHORTWAVE RADIATION

The spectrum of radiation including longwave and shortwave radiation is illustrated in figure 2.6, where longwave radiation is defined as *infrared radiation* and shortwave radiation as the sum of *ultraviolet radiation* and *visible light*.

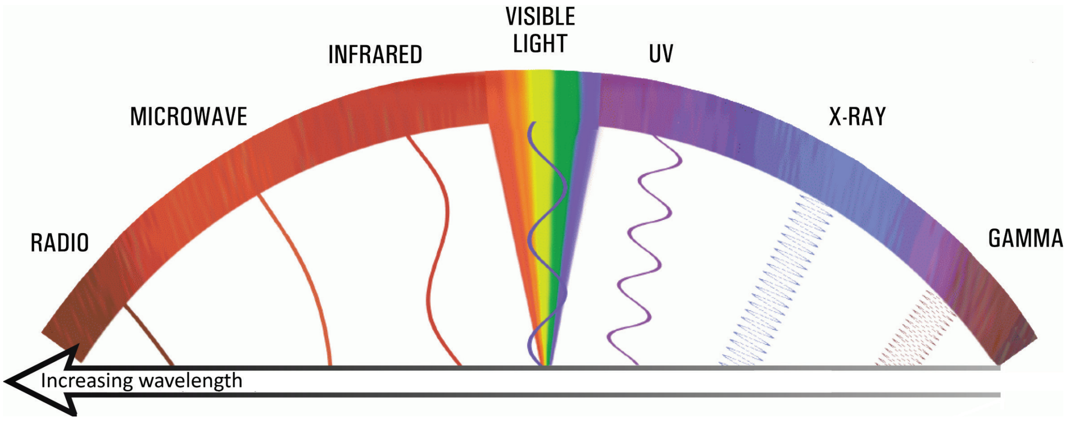

Figure 2.6: *The radiation wavelength spectrum. [Steinle, 2012]*

The normalized relative spectral distribution of global solar radiation representable for the radiation at ground level is given from the standards and is shown in figure 2.7. [Standard, 2011b]

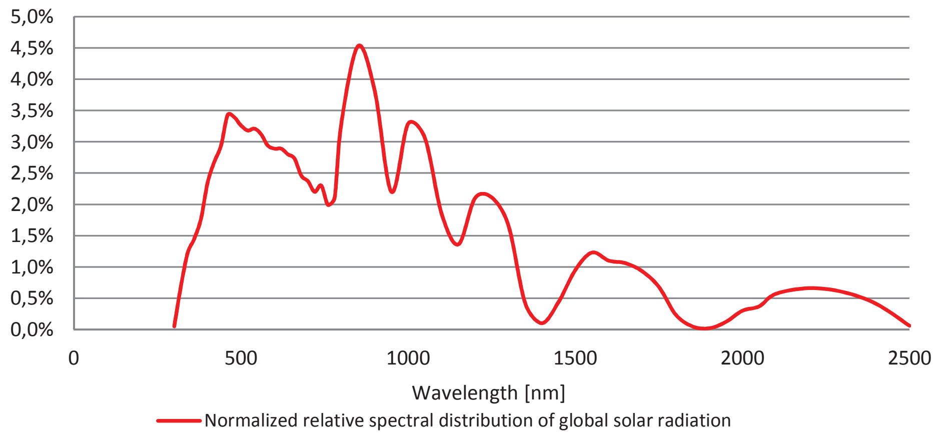

Figure 2.7: *Normalized relative spectral distribution of global solar radiation.*

Shortwave radiation accounts for approximately 55 % of the radiation received from the sun with the remaining 45 % being longwave radiation. As mentioned, the shortwave radiation is defined as the sum of *ultraviolet radiation* and *visible light* and longwave radiation as *infrared radiation*. The distribution of the solar relative spectrum in these types of radiation is as follow: [Duffie and Beckman, 2006]

- Ultraviolet radiation at wavelengths below 380 nm
- Visible light at wavelengths in the interval 380-780 nm
- Infrared radiation at wavelengths above 780 nm

When designing solar shadings the radiation of interests is the shortwave radiation due to its ability to transmit the glazing. Longwave radiation is the radiation from and in between surfaces, for instance inside the building in between walls as a function of temperature differences or outside from the earth to the atmosphere. Likewise longwave radiation is radiated from the surfaces in a room to the windows. The longwave radiation becomes more and more important with decreasing reflectance of the solar shading, which is the case with dark and rough shading where a lot of radiation is absorbed in the shading. The opposite happens when a light and shiny type of shading is used. [Stampe et al., 2006]

Chapter 3

Window

This chapter contains history about the window and what the window consists of. Furthermore the chapter contains a description of the main energy characteristics of a window. Those are for instance the U-value and the g-value of the glazing which will be described further together with appendix A and B. The energy characteristics will be used to describe the difference between the glazing and the glazing system including Venetian blinds. In the end the glazing used in the theoretical and experimental part is presented.

3.1 History of the window

The development of a window is in close connection to the architectural trend and the technological development. The primary functions of a window are to let daylight into the building, to provide visual contact with the surroundings and to transmit solar energy to the building in order to reduce the energy consumption of the building in case of heating. The fact that windows both transmit solar energy and have a poor insulating ability compared to the remaining building envelope can be considered a weakness. This may result in both a cooling demand during sunny days and in a heating demand in cold winter days. In the past the U-value of windows was so high that the luxury of having large window areas was not a possibility. Instead very small window areas were used, even though it gave a very low level of daylight. Later on when the technological development of the window occurred, the U-value of the window was reduced and at the same time the window areas became larger. With increasing window sizes the primary functions of the window was utilized to a greater extent. An increasing window size gives some problems with overheating and therefore the facades are now going in the direction of being dynamic. [Mróz, 2003] Dynamic facades are an attempt to adapt to changing weather conditions like the nature and people does [Hodapp, 2011]. An example of a dynamic facade is seen in figures 3.1 where the system is seen from the outside and the inside. In the figure, number one is the glass of the window, number two is an insulating layer, number three is solar shading and number four is photovoltaics. The layers are dynamic, meaning that they are able to go in and out of place for comfort reasons.

Figure 3.1: *An example of a dynamic facade. Left: Seen from the outside. Right: Seen from the inside. [Hodapp, 2011]*

Windows are build of a number of components. The fixed components are the frame and the glass. The glass is sometimes mounted with a coating. If there are more than one pane there is a gas type, typically argon, krypton, air or a mix with air, in the cavity between the panes [Mróz, 2003]. Argon and krypton are more insulating than air. In the past windows contained only one pane. Later on windows with one pane were either mounted with a secondary glazing or they were replaced with new windows with two or more layers of glazing. A Double-glazed window is a more insulating window than a window with only one layer of glass and a triple-glazed window is even more insulating etc. Today both regular glazed windows and energy glazed windows are used. [Glasindustrien, 2010] The difference between the two types of windows is the use of a low emissivity coating on the outer surface on the inner pane, reflecting longwave radiation [Termoruder.dk, 2012]. This is illustrated in figure 3.2.

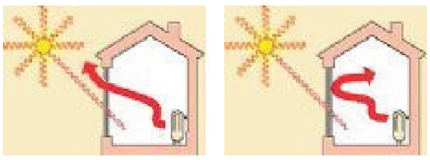

Figure 3.2: *Left: Regular glazed window. Right: Energy glazed window. [Termoruder.dk, 2012], edited*

The frames are often made of wood, plastic or aluminium. For windows with a U-value less than 1,4-2 $^{W}/_{m^2K}$, the frame is the part of the window that have the worst insulating abilities. [Mróz, 2003]

Glazing has some main energy characteristics. Those are the U-value, the g-value and the light transmittance. The LT-value is describing the amount of daylight that is passing through the pane. [Mróz, 2003] The U-value and the g-value are described in the following.

3.2 THERMAL TRANSMITTANCE, U-VALUE, OF GLAZING SYSTEMS

The U-value is describing how much energy is lost from the inside to the outside or the other way around depending on the inside and outside temperatures. The U-value of glazings can be described in two different ways; one describing the entire window including the frame and one only considering the glazing. In the following the calculation of the U-value of the glazing system is described, based on the European Standard: *DS/EN 673: Glass in building - Determination of thermal transmittance (U-value) - Calculation method* [Standard, 2011c].

The U-value of the glazing system is found from equation 3.1.

$$\frac{1}{U} = \frac{1}{h_e} + \frac{1}{h_t} + \frac{1}{h_i} \tag{3.1}$$

where:

h_e	*External heat transfer coefficient* $[\mathrm{W}/\mathrm{m^2 \cdot K}]$
h_t	*Thermal conductance of the glazing* $[\mathrm{W}/\mathrm{m^2 \cdot K}]$
h_i	*Internal heat transfer coefficient* $[\mathrm{W}/\mathrm{m^2 \cdot K}]$

The description of the external and internal heat transfer coefficients and the calculation of the thermal conductance are seen in appendix A.

3.3 TOTAL SOLAR ENERGY TRANSMITTANCE, G-VALUE, OF GLAZING SYSTEMS

The g-value is describing the amount of solar energy passing through the pane. In the following the calculation of the g-value of glazing systems are described, based on the European Standard: *DS/EN 410: Glass in building - Determination of luminous and solar characteristics of glazing* [Standard, 2011b].

The incident solar radiant flux on a glazing consists of three parts; a transmitted part, a reflected part and an absorbed part. This is illustrated in figure 3.3.

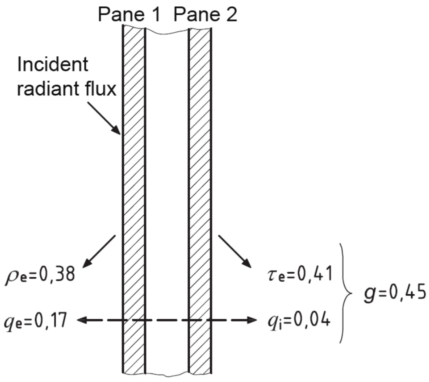

Figure 3.3: *An example of the division of the incident solar radiant flux on a glazing. [Standard, 2011b], edited*

The relation between the three parts is given in equation 3.2.

$$\tau_e + \rho_e + \alpha_e = 1 \tag{3.2}$$

where:

α_e	*Solar direct absorptance* [−]
ρ_e	*Solar direct reflectance* [−]
τ_e	*Solar direct transmittance* [−]

The absorptance is divided into two parts which can be seen in equation 3.3.

$$\alpha_e = q_i + q_e \tag{3.3}$$

where:

q_e	*Secondary heat transfer factor of the glazing towards the outside* [−]
q_i	*Secondary heat transfer factor of the glazing towards the inside* [−]

The g-value is given as the fraction of the incident solar radiation that is transmitted through the glazing system and absorbed in the inner layer of glass. This is seen in equation 3.4.

$$g = \tau_e + q_i \tag{3.4}$$

The calculation of the g-value for one pane, two panes and three panes are seen in appendix B.

3.4 THE WINDOW OF THE EXPERIMENTS

The glazings used in the experiments and in the calculations are from Pilkington. The window consist of two layers of glazing; the first layer is Optifloat Clear of 4 mm, the second layer is Optitherm S3 of 4 mm and in between the glazing 15 mm of gas is used; 90 % argon and 10 % air. Optifloat Clear glass is a normal pane facing the outside while Optitherm S3 is an energy glass with a coating. The purpose of the coating is to reflect long-wave radiation, from the surfaces into the room to reduce the heat loss through the glazings and from the surfaces to the outside to reduce the incident solar radiation through the glazings. A sketch of the glazings and the location of the coating, the red line, is shown in figure 3.4.

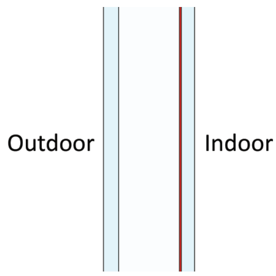

Figure 3.4: *A sketch of the glazings used in the experiments and calculations.*

A picture of the window is seen in figure 3.5.

Figure 3.5: *The window used in the experiments and calculations.*

The glazing has a center U-value of 1,1 $^{W}/_{m^2K}$ and a g-value of 0,63.

The transmittance and reflectances as a function of the wavelength for the two glass panes Optifloat Clear and Optitherm S3 is shown in figures 3.6 and 3.7 respectively.

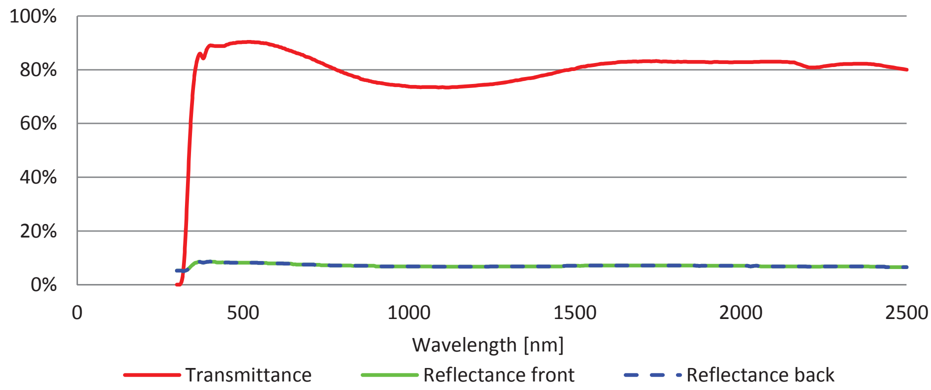

Figure 3.6: *Optical properties as function of wavelength for the Pilkington Optifloat Clear.*

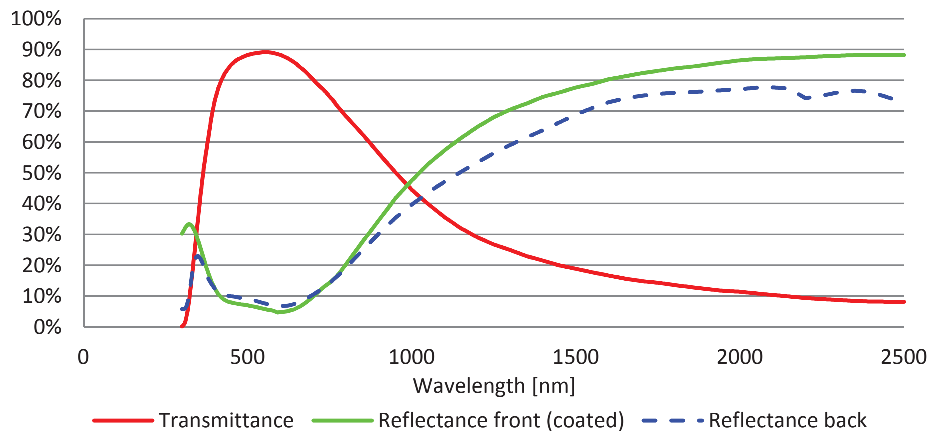

Figure 3.7: *Optical properties as function of wavelength for the Pilkington Optitherm S3.*

The effect of the coating is obvious, as the reflectances on both surfaces of the Optifloat Clear shown in figure 3.6 are the same, while the reflectances are different for the Optitherm S3 shown in figure 3.7.

CHAPTER 4

SOLAR SHADING

Solar shading comes in many varieties both static and dynamic. Static solutions include overhangs which cannot be adjusted or moved to the side while dynamic solutions is any kind of shading type which can be adjusted to increase or decrease the coefficient of shading. This chapter includes a small description of the type of shading used throughout this project along with the main purposes of solar shading. In the end of the chapter the exact shading used in the theoretical and experimental part is described.

4.1 VENETIAN BLINDS

The most common type of shading system are the exterior venetian blinds as shown in figure 4.1. [Investment, 2012]

Figure 4.1: *Solar shading in case of venetian blinds. [Materials and Sources, 2012]*

Solar shading basically have two main purposes; firstly reduce the amount of energy into the room received from the sun and secondly prevent glare [Baker and Steemers, 2000]. While achieving these two things, some side effects occur; reduced external heat gain, reduced daylight factor and loss of visual exterior contact. Obviously reduced external heat gain can be both bad and good, but glare is usually a bigger problem during winter when the solar altitude angle is low and this is typically the period where heating demands are present. One of the ideas of this project is to investigate the difference of the effect on the LT-value and the g-value of a glazing system due to the Venetian blinds.

The properties known for glazings as transmittance, reflectance and absorptance are the same properties of interest when considering solar shading. The transmittance is usually of biggest influence on the total g-value of the system since this accounts for solar energy, going straight through the shading system. Dependent on the angle of incidence and the slat angle the reflectance from the slats into the room may be of great importance.

4.2 SHADING FACTOR

When calculating the energy frame of a building or the energy balance of a room with applied solar shading, by using the standards presently valid, the shading factors are chosen from a table similar to that shown in figure 4.2 [Standard, 2011a] [Heiselberg et al., 2002]. It is seen in the figure that the effect of the solar shading is varying dependent on the type of window in case of medium and dark shading colour. This is because a double-glazed energy window includes a coating which reflects longwave radiation while a normal double glazed window does not. Thereby the energy window shades more than the other window. It is also seen that the effect of the solar shading is varying dependent on the shading colour. The dark shading colour reflects less energy between the glazing and the solar shading than shading with a bright colour, hence a greater reduction when using dark shadings.

Shading type	Window type and shading colour					
	Double-glazed window			Double-glazed energy window		
	bright	medium	dark	bright	medium	dark
External shading						
Roller blinds	0,35	0,20	0,20	0,35	0,20	0,15
Venetian 30°	0,30	0,20	0,15	0,30	0,15	0,10
Venetian 60°	0,15	0,15	0,10	0,15	0,15	0,05

Figure 4.2: *Shading factor as a function of shading type, angle of slats and glazing type. [Heiselberg et al., 2002], edited*

This procedure is not as accurate as it could be and leaves the engineer to estimate the shading factor based on prescribed static values for windows most likely not matching the ones intended. As seen from figure 4.2 a shading factor is given for Venetian blinds with e.g. a slat angle of 30°. This angle of 30° would only have this same shading factor if the sun was stationary perpindicular to the blinds. But as the sun is moving across the sky this angle of 30 ° will not have this same shading factor since the angle of incidence is varying throughout the day. A more accurate way of handling this issue would be to set up a model being able to calculate the shading factor as a function of the incident angle and slat angle. This could be beneficial in developing a control strategy where the slats continuously could adjust to the incident angle as the sun moves across the sky. This in order to sustain the same shading factor or even be able to adjust the shading factor in relation to the thermal comfort in the room.

4.3 THE SOLAR SHADING OF THE EXPERIMENTS

The solar shading used for theoretical calculations and experiments throughout this report, is an exterior Venetian blind type C80 from the company Climatic. The slats are made of aluminium and are curved with a width of 8 cm. The vertical distance between the slats is 7 cm. The shading can be seen in figure 4.3

Figure 4.3: *Front view picture of the Venetian blinds.*

The properties of the shading which are of importance when doing calculations on the energy characteristics are the following three:

- Reflectance of the front and the back of the slats $\rho = 0{,}37$
- Emissivity of the front and the back of the slats $\epsilon_f = \epsilon_b = 0{,}25$

These properties are assumed to be constant no matter the wavelength and hereby not varying like the properties of the glazing shown in figures 3.6 and 3.7. Even though this assumption most likely differs from reality, wavelength dependent properties could not be found for the shading.

CHAPTER 5

ENERGY BALANCE

This chapter gives a description of the energy balance of windows. This is done because it is a way of describing windows, where both the U-value and the g-value of the window are taken into consideration. The mean energy balance equation for Danish conditions will be used to evaluate the window without shading in the theoretical part of this report.

5.1 DESCRIPTION OF WINDOWS ENERGY BALANCE

The energy balance of a window is taking both the windows U-value and g-value in to consideration along with the climate and the orientation of the windows. The energy balance is given in kWh per m^2 per year and according to regulations it is, for new windows, not allowed to be less than -33 $^{kWh}/_{m^2}$ per year [Enterprise and Authority, 2011]. Evaluating windows performance based on the energy balance, E_{ref}, instead of just looking at the U-value, is a more reasonable way of comparing different windows since the heat gain is also considered in a combined evaluation of both the U-value and g-value as shown in figure 5.1 [Velfac, 2012].

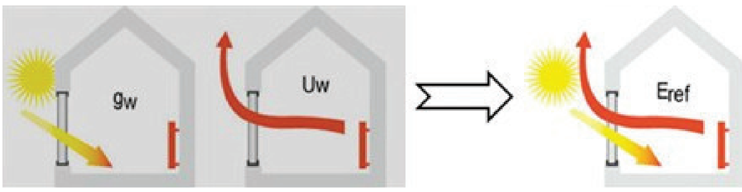

Figure 5.1: *Depiction of a windows energy balance. [Rationel, 2012]*

The energy balance expresses how much energy that is received through the window subtracted with the amount of energy lost through the window during the heating season. I.e. if the energy balance is positive the window results in a net energy gain and vice versa if the energy balance is negative [Velfac, 2012]. The way of calculating the energy balance of a window is different for each orientation due to the fact that the amount of energy received by the sun is varying as a function of the orientation. The summed up weighted mean equation for the energy balance, in case of Danish climate, is given in equation 5.1.

$$E_{ref} = 196{,}4^{kWh}/_{m^2} \cdot g - 90{,}36 kKh \cdot U \tag{5.1}$$

The 196,4 $^{\mathrm{kWh}}/_{\mathrm{m}^2}$ is a weighted average of the irradiation in Denmark, assuming a typical distribution of windows regarding their orientation; 41 % towards south, 33 % towards east or west and 26 % towards north [Enterprise and Authority, 2011]. This assumption is valid for a typical Danish single family house. The value of 90,36 kKh represents the amount of degree hours for Denmark. Both values are calculated based on the Danish Design Reference Year for the heating season from September 24th - May 13th. [Jensen and Lund, 1995]

The evaluation of the performance of glazing systems based on the energy balance does not make sense when the glazing system includes dynamic shading. If it should be applicable a control strategy should be made for the shading. This is not done in this project and therefore the energy balance is only calculated for the window without shading. In case of shading U- and g-values are calculated.

Part 2

Theory

- Theoretical literature survey
  - Window
    - Window with a Venetian blind
    - Window with a curtain

CHAPTER 6

THEORETICAL LITERATURE SURVEY

This chapter contains a literature review addressing techniques given in different academic journals along with assumptions and simplifications. The methods used in the various papers are briefly addressed in order to give an overview of these. The literature survey is made as inspiration to the theoretical models.

6.1 SIMPLIFIED SOLAR OPTICAL CALCULATIONS FOR WINDOWS WITH VENETIAN BLINDS [KOTEY AND WRIGHT]

The methodology presented in this paper deals with solar optical properties of a complex fenestration system, i.e. glazing and a Venetian blind. The scope of this paper was to create a model which could be integrated into a building energy simulation program. This leads to the decision of creating a simple model, since long simulation times are not favourable when integrating a model into a simulation program. Due to this the slats were assumed to be perfect diffusers, i.e. they transmit and reflect any incident solar radiation diffusely. This approach eliminates the intensive computational ray tracing techniques like seen in other studies.
Considering the glazing layers the solar optical properties are calculated by use of Fresnel's derived expressions and Snell's Law.

The optical properties of the blinds are, due to the simplifications, functions of the geometry and material of the slats along with the angle of incidence. In this paper these properties are modelled in a similar way as in the simulation program EnergyPlus, with the addition of some simplifying assumptions:

- The slats are flat with negligible thickness
- Incident diffuse radiation is uniformly distributed
- The slats reflect diffusely any incident beam radiation (measurements have shown that more than 90 % of reflected beam radiation is diffuse)

The solar optical properties of the Venetian blind is divided into three parts; beam-beam, beam-diffuse and diffuse-diffuse solar optical properties. The properties are determined by considering an enclosure which is representative for the entire shading. The beam-beam properties are easily determined as a function of the ratio between the beam radiation passing through the slats and the incident radiation on the slats, like seen to the left in figure 6.1. Considering beam-diffuse solar optical properties this calculation is subdivided into two methods; 4-surface and 6-surface method as seen in figure 6.1. The 4-surface model is used when the slats are fully illuminated, while the 6-surface model is used when the slats are partially illuminated, subdividing the slats into two surfaces; one being illuminated while the other being shaded.

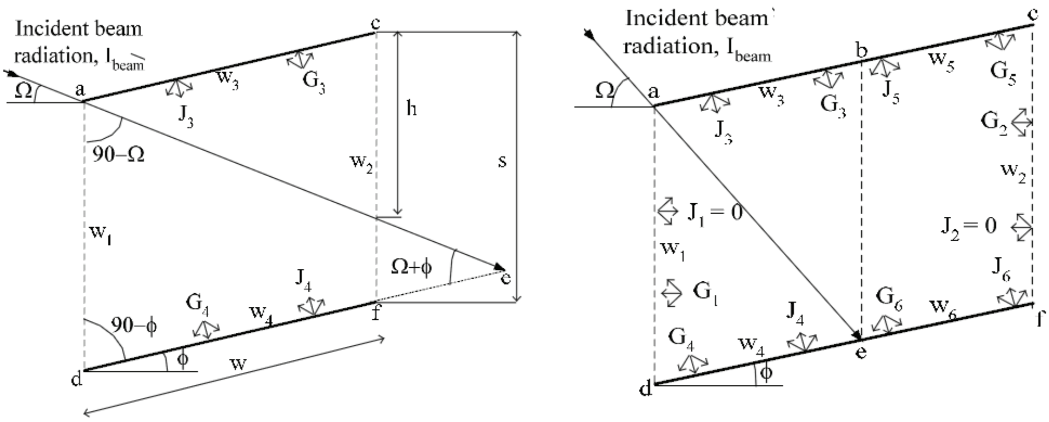

Figure 6.1: *Enclosure of a Venetian blind illustrated as 4-surface model shown to the left and 6-surface model shown to the right. [Kotey and Wright]*

Where s is the slat separation length, w is the slat width, ϕ is the angle of the slats, Ω is the profile angle, J_i is the radiation flux leaving surface i while G_i is the irradiance on surface i.

For diffuse-diffuse solar optical properties a 4-surface model like seen in figure 6.2 is used for the calculations.

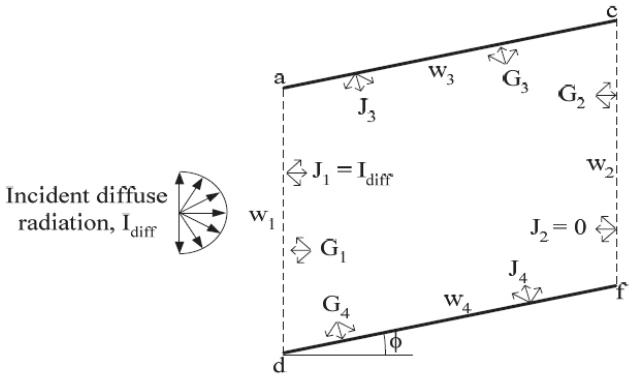

Figure 6.2: *Enclosure of a Venetian blind illustrated as 4-surface model used for determining diffuse-diffuse solar optical properties. [Kotey and Wright]*

The results of this paper were not compared to other calculations nor measurements and the conclusions to the study are that the method is useful for integration in building energy simulation programs due to quick simplified model.

6.2 A Simplified Method for Calculating the Effective Solar Optical Properties of a Venetian Blind Layer for Building Energy Simulation [Kotey et al., 2009]

This paper deals with the same methodology as presented in section 6.1, but in addition to the approximation where the slats are assumed to be flat with negligible thickness, a correction taking the curvature of the slats into account is developed. Two mentionable errors of the flat-slat zero-thickness assumption are the view-factor error and the fact that the transmission of Venetian blinds at a negative slat angle opposite to the profile angle is not 100 %. This is not the case in reality as the slats of a Venetian blind system are curved. The effect is seen in figure 6.3.

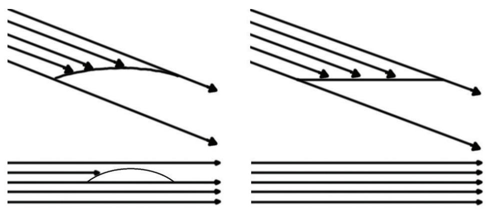

Figure 6.3: *Left side shows the effect with a curving slat while the right side shows the effect of a flat-slat zero-thickness assumption. [Kotey et al., 2009]*

Another Ashrae journal used as reference in this paper compared theoretical data, based on the flat-slat zero-thickness assumption, with measured data. This study showed that the model predicts 100 % transmittance with an incident angle perpendicular to the shading system and a slat angle of 0°, i.e. horizontal slats. This showed to be as much as 10 % higher than the measured results. But as the slat angle was increased, the model results and the experimental results were in better agreement. [Collins and Jiang, 2008]

In order to improve this, a curvature correction model was created defining the geometry of the slats as a perfect arc instead of being flat like the previous assumptions. The results of this implementation is shown in figures 6.4, 6.5 and 6.6 which shows measurements [Collins and Jiang, 2008] and calculated values [Kotey et al., 2009] of the total transmittance of the shading from both the flat slat model and the curved model at a slat angle of 0°, 30° and 60° respectively.

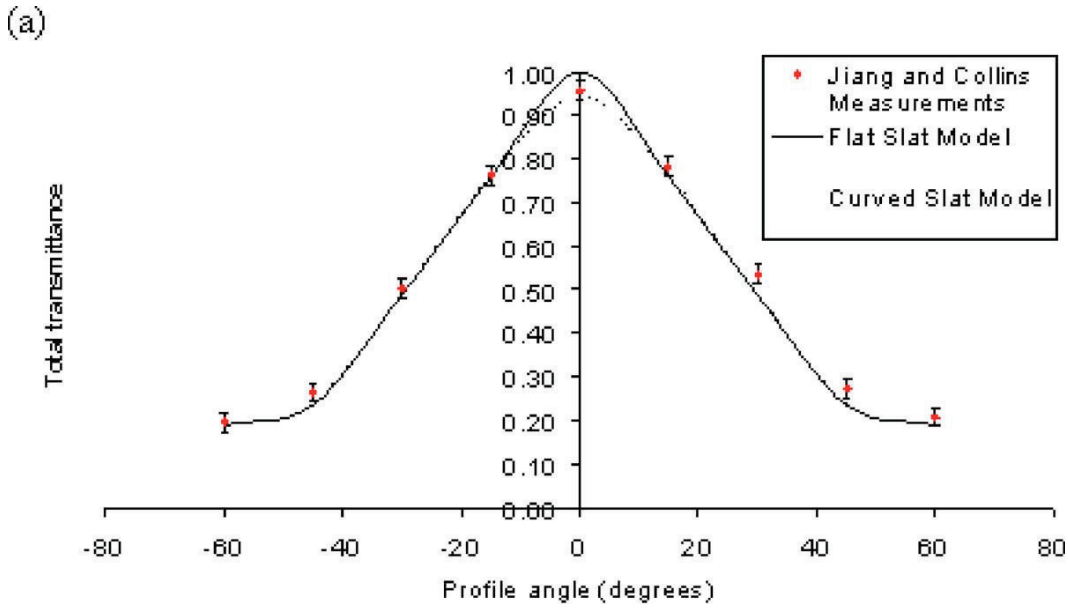

Figure 6.4: *Total transmittance at a slat angle of 0°. [Kotey et al., 2009]*

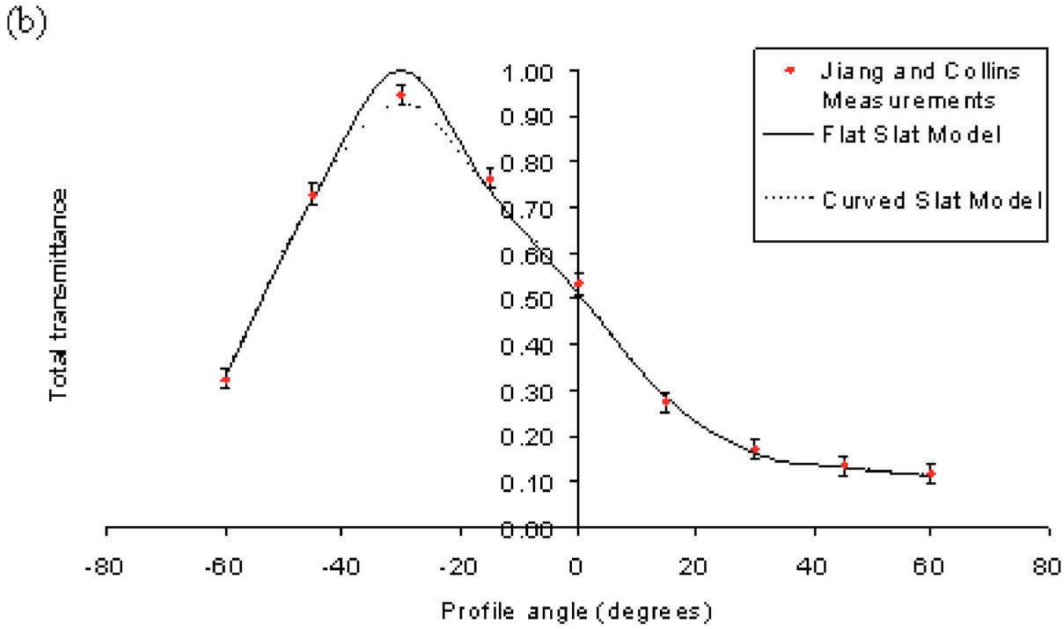

Figure 6.5: *Total transmittance at a slat angle of 30°. [Kotey et al., 2009]*

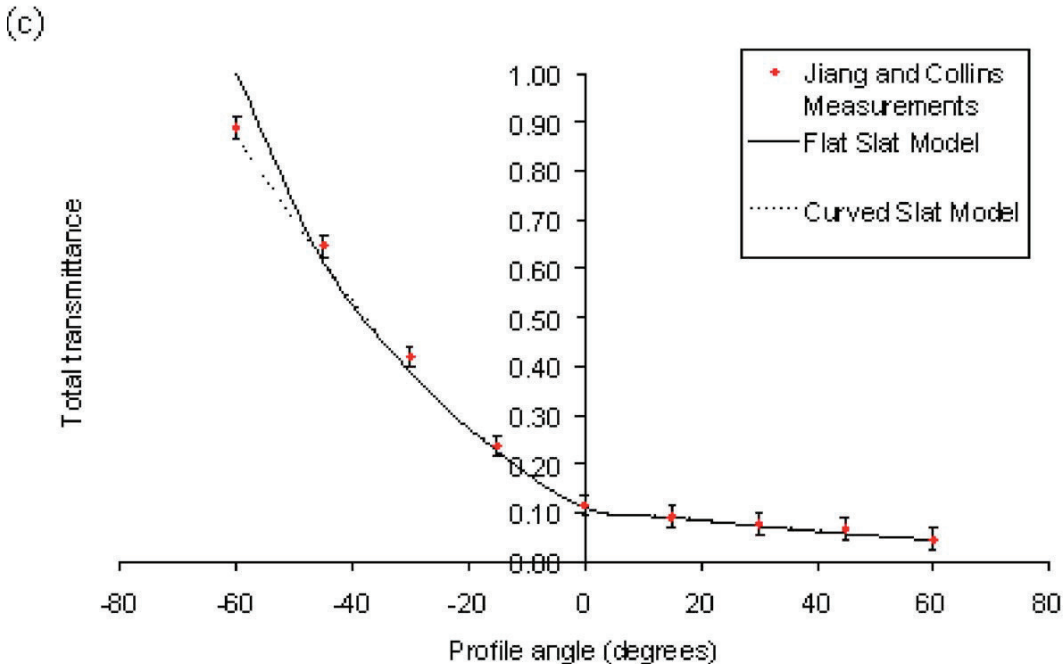

Figure 6.6: *Total transmittance at a slat angle of 60°. [Kotey et al., 2009]*

As seen in figures 6.4, 6.5 and 6.6 the model containing the curved slat correction fits better with the measured values. A slat thickness correction was not attempted due to the fact that the slats of Venetian blinds typically are very thin. Likewise a thickness correction model once developed showed minimal effect on the calculated blind properties [Parmelee and Aubele, 1952].

6.3 METHODS FOR CALCULATING THE EFFECTIVE... [YAHODA AND WRIGHT, 2004] [YAHODA AND WRIGHT, 2005]

The next two papers made by the same authors, are closely connected but are dealing with two different properties regarding Venetian blinds; Solar-optical properties and longwave radiative properties.

By giving the back and front surfaces of the shading layer averaged properties, named "effective" optical properties, the centre-glass method calculations can be used, because the shading layer can be considered homogeneous when using the "effective" properties. Doing this allows the shading layer to be treated as a planar layer within the glazing system just like the glass panes as shown in figure 6.7.

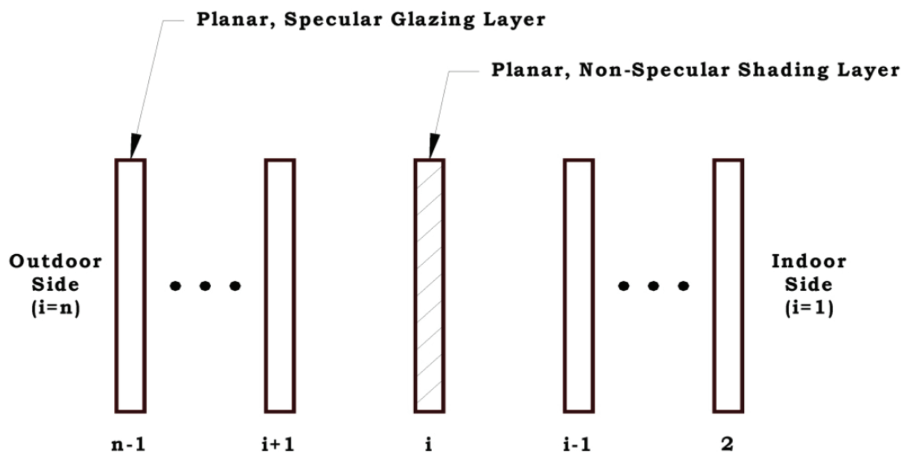

Figure 6.7: *Example of a layer representation of a glazing system with a Venetian blind. [Yahoda and Wright, 2005] [Yahoda and Wright, 2004]*

As for some of the previous papers of this literature survey a 4-surface and 6-surface model is used to model the blind enclosure, as seen in figure 6.8 where the Venetian blind layer from figure 6.7 is zoomed in upon and showed as a 4-surface model.

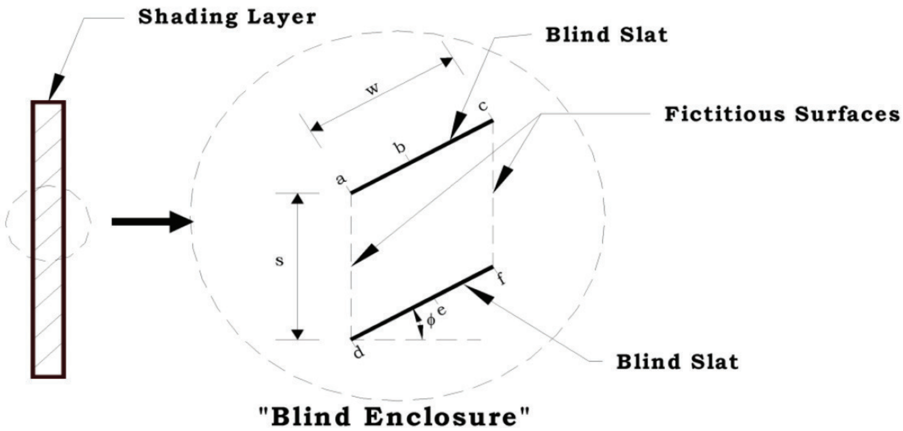

Figure 6.8: *Blind enclosure representing the entire Venetian blind layer. [Yahoda and Wright, 2005]*

6.3.1 METHODS FOR CALCULATING THE EFFECTIVE SOLAR-OPTICAL PROPERTIES OF A VENETIAN BLIND LAYER [YAHODA AND WRIGHT, 2005]

The purpose of this paper was to develop methods for determining the effective solar-optical properties of a Venetian blind shading layer. The results obtained from this research, compared to results obtained in well established literature were made in order to verify the model.

6.3.1.1 EFFECTIVE SOLAR-OPTICAL PROPERTIES

The model developed for determination of the effective solar-optical properties is based on fundamental radiative analysis and geometrical analysis. The solar-beam radiation incident on a Venetian blind layer can be modelled as being transmitted or reflected by the Venetian blind layer through five different paths. These paths are seen in figure 6.9 and can be defined as being:

1. transmitted without encountering the slat surfaces
2. transmitted through the shading layer by being specularly reflected on the slat surfaces
3. transmitted through the shading layer by being diffusely reflected from the slat surfaces
4. specular reflected from the shading layers surface to the outside
5. diffusely reflected from the shading layers surface to the outside

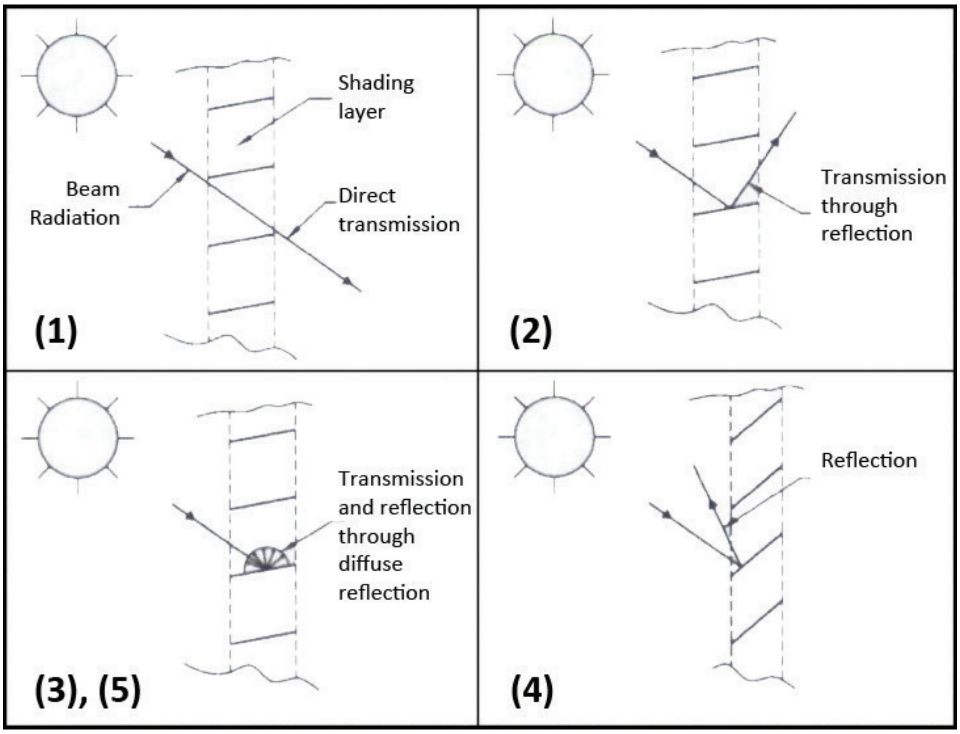

Figure 6.9: *Paths of transmission and reflection of incident radiation. [Yahoda and Wright, 2005], edited*

Commonly used in the literature is the assumption that the slat surface will reflect incident radiation either specularly or diffusely. This is not entirely true as the slat will reflect a portion of the incident radiation specularly and the remainder diffusely [Parmelee and Aubele, 1952]. These three cases of handling the reflection from the slats is illustrated in figure 6.10.

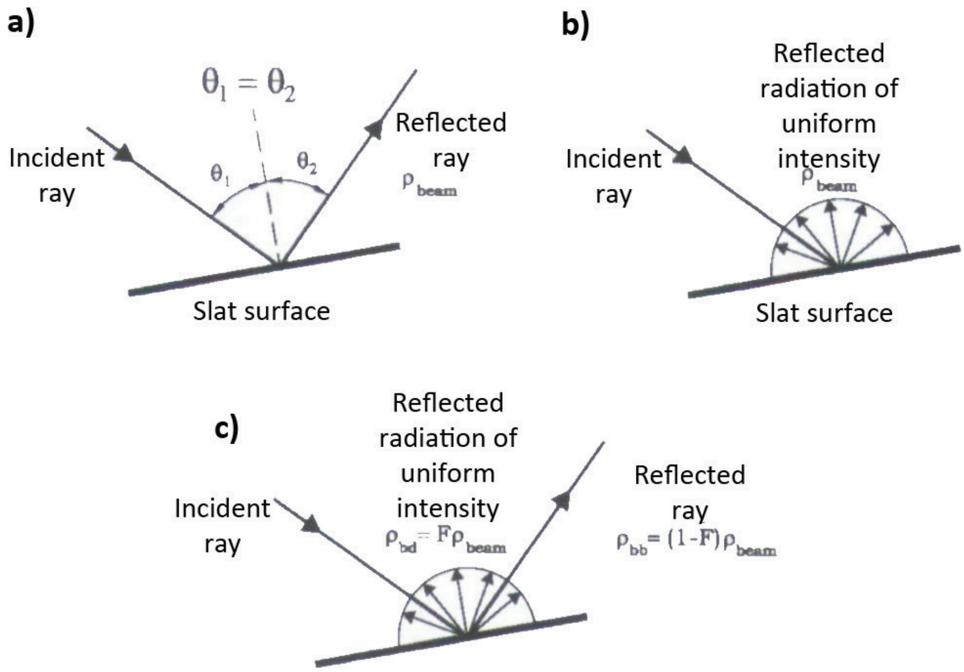

Figure 6.10: *Reflection from the slat surface: (a) specularly, (b) diffusely, (c) specularly and diffusely. [Yahoda and Wright, 2005]*

Where ρ_{bb} and ρ_{bd} describes the specularly reflection and the diffusely reflection respectively. These two types of reflectance are related by the beam/diffuse split factor F, which describes how specularly and diffusely the slat material reflects radiation. F equal 0 implies purely specular properties while F equal 1 implies purely diffusely properties. This factor F is assumed to be a constant, independent on the direction and wavelength of the incident radiation. Measurements from earlier literature indicates that approximately 10 % of the reflection is specularly and the remaining 90 % is diffusely, suggesting a F factor of 0,9 for slat materials [Parmelee et al., 1953] [Rosenfeld et al., 2001].

In this paper the reflection was modelled as in figure 6.10 c.

6.3.1.2 RADIANT ANALYSIS

The radiant analysis is performed in a similar way as in the other papers of this literature survey but through an eight-surface slat model with each slat being divided into three surfaces and each side of the shading layer, front and back, being a surface. This is illustrated in figure 6.11.

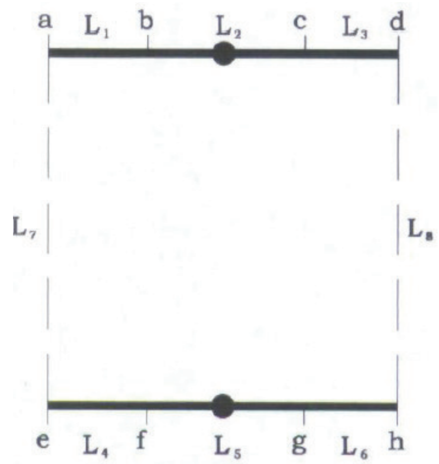

Figure 6.11: *Eight-surface blind enclosure model. [Yahoda and Wright, 2005]*

The radiosity equations are simplified using the flat-slat zero thickness assumption as seen before.

Based on this, a model for calculation of the effective solar-optical properties of a Venetian blind with respect to incident radiation and direction was developed. This model can be used for centre-glass heat transfer analysis of a glazing system with Venetian blinds applied anywhere in the glazing system. Through comparisons the model showed to be in good agreement with results obtained in other literature.

6.3.2 Methods for calculating the effective longwave radiative properties of a Venetian blind layer [Yahoda and Wright, 2004]

In the analysis of the longwave radiative properties the following assumptions were made:

- The blind slats are flat with uniform non-temperature-dependent properties
- The blind slats are opaque with respect to longwave radiation and the slat material is assumed to be gray and emit and reflect diffusely
- The blind slats are assumed to be long so the geometry can be treated as two-dimensional

The analysis contains methods for calculating the effective longwave absorptance, reflectance and transmittance of the Venetian blind layer where the influence of the 4-surface and 6-surface model was tested along. Furthermore the error of using a flat-slat model was looked upon by creating a model taking the curve of the slats into account.

6.3.2.1 EFFECTIVE LONGWAVE ABSORPTANCE

In obtaining the effective longwave absorptance two methods have been presented. The first method is based on an energy balance from which the fraction of the absorbed irradiance, G, can be determined, by using the reasoning that the amount of supplied energy which is absorbed by either the front or back surface of the shading layer should equal the total amount of energy absorbed at the slat surfaces. The rate of energy supplied to the enclosure equals the incident irradiance, G, multiplied with the area A on which G is incident. The absorption is then found by multiplying this with the slat materials absorptance. A second method deals with the fact that the fraction of G which is not reflected or transmitted must be absorbed.

6.3.2.2 EFFECTIVE LONGWAVE REFLECTANCE

The effective reflectance is defined as the fraction of G that is reflected by the blinds and is determined through an energy balance of the blind enclosure. The enclosure is seen in figure 6.8. The reflectance is determined from the rate of energy that leaves the blind enclosure compared to the incident rate of energy. I.e. in order to achieve the effective longwave reflectance, the energy that is reflected back from the blind layer is divided by the incident radiation on this blind layer.

6.3.2.3 EFFECTIVE LONGWAVE TRANSMITTANCE

The transmittance is determined through an energy balance as well as the absorptance and reflectance. The transmittance is found as the ratio of the incident radiation and the energy leaving the blind enclosure on the opposite side of the incident radiation.

6.3.2.4 CURVATURE AND SURFACE MODEL

Regarding the flat-slat model vs. the curved slat model made in this paper, the error of the flat-slat model was analysed for Venetian blinds with different properties, regarding curvature. This is illustrated in figure 6.12.

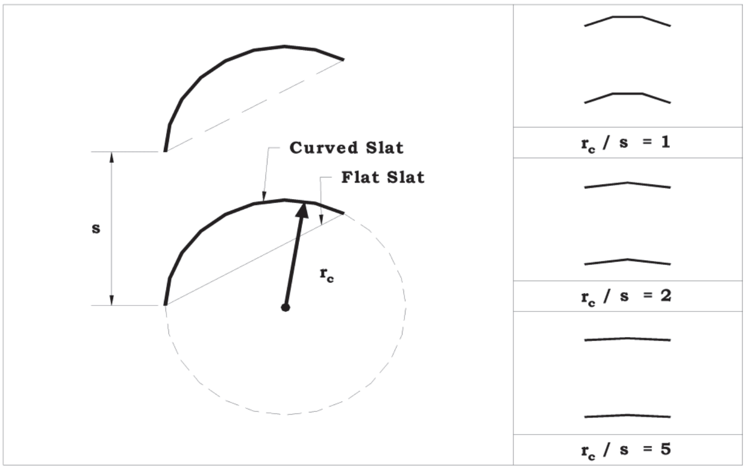

Figure 6.12: *Illustration of how the curvature of the slats is defined. [Yahoda and Wright, 2004]*

The analysis resulted in a maximum error of as little as 4 %, with the discrepancy approaching 0 % as the radius of the slats curve is decreasing. This is graphed in figure 6.13 for four different types of Venetian blinds at a slat angle of 0°, where the discrepancy is shown on the ordinate and the abscissa depicts the radius of the slat curvature, r_c, divided by the slat distance, s. Low value means high slat curvature radius, while high value means smaller radius.

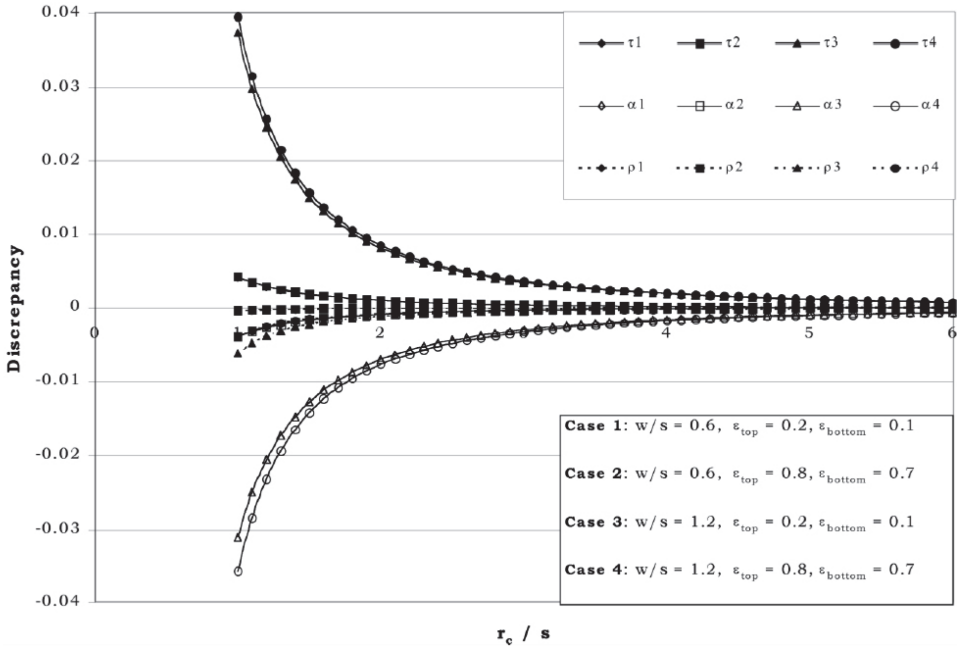

Figure 6.13: *Discrepancy in effective longwave properties between curved and flat slat models as a function of r_c/s at a slat angle of 0°. [Yahoda and Wright, 2004]*

Comparing the results of the 4-surface and 6-surface models the 4-surface model produces a small error. This error occurs when the slats have an angle where overlap is possible. Overlap is possible at specific angles when the width w of the slats is greater than the distance s in between the slats, see figure 6.8. The error is seen in figure 6.14 where e.g. the transmittance does not approach 0 when the slats are fully closed at ± 90°. This is because of the fact that the slats are considered fully uniformly irradiated in the 4-surface model which is not the case when the slats overlap.

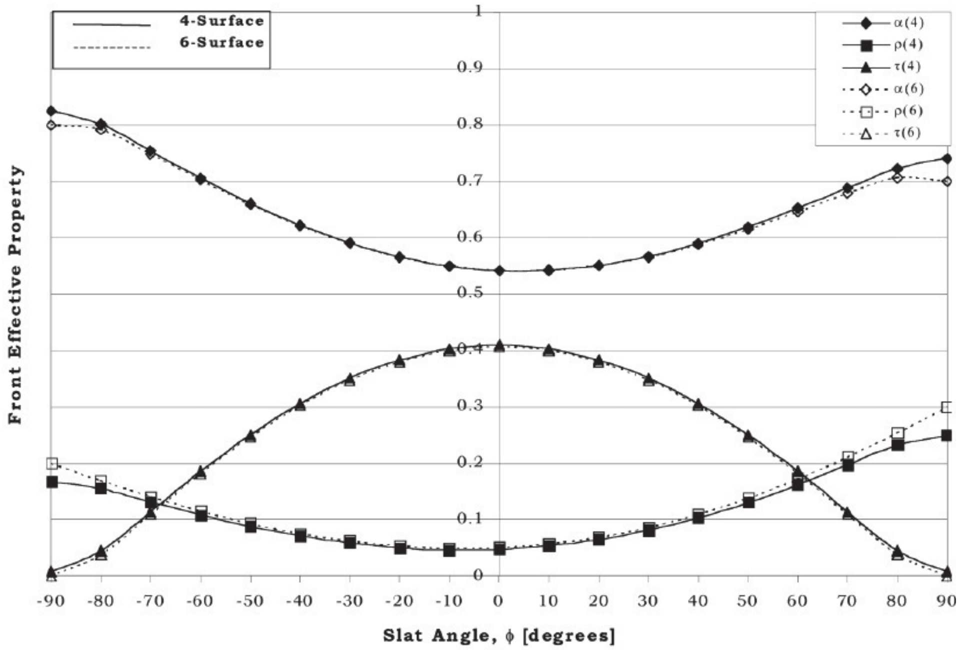

Figure 6.14: *Comparison of effective properties using 4-surface and 6-surface models with slat overlap. [Yahoda and Wright, 2004]*

6.4 SOLAR CONTROL: A GENERAL EVALUATION METHOD FOR FACADES WITH VENETIAN BLINDS OR OTHER SOLAR CONTROL SYSTEMS [KUHN, 2006]

The aim of this paper was to develop a model for calculating the total g-value g_{tot}, of a glazing system including a window and a Venetian blind layer. The model can be implemented in building simulation programs and opposite to many models from other literature it is able to account for the complex angular dependency of g_{tot}. Methods for determining g_{tot} were made for blinds at different locations in the glazing system, i.e. internal and external shading. Due to the scope of this project only the methodology used for the external shading will be addressed during the literature survey on this paper.

6.4.1 ANGLE-DEPENDENT CHARACTERISATION OF GLAZING PROPERTIES

In order to determine the angular dependent properties of a glazing, in this case g-value, direct solar transmittance and direct solar reflectances, a total of four different steps is looked upon:

- Experimental determination of the properties at an incident angle of 0°.

- Experimental determination of the properties at an incident angle greater than 0°. Due to very small variation in the properties at angles close to 0°, an angle of 60° is recommended.
- Theoretical determination of the glazing properties for arbitrary angles of incidence.
- Theoretical determination of the properties for diffuse irradiation.

Determining glazing characterisations at an incident angle of 0° is well described in the literature, while the same properties is more difficult to determine at incident angles different from 0°. This was handled by use of theory according to *DS/EN 410: Glass in building - Determination of luminous and solar characteristics of glazing* [Standard, 2011b] for the calculations of the properties at an incident angle of 0°. The results achieved through this process was generalised to account for arbitrary angles of incidence with an empirical model.

6.4.2 ANGLE-DEPENDENT CHARACTERISATION OF BLIND PROPERTIES

The optical properties of the Venetian blinds are determined with use of ray-tracing techniques. The principle of ray-tracing is illustrated in figure 6.15.

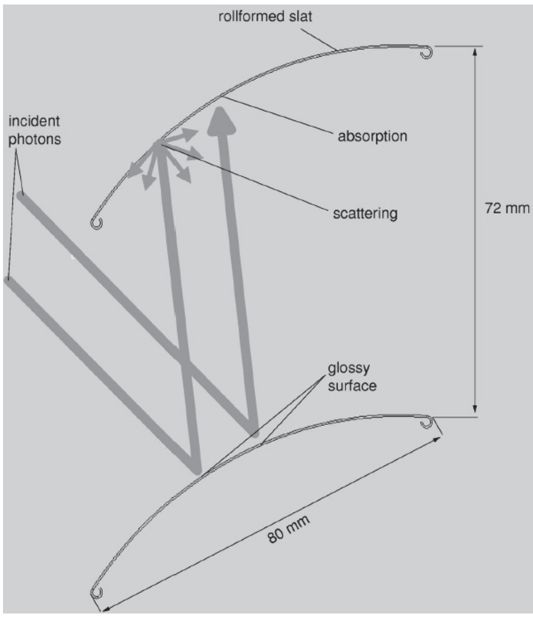

Figure 6.15: *Schematic drawing of the mechanisms considered in the ray-tracing method. [Kuhn et al., 2000]*

Compared to methods use in standards and for instance the software WIS, described in appendix C, which uses radiosity methods with the assumption of non curved slats, the model developed by the authors of this paper is dealing with ray-tracing methods on curved slats as seen in figure 6.15.

Within building simulations it is common practice to model external blinds as an extra glass pane with other properties. When doing so the angular dependent properties of the Venetian blind are treated as if they were rotationally symmetric, i.e. the blinds are assumed to have rotationally symmetric reflectance and transmittance instead of profile angle symmetry. The difference between profile angle and rotationally symmetry is shown in figure 6.16.

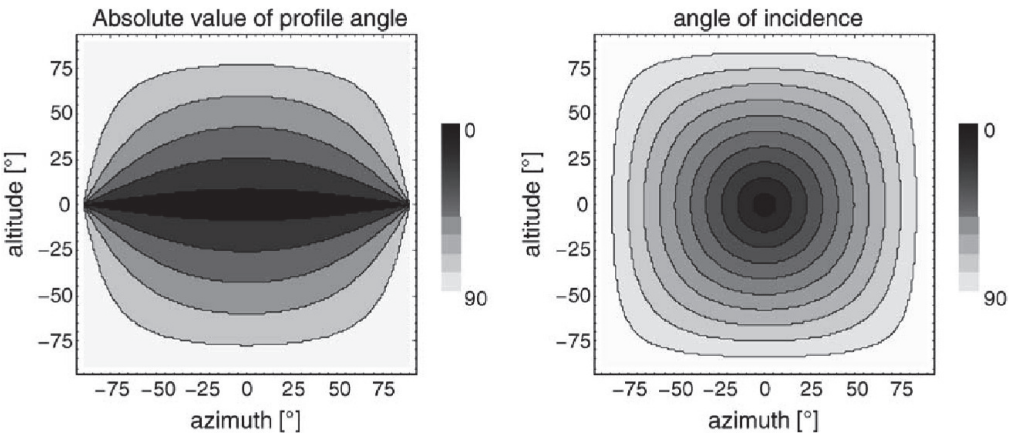

Figure 6.16: *Difference between profile angle symmetry and (rotationally symmetric) incidence angle symmetry. [Kuhn, 2006]*

In the case of Venetian blinds the rotationally symmetric assumption have shown to be very inaccurate in case of significantly underestimation of the solar gains for external blinds and that profile angle symmetry provides sufficiently accurate results when calculating angle dependent total g-values. [Kuhn et al., 2000]

6.4.3 DETERMINATION OF THE TOTAL G-VALUE OF THE GLAZING SYSTEM

In the calculations of the g-value of the glazing system including external Venetian blinds, an improved generalised version of the method given in *DS/EN 13363-1: Solar protection devices combined with glazing - Calculation of solar and light transmittance - Part 1: Simplified method* [Standard, 2007] was used.
This model has shown to be more accurate than other methods and that it is able to provide a general expresion for the total g-value for arbitrary boundary conditions, i.e. slat angles, solar azimuth and altitude angle.

Chapter 7

Window

This chapter deals with the calculation of the energy balance for the glazing. To do this the U-value and g-value of the glazing system is found. The g-value is a function of the transmittance, reflectance and absorptance of the glazing which will be described. An analysis is also made of how sensitive the U-value of the glazing is to the internal and external heat transfer coefficients.

7.1 Energy characteristics of the glazing system

A simple calculation of the energy balance is made for the glazing of the experiment. As mentioned in chapter 5 the energy balance of a glazing is taking both the U-value and g-value into consideration along with the climate and the orientation of the window. To calculate the U-value and the g-value of the glazing an excel sheet is made which can be seen in annex 2 on DVD. The g-value is a function of the transmittance, reflectance and absorptance of the glazing, which are dependent on the angle of incidence. This is described in section 7.2. The calculation method of the U-value and the g-value is shown in appendix A and B. To calculate the U-value, the temperature distribution through the glazing system is needed.

The temperature distribution through the window is found from the outdoor air temperature, the indoor air temperature and longwave radiation in between the glazings. The temperatures are found on the outside of the outer pane, in the middle of the outer pane, on the inside of the outer pane, in the middle of the gas layer and so on. Those temperatures will be used in the calculation of the U-value. The calculation of the temperature distribution is described in appendix D.

7.2 Angle dependent transmittance, reflectance and absorptance

Most standards are calculating the characteristics of glazings assuming an incident angle of 0°, i.e. with solar radiation perpendicular to the window. This phenomenon only occurs a few times of the year during certain months depending on the orientation of the window. In this case an east oriented vertical window will only have an angle of incidence of 0° at sunrise, where the solar altitude angle is just above 0°. The same goes for a west oriented vertical window at sunset.

Because of this is important to be able to evaluate the properties of glazing systems at different angles of incidence. A model calculating the transmittance τ, the reflectance ρ and the absorptance α, depending on the incident angle, is described in appendix E. In this model a refractive index, n, and an extinction coefficient, K, is used. For glass the refractive index is given at 1,526 meaning that the speed of light is 1,526 times faster in vacuum than in glass. The extinction coefficient for the uncoated glazing is set to 16,1 due to [Duffie and Beckman, 2006]. For the coated glazing it is determined in the way that the transmittance, reflectance and absorptance at an incident angle of 0° are as close as possible to the calculations in annex 4.1 on DVD, where the standardised spectral distribution is used.

It was not possible to reach a transmittance, reflectance and absorptance at an incident angle of 0° close to the calculations. Therefore a similar calculation is made in WINDOW 7 of the panes used in the experiment and the result is seen in figure 7.1. The calculation is given in annex 4.2 on DVD.

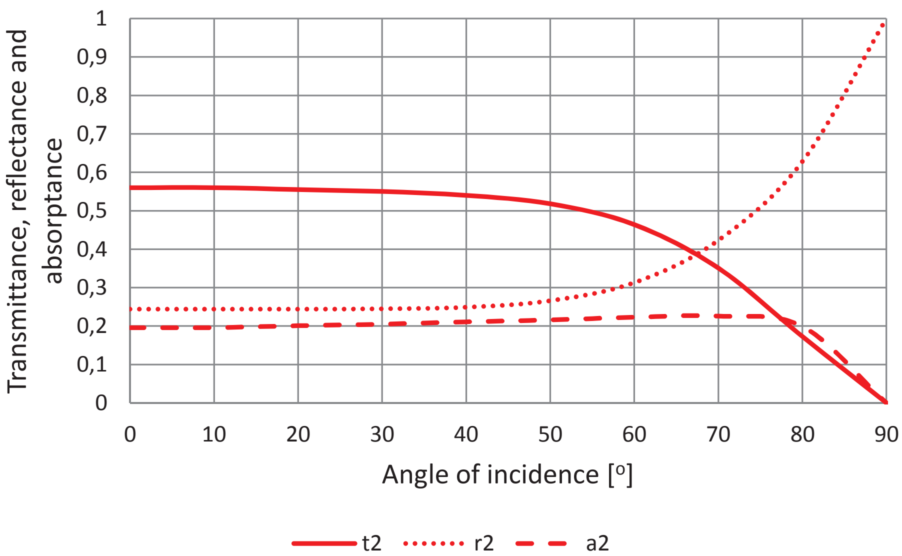

Figure 7.1: *Angle dependent transmittance, reflectance and absorptance found from WINDOW 7.*

Based on the incident angle dependent results given in figure 7.1 a curve fit was made for the transmittance and reflectance based on the expressions given in equations 7.1 and 7.2.

$$\tau(i) = \tau(0)\left(1 - tan^{p_1}\left(\frac{i}{2}\right)\right)^{p_2} \tag{7.1}$$

$$\rho(i) = \rho(0) + (1 - \rho(0))\left(tan^{p_3}\left(\frac{i}{2}\right)\right)^{p_4} \tag{7.2}$$

The absorptance is found through the fact that the sum of the transmittance, reflectance and absorptance equals 1. The angle dependent parameters p, is found through the *least square method* by iteration. These are found to be the values given in table 7.1.

p_1	4,09
p_2	1,75
p_3	2,46
p_4	1,65

Table 7.1: *Angle dependent parameters p.*

The curve fits of the graphs given in figure 7.1 are calculated through equations 7.1 and 7.2 with the parameters given in table 7.1. These are shown in figure 7.2.

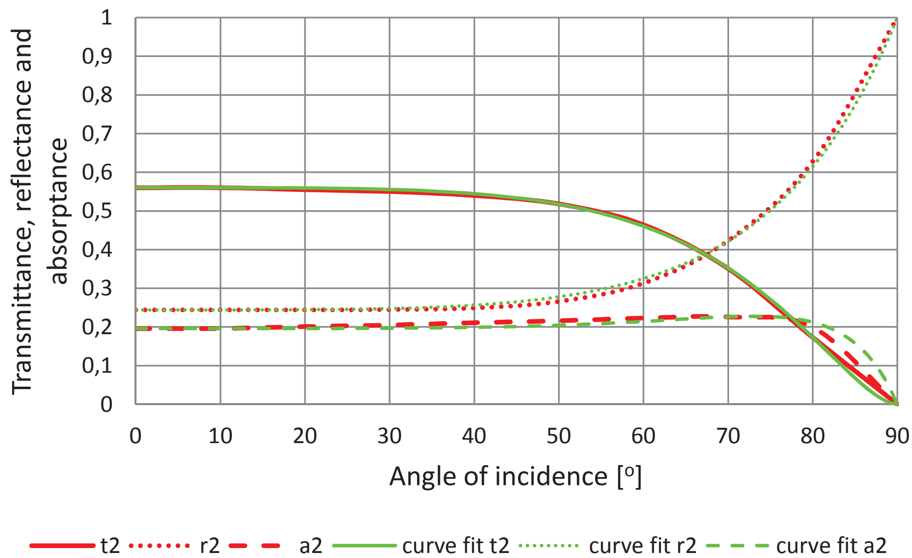

Figure 7.2: *Curve fits of the values found in WINDOW 7.*

In addition to the calculation of the angle dependency of the transmittance, reflectance and absorptance, the angle dependency of the g-value was found in a similar way in WINDOW 7. A curve fit for the g-value is shown in figure 7.3 which is found through the expression given in equation 7.3, with p_5 and p_6 found to be 1,67 and 4,21 respectively.

$$g(i) = g(0)\left(1 - tan^{p_5}\left(\frac{i}{2}\right)\right)^{p_6} \tag{7.3}$$

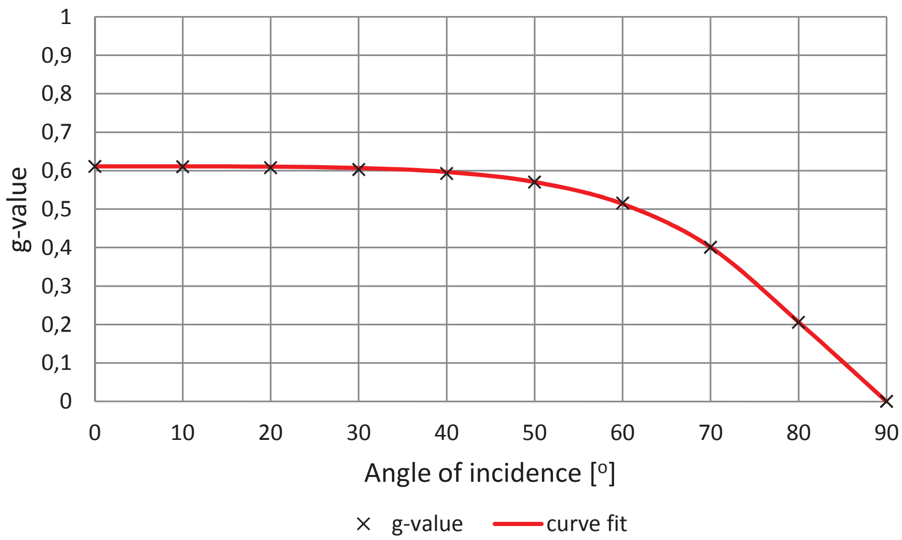

Figure 7.3: *A curve fit of the g-value.*

7.3 SENSITIVITY ANALYSIS OF EXTERNAL AND INTERNAL HEAT TRANSFER COEFFICIENTS

Standard values are normally used for the external and internal heat transfer coefficients, h_e and h_i, of 25 $^{W}/_{m^2K}$ and 7,71 $^{W}/_{m^2K}$ respectively. In reality the coefficients can vary and because of this, an analysis of how sensitive the U-value of the glazing are to these coefficients is made. The analysis is made with four different types of windows as seen in table 7.2. The window used in the calculations of the energy balance and in the experiments in this report is the third window which therefore will be the most interesting in this case. The fourth pane is interesting for future investigations and the two first panes are only for comparison with the past.

	Thickness of the layers	Gas type
Old-fashioned double-glazed window with a U-value of 2,9 $^{\mathrm{W}}/_{\mathrm{m^2K}}$	4-12-4	Air
New double-glazed window with a U-value of 1,8 $^{\mathrm{W}}/_{\mathrm{m^2K}}$	4-12-4*	Air
Experimental window with a U-value of 1,1 $^{\mathrm{W}}/_{\mathrm{m^2K}}$	4-15-4*	90 % Argon 10 % Air
New triple-glazed window with a U-value of 0,6 $^{\mathrm{W}}/_{\mathrm{m^2K}}$	4*-12-4-12-4*	Krypton

Table 7.2: *The different types of windows used in the sensitivity analysis. * is energy glass. [Glasindustrien, 2010], [Mróz, 2003], [UK, 2012]*

The given U-values are based on an external and an internal heat transfer coefficient of 25 $^{\mathrm{W}}/_{\mathrm{m^2K}}$ and 7,71 $^{\mathrm{W}}/_{\mathrm{m^2K}}$ respectively.

In the analysis of how sensitive the U-value of the glazing is to the internal heat transfer coefficient, a constant external heat transfer coefficient of 25 $^{\mathrm{W}}/_{\mathrm{m^2K}}$ is used while the internal heat transfer coefficient is varied. This analysis is seen in figure 7.4.

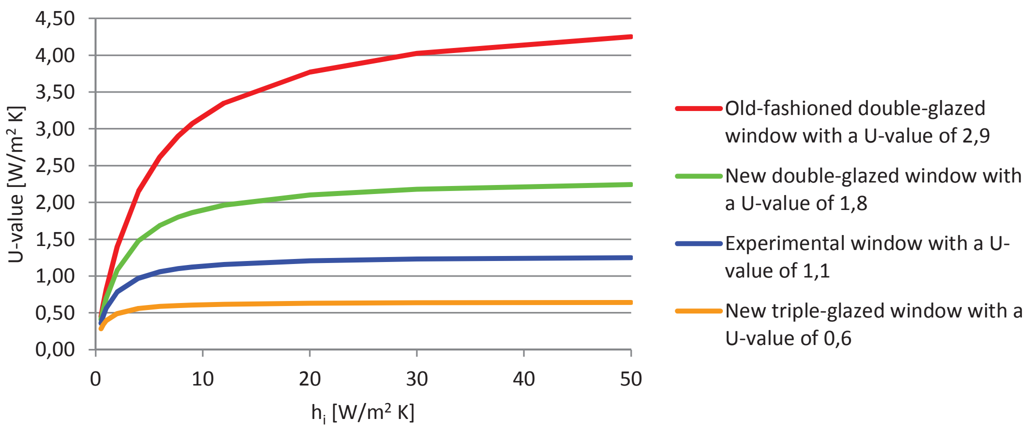

Figure 7.4: *h_i as a function of the U-value.*

In the analysis of how sensitive the U-value of the glazing is to the external heat transfer coefficient a constant internal heat transfer coefficient of 7,71 $^{\mathrm{W}}/_{\mathrm{m^2K}}$ is used while the external heat transfer coefficient is varied. This analysis is seen in figure 7.5.

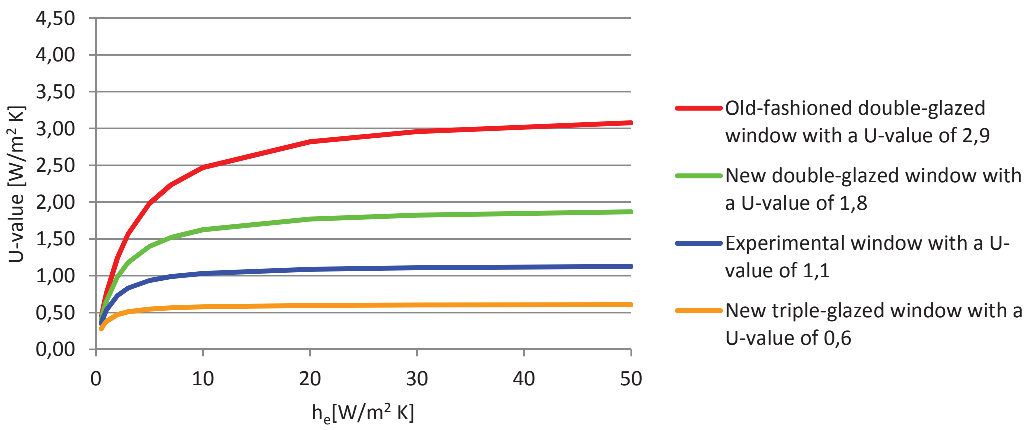

Figure 7.5: *h_e as a function of the U-value.*

It can be seen from those figures that the h_e-value and the h_i-value is most important for the U-value in the case of an old-fashioned double-glazed window with a U-value of 2,9 $^{W}/_{m^2K}$. In the other cases of windows with lower U-values, the h_e-value and the h_i-value is only important for the U-value if the heat transfer coefficients are less than 5-10 $^{W}/_{m^2K}$. From this it can be concluded that h_e and h_i is of less influence the lower the U-value is. Because this project deals with an energy glazing where the heat transfer coefficients is of modest importance the coefficients will not be investigated further as long as the glazing system is considered without any shading.

The sensitivity analysis is seen in annex 3 on DVD.

7.4 RESULTS OF THE WINDOW

To find the g-value of the glazing used in the experiments the optical properties of the glazing is needed. Those are given in table 7.3 at an incident angle of 0°, both in case of a standardized and a experimental relative spectral distribution.

	$\tau_e\,[-]$	$\rho_e\,[-]$	$\alpha_e\,[-]$	$q_i\,[-]$
Standard	0,55	0,25	0,20	0,07
Experiment	0,30	0,43	0,27	0,06

Table 7.3: *Optical properties in case of an incident angle of 0°, comparable with theory and experiments.*

The energy characteristics in case of the U-value and g-value was through calculation found to the values shown in table 7.4 both in case of a standardized and an experimental relative spectral distribution. The g-value is given for an incident angle of 0°. The same data given by Pilkington [UK, 2012] is also seen in the table along with the percentage deviations.

	U-value [$^{W}/_{m^2K}$]	g-value [$-$]
Standard	1,08	0,61
Pilkington	1,1	0,63
Deviation	1,08 %	3,2%
Experiment	1,08	0,36
ParaSol 6.6	1,13	0,6
WINDOW 7	1,26	0,63

Table 7.4: *Calculations of the U-value and the g-value compared to values from Pilkington, ParaSol 6.6, WINDOW 7 and the experimental relative spectral distribution.*

It is seen from table 7.4 that the calculated U- and g-values are very close to the ones from Pilkington. Due to a different relative spectral distribution in the experiments the g-value is diverging from the standard value.

The energy balance E_{ref}, for the glazing is found from equation 5.1 in chapter 5 to be 22,2 $^{kWh}/_{m^2}$ at an incident angle of 0 °, which is well above the minimum allowed value of -33 $^{kWh}/_{m^2}$.

For further comparison the U-value and g-value was calculated with use of the programs ParaSol 6.6 and WINDOW 7 described in appendix C. Results from ParaSol 6.6 and WINDOW 7 are shown in table 7.4. The boundary conditions for the calculations in the two programs are described in appendix C. ParaSol 6.6 calculates according to *DS/EN 673* [Standard, 2011c] and WINDOW 7 does not. This may be the reason why the calculation of the U-value is higher in WINDOW 7 than the other U-values.

7.4.1 ANGLE DEPENDENT RESULTS

The g-value is different at incident angles different from 0°. The solar direct transmittance τ_e is found from equation 7.1, also shown in figure 7.2, in section 7.2 dependent on the incident angle. The g-value dependent on the incident angle is found from equation 7.3 and is shown in figure 7.3 in section 7.2. The results of this is not commented further during this report as the theoretical calculations are compared to measurements which only is made for an incident angle of 0°.

CHAPTER 8

WINDOW WITH A VENETIAN BLIND

This chapter contains the description of the procedure used to determine the energy characteristics of the glazing system containing a Venetian blind. The approach used for the glazing itself is similar as in chapter 7 but with different boundary conditions in order to account for the Venetian blind. To determine the U-value and g-value, the shading factor of the Venetian blind and the external heat transfer coefficients on the outside of the pane are recalculated.

8.1 ENERGY CHARACTERISTICS OF THE GLAZING SYSTEM

In order to determine the energy characteristics of a glazing system containing solar shading in case of a Venetian blind, the following parameters needs to be addressed:

1. Energy characteristics of the glazing
2. Optical properties of the Venetian blind
3. Shading factor of the Venetian blind
4. Heat transfer coefficient in between Venetian blinds and glazing including long-wave radiation in between slats and pane

The four parameters listed above, are used to describe the energy characteristics of the glazing system including the Venetian blind. Excluding the first parameter which is described in chapter 7, the remaining four parameters are separately dealt with in the following sections, where detailed description on how these are found are presented. The Venetian blind is described in chapter 4.

8.1.1 OPTICAL PROPERTIES OF THE VENETIAN BLIND

The Venetian blind is considered as a volume consisting of two slats, as shown in figure 8.1.

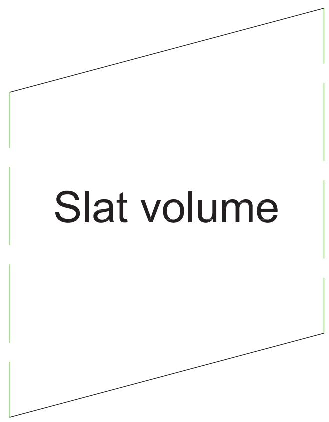

Figure 8.1: *Two slats of a Venetian blind, considered as a volume.*

The optical properties of the slat volume are categorised under the parameters; transmittance τ, reflectance ρ and absorptance α, which through Kirchoff's relation is related in the following way, as presented in section 3.3 equation 3.2.

$$1 = \tau + \rho + \alpha$$

These parameters says something about how much energy is transmitted through the slat volume, how much that is reflected either back towards the outside or reflected from the volume towards the window and finally how much of the energy that is absorbed in the volume.

8.1.1.1 TRANSMITTANCE

The transmittance of the slat volume, which is reaching the window directly is determined as the fraction of the vertical distance between the slats s, and the irradiated height W. This is given in equation 8.1 and illustrated in figure 8.2.

$$\tau = \frac{W}{s} \tag{8.1}$$

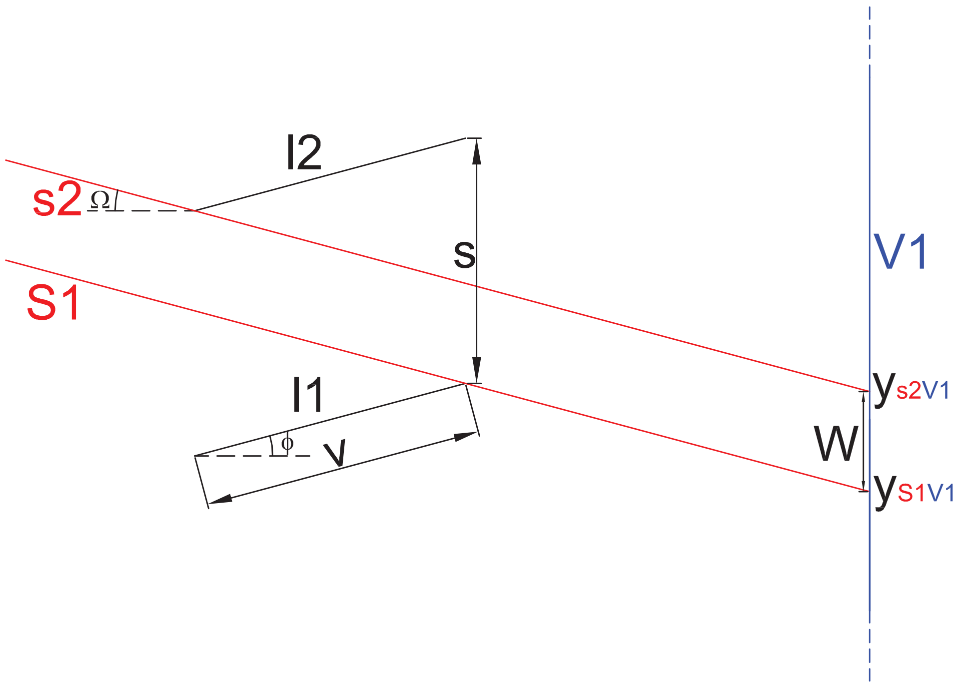

Figure 8.2: *Definition of the transmittance for a Venetian blind layer.*

An example of the calculation of the transmittance τ, is given in appendix F section F.2.

8.1.1.2 REFLECTANCE

The possible radiative scenarios that can occur are described in the literature survey section 6.3.1 and shown in figure 6.9. Based on this knowledge three sub-parameters are defined for the reflectance of the shading layer. These are given below and shown in figure 8.3.

A Beam-beam reflectance ρ_{bb}, i.e. incident beam-radiation is reflected specularly

B Beam-diffuse reflectance ρ_{bd}, i.e. incident beam-radiation is reflected diffusely

C Diffuse-diffuse reflectance ρ_{dd}, i.e. diffuse radiation is reflected diffusely

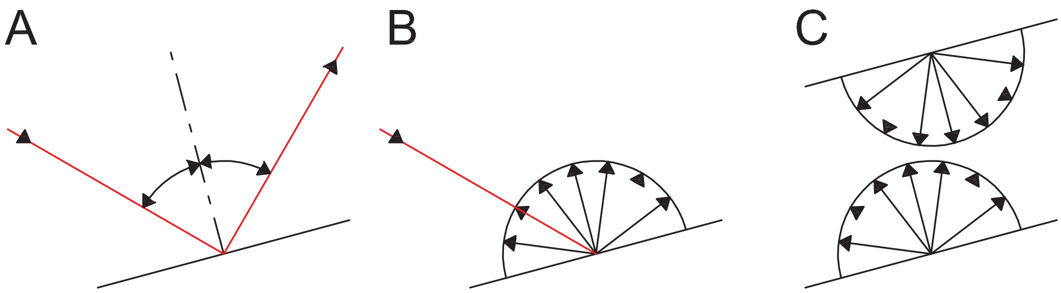

Figure 8.3: *A: Beam-beam reflectance. B: Beam-diffuse reflectance. C: Diffuse-diffuse reflectance.*

The reason for defining three types of reflectances are the fact that slat materials typically reflect a portion of the incident beam radiation specularly and the remaining diffusely, while diffuse radiation is reflected diffuse. I.e. when the slats are irradiated, the radiation is reflected partly as A and partly as B as described above and shown in figure 8.3. These two optical properties are related through the concept of the beam/diffuse split, which is a measure of how specularly or diffusely the slats reflects incident beam radiation independent of direction or wavelength of the incident radiation. For slats only reflecting beam radiation specularly, as shown in A above, the beam/diffuse split factor F, equals 0. For cases with purely diffuse reflection, as B shown above, F equals 1. Through measurements of common slat materials the specular fraction was found to be 10 % giving a diffuse fraction of 90 %, implying F=0,9 [Parmelee et al., 1953] [Rosenfeld et al., 2001]. This leads to the following two expressions given in equation 8.2 and equation 8.3.

$$\rho_{bb} = (1 - 0{,}9)\,\rho \tag{8.2}$$

$$\rho_{bd} = 0{,}9\rho \tag{8.3}$$

where:

ρ	*Reflectance of the slat material* $[-]$

The diffuse-diffuse reflectance is given as the reflectance of the slat material. [Yahoda and Wright, 2005] When calculating the reflectances the view factors between the slats, between the slats and the window and between the slats and the outside are used for calculating the fraction of energy leaving one surface being intercepted by the opposite surface. The view factor in between two surfaces is found as the angle between the two surfaces divided by 180°, where 180° is the total view from the surface. Every surface, when considering view factors, are divided into five subsurfaces and a mean of those five view factors is found. An illustration of the view factor is shown in figure 8.4, where the angle between the third subsurface of the lower slat and the upper slat is found. In this example the view factor from the third subsurface of the lower slat to the upper slat is calculated to be $\psi = 0{,}69$.

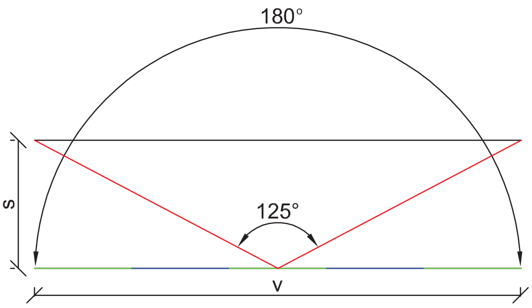

Figure 8.4: *Illustration of a view factor from one surface to another.*

The reflecantes from the slats can be summed up to contain the following; diffusely to the outside, diffusely to the window, specular to the outside and specular to the window. Those reflectances are found dependent on the specular and diffuse reflectances in between two slats.

The model which has been made to calculate the optical properties for the Venetian blinds differs from the typical models described in the literature survey in chapter 6. In the literature it is common to use af four-surface or six-surface model for the calculations. The model which are about to be described uses different amount of surfaces dependent on the given situation, in case of the position of the sun and the slat angle. Based on a ray-tracing method the algorithm calculates the intersections both between the incident radiation and the slat and between the reflectances and the slats. Based on these, the amount of necessary surfaces is determined. The model is therefore named ***optimal-surface model***. An illustration of this model is shown in figure 8.5 in two different cases; one with a radiation angle of 45° and a slat angle of 30° and another with a radiation angle of 60° and slat angle of 0°.

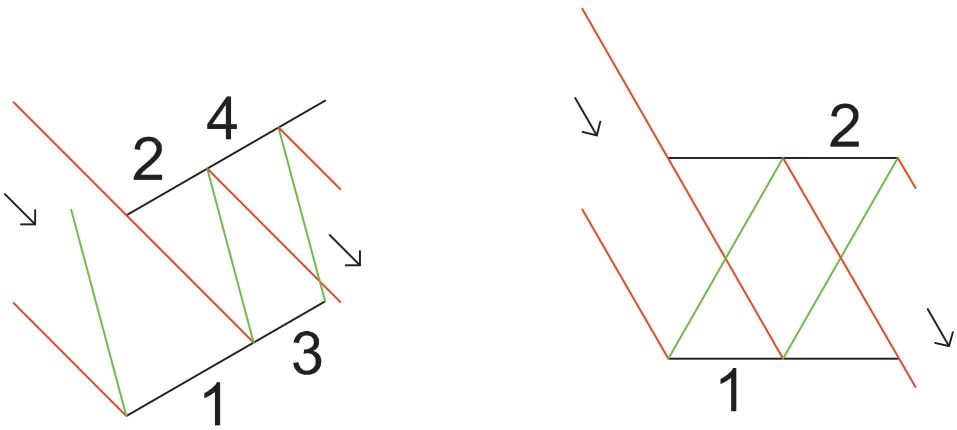

Figure 8.5: *Left: In case of a radiation angle of 45° and a slat angle of 30°. Right: In case of a radiation angle of 60° and a slat angle of 0°. The numbers represents the number of surfaces on the slats in case of specular reflections.*

The ***optimal-surface model*** is made of a ray-tracing technique based on simple linear equations expressed by equation 8.4.

$$y = ax + b \tag{8.4}$$

The linear equations are found for all the downward and upward going radiations, as seen in figure 8.5. Besides that, equations for some helping lines are found. The lines, their intersections and distances of lines used in the ***optimal-surface model*** are described in appendix F. An example of the calculations is also shown in appendix F section F.2.

8.1.1.3 ABSORPTANCE

The absorptance of the shading layer is found through Kirchoff's relation. By considering the volume between two slats as a box, it can be stated that the amount of energy leaving this volume either as being transmitted or reflected subtracted from the total amount of energy incident on the volume, must equal the amount of energy being absorbed by the volume. This is given in equation 8.5 and illustrated in figure 8.6.

$$\text{Absorptance} = 1 - \frac{\text{Entering}}{\text{Leaving}} \tag{8.5}$$

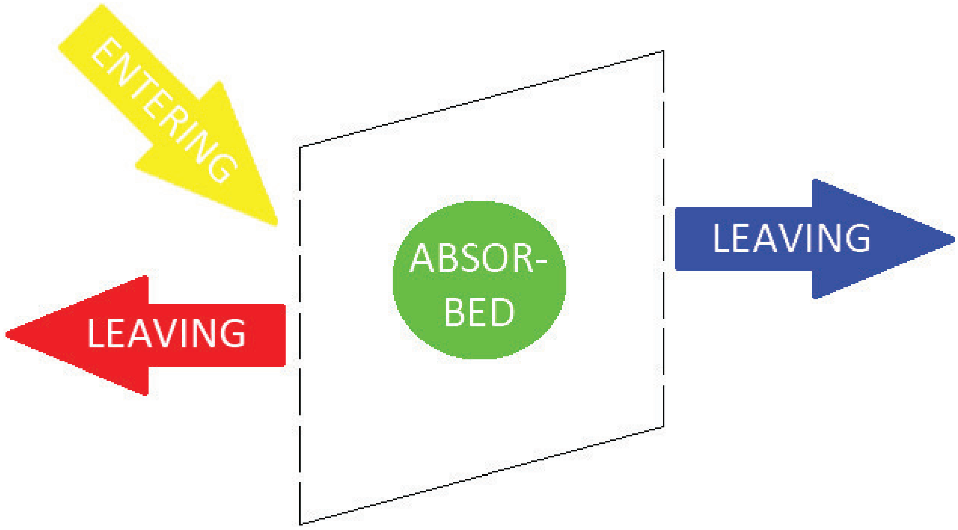

Figure 8.6: *Illustration of the radiative energy balance of the volume of a shading layer. The energy leaving the volume is given as the sum of the transmittance and reflectances.*

The absorptance by the slats, when considering the volume between two slats, is used later on in the calculation of the convective heat transfer coefficient in case of measurements.

From the optical properties presented, the shading factor of the Venetian blind can be determined.

8.1.2 SHADING FACTOR OF THE VENETIAN BLIND

The solar shading factor s_f indicates how efficient a shading is. It is found as the relation in between the amount of energy reaching the window with and without solar shading, in this case the radiative energy without considering the effect of the temperature. In case of no solar shading the radiative energy reaching the window is found from equation 8.6. With use of solar shading the energy reaching the window is found from equation 8.7.

$$E_{no-shading} = E \cdot A_{window} \tag{8.6}$$

where:

A_{window}	*Area of the window* [m^2]
E	*Energy reaching the window* [$^{W}/_{m^2}$]
$E_{no-shading}$	*Energy reaching the window without shading* [W]

The incident radiation, E, used in these calculations can be found from the weather data from DRY. In DRY the radiation is given on a horizontal surface, which needs to be transformed into a radiation on a vertical surface, as the window is vertical.

$$E_{shading} = \sum \tau_{energy} + \sum \rho_{energy} \tag{8.7}$$

where:

$E_{shading}$	*Energy reaching the window with shading* [W]
ρ_{energy}	*Specular and diffuse reflected energy through the shading* [W]
τ_{energy}	*Transmitted energy through the shading* [W]

τ_{energy} is the transmission given in equation 8.1 and ρ_{energy} is the sum of the diffuse and the specular reflection reaching the window.

From the statements above, the solar shading factor of the Venetian blind only taking the radiation into account is found from equation 8.8.

$$s_f = \frac{E_{shading}}{E_{no-shading}} \tag{8.8}$$

The reason for only taking the radiation into account is due to the fact that the addition in energy entering through the glazing through absorption cannot be measured without the use of a hotbox.

The shading factor is valid for an endless height of the window/shading. Due to this the error of the shading factor will increase with decreasing amount of slats.

All the calculations are made in MATLAB and can be seen in annex 5 on DVD.

8.1.3 HEAT TRANSFER COEFFICIENT IN BETWEEN VENETIAN BLINDS AND GLAZING

In the cavity between the Venetian blind and the window, convection will occur as a function of temperature differences in between the air of the cavity and the bounding surfaces, i.e. slats and window. This flow will influence the heat transfer coefficient, in a way that might be different from the prescribed exterior heat transfer coefficient given in the standard as $25\,{}^{W}/_{m^2K}$ [Standard, 2011b]. This value is set as a worst case scenario to ensure that the effect on the U-value will not be more positive than it really is. In this case with solar shading it is necessary to calculate a more precise exterior heat transfer coefficient on the outside of the window. The way of calculating the exterior heat transfer coefficient is presented in this section and will be done for different slat angles, similar to the ones used through the experiments. The interior heat transfer coefficient is not investigated further due to expectations of low variations of experimental h_i compared to the standardized value.

The heat transfer at a surface happens as a function of both radiation and convection and the heat transfer coefficient is calculated as shown in equation 8.9.

$$h_e = \alpha_r + \alpha_c \tag{8.9}$$

where:

h_e	*Heat transfer coefficient* [W/m²K]
α_c	*Heat transfer coefficient due to convection* [W/m²K]
α_r	*Heat transfer coefficient due to radiation* [W/m²K]

The two parts of the heat transfer coefficient is calculated independently. The procedure is shown in the following, while calculations are given in annex 6 on DVD.

8.1.3.1 HEAT TRANSFER COEFFICIENT DUE TO RADIATION

The radiation from a surface to another can be written as shown in equation 8.10 [Stampe et al., 2006].

$$\Phi_{12} = \alpha_r \cdot A_1 \cdot (t_1 - t_2) \tag{8.10}$$

where:

A	*Surface area* [m²]
t	*Surface temperature* [°C]
Φ_{12}	*Heat flow* [W]

This is achieved from equation 8.11.

$$\Phi_{12} = \psi_{12} \cdot \epsilon_1 \cdot \epsilon_2 \cdot \sigma \cdot A_1 \cdot \left(T_1^4 - T_2^4\right) \tag{8.11}$$

where:

T	*Surface temperature, absolute* [K]
ψ_{12}	*View factor* [−]
σ	*Stefan Boltzmanns constant* [$^{W}/_{m^2K^4}$]

Having equation 8.10 and 8.11 in mind, the radiative contribution to the heat transfer coefficient is found from equation 8.12.

$$\alpha_r = \frac{\psi_{12} \cdot \epsilon_1 \cdot \epsilon_2 \cdot \sigma \cdot \left(T_1^4 - T_2^4\right)}{(t_1 - t_2)} \tag{8.12}$$

8.1.3.2 HEAT TRANSFER COEFFICIENT DUE TO CONVECTION

In order to determine the exterior heat transfer coeffiecient, some characteristics regarding the flow in the cavity between the shading and window needs to be known, since the heat transfer coefficient is determined on behalf of the model numbers; Prandtl's, Grashof's and Nusselt's. These values consist of the flow density, temperature, viscosity, thermal conductivity and the heat capacity. Prandtl's number is a fluid material parameter and Grashof's number approximates the ratio of the buoyancy to viscous force acting on a fluid while Nusselt's number is defined as the ratio of convective to conductive heat transfer. Before being able to calculate the heat transfer coefficient the type of flow needs to be determined, i.e. is the flow made by free or forced convection. Free and forced convection are described in appendix G. For the experimental setup of this project the air flow in the cavity was investigated through measurements of the velocity profile. These results are seen in appendix G.3 and the conclusion is that the flow corresponds most to free convection. Due to this the flow is seen as free convection. The reason for this type of flow may be because of the fact that the experiment is located indoors with no wind induced pressures. This lead to the use of equation 8.13 in order to determine the exterior heat transfer coefficient.

$$Nu = \frac{\alpha_c \cdot l}{\lambda} = A \cdot Ra^n \tag{8.13}$$

$$Ra = Gr \cdot Pr$$

where:

A	*Constant* [$-$]
l	*Characteristic length* [m]
n	*Exponent* [$-$]
Nu	*Nusselt's number* [$-$]
α_c	*Heat transfer coefficient due to convection* [$^{W}/_{m^2K}$]
λ	*Thermal conductivity* [$^{W}/_{mK}$]
Gr	*Grashof's number* [$-$]
Pr	*Prandtl's number* [$-$]
Ra	*Rayleigh's number* [$-$]

The values used for determining the dimensionless Prandtl and Grashof numbers are given for air at a temperature corresponding to the mean temperature of the air and the bounding surfaces, i.e. the shading and the window surface temperatures. The characteristic length corresponds to the height of the shading. Prandtl's and Grashof's number is shown in equation 8.14 and 8.15 respectively.

$$Pr = \frac{\rho \cdot c_p \cdot \nu}{\lambda} \tag{8.14}$$

$$Gr = \frac{g \cdot \beta \cdot \Delta t \cdot l^3}{\nu^2} \tag{8.15}$$

where:

c_p	*Heat capacity* [$^{J}/_{kgK}$]
g	*Gravitational acceleration* [$^{m}/_{s^2}$]
β	*Expansion coefficient* [$^{1}/_{K}$]
Δt	*Temperature difference* [K]
ν	*Kinematic viscosity* [$^{m^2}/_{s}$]
ρ	*Density* [$^{kg}/_{m^3}$]

Different literature have been studied and equation 8.13, valid for free convection, was present in each of these literatures, the only variation being the constant A and the exponent n [Stampe et al., 2006] [Stampe, 1982] [Standard, 2011c]. The values from [Stampe et al., 2006] and [Stampe, 1982] are valid for flows along vertical positioned walls while the values from [Standard, 2011c] are valid for flows in the gas space in between two layers of glass in a window. This is illustrated in figure 8.7.

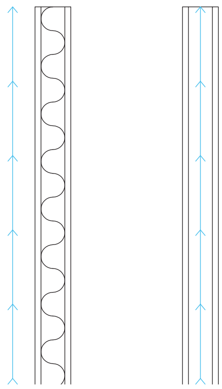

Figure 8.7: *A sketch where the arrows indicate a flow. Left: Flow along vertical positioned walls. Right: Flow in the gas space in between two glass layers of a window.*

The constants A and the exponents n as presented in different literature are shown in table 8.1.

	Laminar		**Turbulent**	
	A	n	A	n
Danvak	0,54	0,25	0,135	0,33
Glent	0,59	0,25	0,135	0,33
	A		n	
DS/EN 673	0,035		0,38	

Table 8.1: *Values of the constant A and the exponent n for various literature in case of free convection. [Stampe et al., 2006] [Stampe, 1982] [Standard, 2011c]*

None of these constants and exponents can rightfully be used, since the cases in where these are valid do not correspond to the situation with Venetian blinds in front of a window as illustrated in figure 8.8. Despite of this, these values will be used for calculation of the exterior heat transfer coefficient and later on compared with the exterior heat transfer coefficient obtained from experiments, to determine whether some of the values of table 8.1 can be used or not.

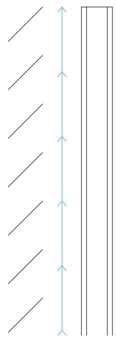

Figure 8.8: *A sketch of the window mounted with the Venetian blind, where the arrows indicate a flow.*

The constant A and the exponent n varies dependent on the type of flow, i.e. whether it is laminar or turbulent. The region of validity of free convection is for a laminar flow at a Rayleigh's number in the region of $10^4 - 10^8$ and for turbulent flow with a Rayleigh's number in the region of $10^8 - 10^{12}$ [Stampe et al., 2006].

With use of equation 8.14 and 8.15 along with the boundary conditions from the experiment, $Gr \cdot Pr = Ra$ is found to be in the region of $1,75 - 2,28 \cdot 10^9$ for slat angles from 0-70 $^\circ$ meaning that the flow is turbulent at every slat angle.

8.2 RESULTS OF THE WINDOW WITH VENETIAN BLINDS

The U-value and g-value of the glazing system, consisting of the window shaded by the Venetian blind used in the experiments, is dependent on the following; the shading factor of the Venetian blind and the external heat transfer coefficient on the outside of the pane, which are described above. Those parameters are varying dependent on the radiation angle and the slat angle. The experiments are made for a radiation angle of 0° and six different slat angles; 0°, 15°, 30°, 45°, 60° and 70°. The results of those parameters are described in the following.

8.2.1 SHADING FACTOR

The results of the shading factors, comparable with the experiments and calculated through equations 8.6-8.8, are seen in table 8.2.

ϕ [°]	0	15	30	45	60	70
s_f [−]	1	0,74	0,48	0,26	0,07	0,04

Table 8.2: *Shading factors in case of a radiation angle of 0°, which are comparable with the experiments.*

The same results are seen in figure 8.9 compared with the total transmittance at slat angles of 0°, 30° and 60° given in the theoretical literature survey in section 6.2 figures 6.4, 6.5 and 6.6.

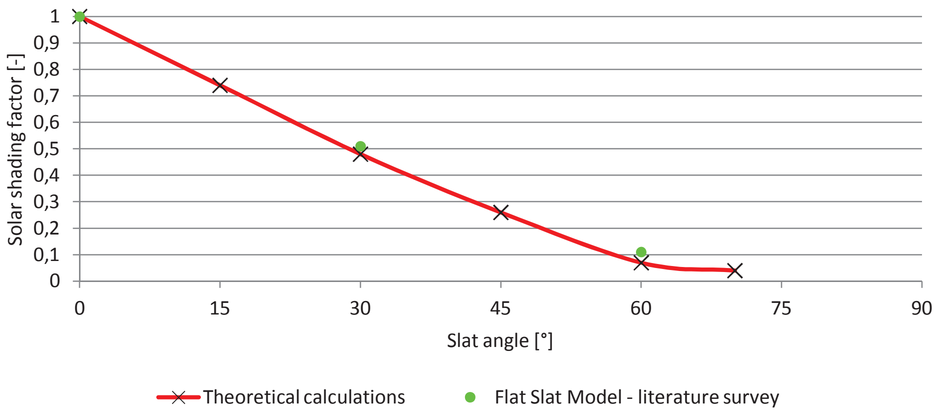

Figure 8.9: *Calculated shading factor compared to the theoretical literature survey.*

It is seen from the graph that the calculated solar shading factors at slat angles of 0, 30 and 60° are in agreement with the ones from the literature survey.

The shading factors from table 8.2 are detailed further and the results of the shading factors for every radiation angle and every slat angle, in an interval of 1° are shown in figure 8.10.

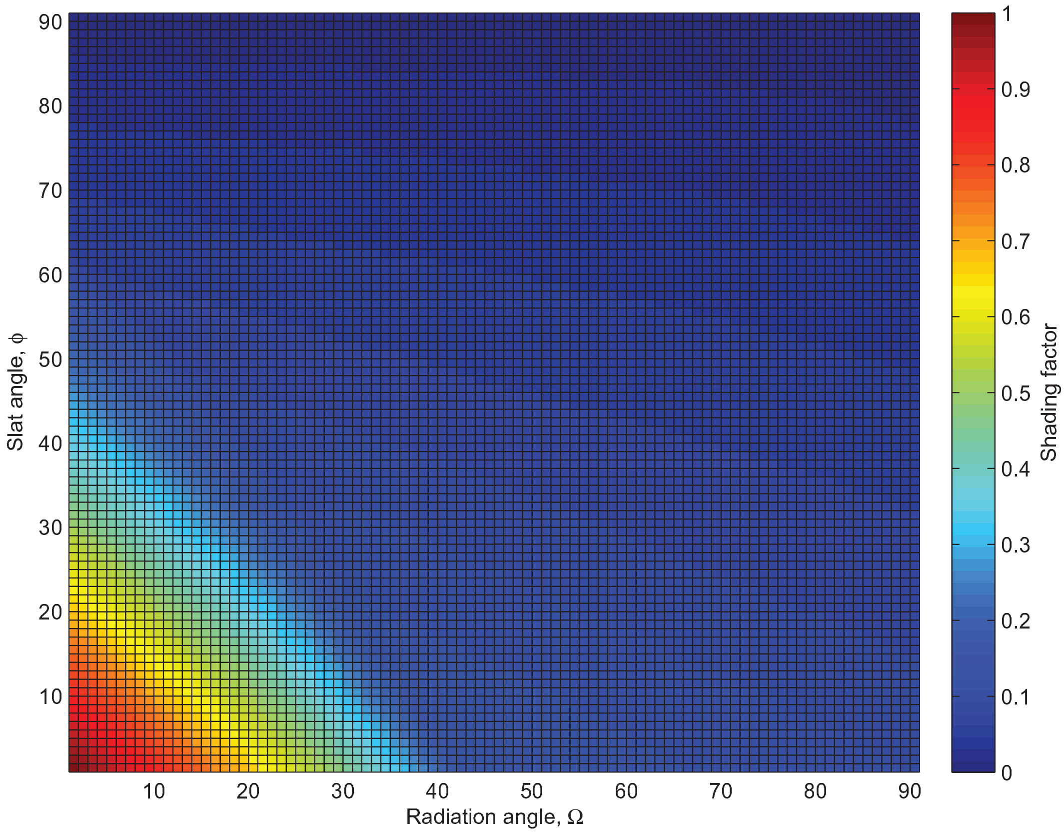

Figure 8.10: *Shading factors for radiation angles and slat angles, in an interval of 1°.*

As expected, the solar shading factors are highest at a low radiation angle and slat angle and lowest at a high radiation angle and slat angle. This is because lower values of radiation angle and slat angle results in higher solar transmission of the blind layer.

8.2.2 EXTERNAL HEAT TRANSFER COEFFICIENT

For comparative reasons, the heat transfer coefficients are calculated with boundary conditions similar to the ones measured through the experiments. These are given in appendix H.

From equation 8.9, different heat transfer coefficients has been obtained dependent on what literature are used for determination of the constant A and the exponent n. As the flow is calculated as being turbulent as stated in section 8.1.3, only the turbulent results are presented. The heat transfer coefficients at different slat angles are given in table 8.3 and illustrated in figure 8.11 where the heat transfer coefficient is the sum of the convective and radiative part. These are found through equation 8.9 section 8.1.3. The calculation of h_e is made in annex 6 on DVD.

ϕ [°]	0	15	30	45	60	70
Danvak	4,83	4,79	4,77	4,62	4,47	4,38
Glent	4,83	4,79	4,77	4,62	4,47	4,38
DS/EN 673	3,92	3,88	3,87	3,74	3,61	3,54

Table 8.3: *The exterior heat transfer coefficient, on the outside of the pane, calculated with different constants and exponents according to the literature. [Stampe et al., 2006] [Stampe, 1982] [Standard, 2011c]*

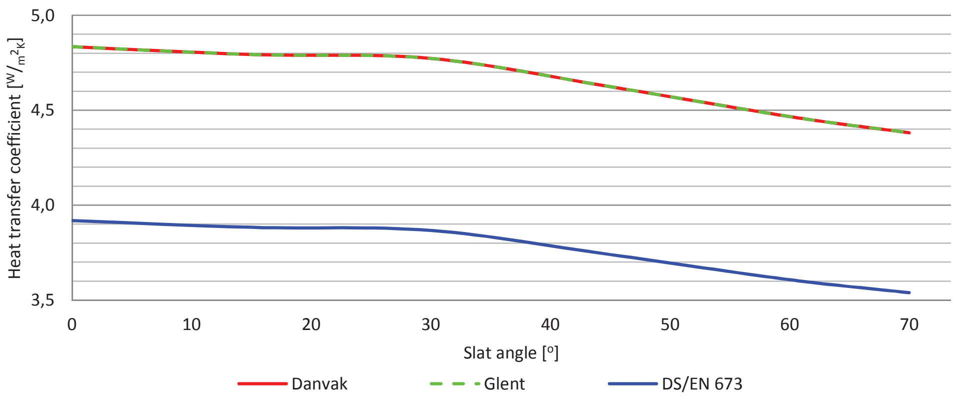

Figure 8.11: *Exterior heat transfer coefficient given for the different literature.*

The results obtained from Danvak and Glent are in good agreement while results from DS/EN 673 are different. The reason for this is because of the fact that the situation in which the A and n values are valid are different in the literature.

8.2.3 THE ENERGY CHARACTERISTICS

To find the total g-value of the glazing used in the experiments including the Venetian blind the optical property in case of the solar direct transmittance τ_e for the system is needed. This is found as the solar direct transmittance of the glazing without solar shading multiplied with the solar shading factor given in table 8.2. The solar direct transmittance of the glazing is calculated in annex 2.1 on DVD for *Standard* and in annex 2.2 on DVD for *Experiment*. The ones for different literatures are equal to the ones from *Standard* as the only difference is the external heat transfer coefficient which only affects he secondary heat transfer factor q_i.

Standard is calculated with use of the standardized relative spectral distribution while *Experiment* is calculated with the experimental relative spectral distribution given in appendix H.

The solar direct transmittance for the glazing system was through calculations found to the values shown in table 8.4 at an radiation angle of 0° as a function of the slat angle. Those will later on be compared to the measured solar direct transmittances.

	τ_e [−]					
ϕ [°]	0	15	30	45	60	70
Standard	0,55	0,40	0,26	0,14	0,038	0,022
Experiment	0,30	0,22	0,14	0,078	0,021	0,012

Table 8.4: *τ_e in case of a radiation angle of 0° and as a function of the slat angle, comparable with experiments.*

Due to different relative spectral distributions τ_e for *Standard* is diverging from *Experiment*.

The secondary heat transfer factor of the glazing towards the inside q_i is calculated in annex 2.1 on DVD for *Standard* and in annex 2.2 on DVD for *Experiment*. For the total glazing system including solar shading q_i is not calculated in this report. This is because no measurements are performed for q_i and due to no measurements to compare with no theoretical model is made.

The g-value was through calculations found to the values shown in table 8.5 for the total glazing system, where a change in q_i due to changing slat angles not is taken into account. If q_i was taken into account, the shading would be less effective, meaning that the g-value would be slightly higher. The different literature is calculating with use of the standardized relative spectral distribution. The calculations with use of various literature are made because of different external heat transfer coefficients as functions of the varying constant A and exponent n. The g-values for the glazing without Venetian blinds are calculated in annex 2.1 on DVD for *Standard* and literatures. For *Experiment* the calculations are found in annex 2.2 on DVD. Those values are multiplied with the shading factors found in table 8.2 for the slat angles used in the experiments to obtain the g-values of the total glazing system including the Venetian blind.

g-value [−]						
ϕ [°]	0	15	30	45	60	70
Standard	0,61	0,45	0,29	0,16	0,043	0,024
Danvak	0,63	0,47	0,30	0,16	0,044	0,025
Glent	0,63	0,47	0,30	0,16	0,044	0,025
DS/EN 673	0,63	0,47	0,30	0,16	0,044	0,025
Experiment	0,36	0,27	0,17	0,093	0,025	0,014

Table 8.5: *Calculations of the g-value according to standardized and experimental relative spectral distribution and different literatures.*

It is seen from the table above that the g-values found from standards differs from the remaining literature with approximately 0 - 4 %. This is due to the different external heat transfer coefficients used in the calculations. For the different literature the external heat transfer coefficients are close to each other which gives similar results as seen in table 8.5. For the calculation with use of *Standard* a higher external heat transfer coefficient is used than for the different literature and this results in a lower but similar g-value than for the literature. The g-value is in case of an experiment relative spectral distribution diverging from the standard value due to the different relative spectral distribution.

The U-value is variable dependent on the slat angle and the value is in between the U-value for the glazing of 1,1 $^{W}/_{m^2K}$ and the U-value for the glazing including a curtain described in chapter 7.4 and 9.2 respectively. This is because it is assumed that the U-value for the glazing corresponds to the U-value of the window including a Venetian blind with a slat angle of 0°, fully open, and that the U-value for the glazing including a curtain corresponds to the U-value of the glazing including a Venetian blind with a slat angle of 90°, fully closed. The U-value is not given for different slat angles in this report due to no investigations of this through the experiments.

CHAPTER 9

WINDOW WITH A CURTAIN

For comparison reasons a more simple form of shading is analysed. The same window as dealt with in chapter 7 is considered as including solar shading in case of a curtain. The results obtained from this study will be compared with the results obtained in chapter 7 and 8.

9.1 ENERGY CHARACTERISTICS OF THE GLAZING SYSTEM

A similar approach as presented in section 7.1 is used to account for the curtain by considering the glazing system as a three-layer system instead of only two layers. This is possible as the curtain can be considered as being homogeneous, while a shading type like Venetian blinds is non-homogeneous [Ferro and Maccari] and would result in a greater error with use of the same method. The spreadsheet used for the calculations given in annex 7 on DVD, calculates the U- and g-value based on the amount of layers in the glazing system and the properties of these layers. In chapter 7 two layers of glazing were used. In order to account for the curtain a third layer is added with optical properties corresponding to the solar shading type but using the same principle as for the glazing system without solar shading. Different from the previous calculations without solar shading, the external heat transfer coefficient may be influenced by the exterior solar shading as was the case for Venetian blinds in chapter 8. The new exterior heat transfer coefficient is calculated in a similar way as in section 8.1.3. This is also seen in annex 6 on DVD.

The U-value and g-value is calculated as shown in appendix A and B, where the g-value is calculated from the equations valid for three layers of glazing.

9.1.1 OPTICAL PROPERTIES OF THE CURTAIN

In lack of information on solar optical properties for a curtain, values have been approximated. These are shown in table 9.1.

Transmittance	0,3
Reflectance	0,5
Absorptance	0,2

Table 9.1: *Estimated solar optical properties for the curtain.*

Unlike the properties of the glazings, these properties are assumed to be independent of the wavelength leaving the transmittance and front and back reflectance of the curtain as shown in figure 9.1.

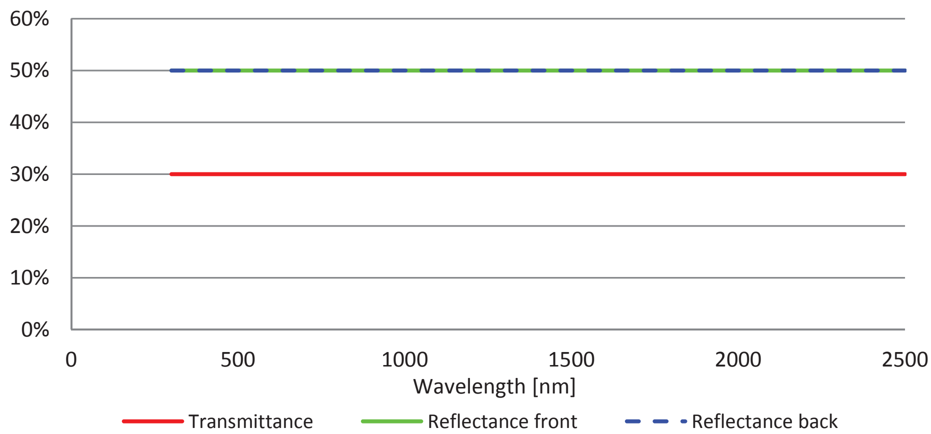

Figure 9.1: *Optical properties of the curtain as a function of wavelength.*

9.1.2 SHADING FACTOR OF THE CURTAIN

The shading factor of the curtain is found through values of the energy passing through the curtain and window, compared to the amount of energy passing through the window without the curtain. This is done through equation 9.1.

$$s_f = \frac{E_{shading}}{E_{no-shading}} \tag{9.1}$$

$E_{no-shading}$ is described in chapter 7 and is calculated in annex 2.1 on DVD. $E_{shading}$ is calculated in annex 7 on DVD.

9.2 RESULTS OF THE WINDOW WITH A CURTAIN

The addition of the curtain changes the energy characteristics of the glazing system due to the fact that the exterior heat transfer coefficient will be different from the usual, along with a change in radiation reaching the window, due to the solar shading factor of the curtain. These parameters are addressed in the following sections.

9.2.1 SHADING FACTOR

The results of the shading factor of the curtain is given in table 9.2 with use of a standardized relative spectral distribution and external heat transfer coefficient. This is found from the amount of energy passing through the curtain and window of 22 % and the amount of energy passing through the glazing without the curtain of 61 %.

s_f [−]	0,36

Table 9.2: *Shading factor of the curtain.*

As seen from table 9.2 the shading factor of the curtain is just above the solar direct transmittance of the curtain. This is to be expected due to the fact that the g-value equals the sum of the solar direct transmittance and the secondary heat transfer factor of the glazing towards the inside. It also depends on the reflectances that occur in between the layers of the system.

9.2.2 EXTERNAL HEAT TRANSFER COEFFICIENT

For comparative reasons, the heat transfer coefficient when considering a curtain is calculated with adjusted boundary conditions based on the measured data from the experiments. I.e. the temperatures of both the cavity and the surfaces are approximated based on the tendency of the measured temperatures as the slat angle increased so that the values would correspond to a Venetian blind layer with a slat angle of 90 ° even though this would not be the case. These are given in appendix H. The calculations are the same as for the Venetian blind and the external heat transfer coefficients are calculated with values based on different literature, the same as presented in table 8.1. The results are shown in table 9.3.

Danvak	4,23
Glent	4,23
DS/EN 673	3,46

Table 9.3: *The exterior heat transfer coefficient, on the outside of the pane, calculated with different constants and exponents according to the literature. [Stampe et al., 2006] [Stampe, 1982] [Standard, 2011c]*

9.2.3 THE ENERGY CHARACTERISTICS

The energy characteristics in case of the U-value and g-value of the glazing including curtain, was through calculation found to the values shown in table 9.4 with use of standardised boundary conditions. The same values were calculated with use of various literatures because of different external heat transfer coefficients. These are also shown in table 9.4. The energy characteristics are calculated in annex 7 on DVD and the boundary conditions are described in appendix H.

	U-value $[\mathrm{W}/\mathrm{m^2K}]$	g-value $[-]$
Standard	0,91	0,22
Danvak	0,77	0,26
Glent	0,77	0,26
DS/EN 673	0,74	0,27

Table 9.4: *Calculations of the U-value and the g-value according to standardized boundary conditions and different literatures.*

It is seen from the table above that the energy characteristics found from standards differs from the remaining with approximately 15 %. This is due to the different external heat transfer coefficients used in the calculations. For the different literature the external heat transfer coefficients are close to each other which gives similar results as seen in table 9.4. For the calculation with use of the standard a higher external heat transfer coefficient is used than for the different literature and this results in a higher U-value and a lower g-value than for the literature.

Part 3

Experiments

- Experimental literature survey
- Description of the conducted experiments
- Results of the conducted experiments

CHAPTER 10

EXPERIMENTAL LITERATURE SURVEY

This chapter contains a literature study of two papers. The first experiment was performed with a test cell placed inside a controlled guarded zone and the second experiment were performed with use of a guarded heater plate. The first method is from [Loutzenhiser et al., 2007] and [Manz et al., 2005] while the second method presented is from [Huang et al., 2006]. The experimental literature survey is made to obtain information about other similar experiments than the ones from this report.

10.1 EMPIRICAL VALIDATION OF SOLAR GAIN MODELS FOR A GLAZING UNIT WITH EXTERIOR AND INTERIOR BLIND ASSEMBLIES [LOUTZENHISER ET AL., 2007]

This section also uses information from the Building and Environment journal from ELSEVIER: *Series of experiments for empirical validation of solar gain modelling in building energy simulation codes - Experimental setup, test cell characterization, specifications and uncertainty analysis* [Manz et al., 2005].

Modern office buildings are often designed with much glazing in the facades, to link the occupants to the environment and to let daylight into the working zones. Blinds are one of the popular shading devices to use in this type of building. Venetian blinds are used to prevent glare and in periods with cooling loads decrease solar gains while in the same time being able to let diffuse light into the room. During periods in need of heating the Venetian blinds can be withdrawn to allow full solar transmittance of the glazing system. When the blinds are installed outside, less heat is transmitted to the inside than if the blinds were located inside. In this literature the effect of external Venetian blinds has been investigated through experiments. This is described in the following.

10.1.1 KNOWN PARAMETERS

In this study, experiments were performed for empirical validation of two building energy simulation programs; EnergyPlus and HELIOS described in appendix C. The focus in this study was on the required cooling power needed to keep a constant temperature in the test cell, i.e. controlling the amount of applied energy by removing the same amount of energy through cooling. By doing so, the total energy transmittance g-value can be determined. To make as few sources of errors as possible the test cell was placed inside a guarded zone. Only the experiments performed with exterior Venetian blinds are commented in this section. Two experiments were made in this study; one with the blind slats in a horizontal position and one with the blind slats tilted 45° downward. The experiments were made for two 20-day periods from July 24 to August 12 2005 and from August 17 to September 5 2005.

The experiments were made in such a way that the interior of the test cell was facing a temperature controlled guarded zone, for better control and thereby better definition of the boundary conditions. The experimental setup was located outdoor in Switzerland. The location is given in table 10.1.

Longitude	8,6° E
Latitude	47,4° N
Orientation of window in external wall	29° West of South

Table 10.1: *Location of the experimental setup.*

A picture of the experimental setup seen from the outside with external Venetian blinds is shown in figure 10.1.

Figure 10.1: *The experimental setup seen from the outside. [Loutzenhiser et al., 2007]*

- The floor, ceiling, north wall, east wall and west wall of the test cell were made of sheet steel insulated with about 140 mm of PU foam.
- All the external walls were made of wood insulated with about 130 mm of glass wool or polystyrene.

- Five surfaces of the test cell were facing the guarded zone.
- Both the test cell and the guarded zone have their own air conditioning unit.
- To control the temperature in the test cell, an air-water heat exchanger was used.

An illustration of the test cell, the guarded zone and the ventilation system is seen in figure 10.2. The figure is also showing an optional external chamber for controlling the outdoor temperature.

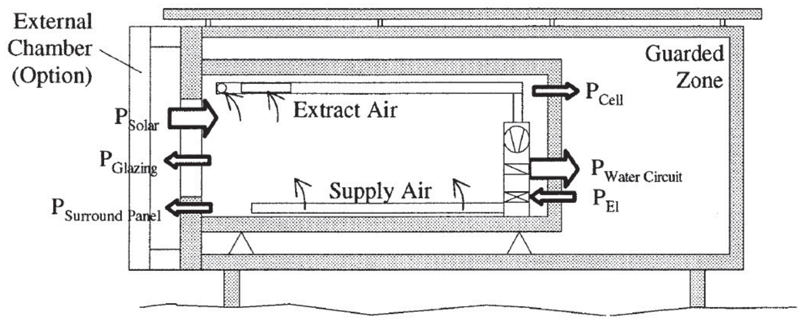

Figure 10.2: *The concept of the experimental setup in this study. [Manz et al., 2005]*

10.1.2 INVESTIGATIONS

Through the experiment different parameters were investigated. Some of the measured parameters are listed underneath:

1. Air temperatures inside the test cell
2. Experiments without solar gains to identify the magnitude of the thermal bridge losses
3. The air tightness of the test cell
4. Wavelength dependent reflectances at near-normal incident angles from 250 to 2500 nm with the use of Venetian blinds. By the study from [Loutzenhiser et al., 2007], the solar reflectance was computed according to [Standard, 2011b]
5. Emittance of the blind slats

A parameter which can be of great importance in this experiment and can lead to a huge source of error is thermal bridge losses as mentioned above, because test cells are smaller than real buildings. Therefore it is important to investigate the locations of those thermal bridges and seal them as much as possible.

To avoid a few other sources of errors the following initiatives were made in the study:

1. To reduce temperature stratification in the test cell and obtain a uniform air temperature distribution, conditioned air were entering the test cell through two large textile ducts on the floor at low speed and was extracted from the test cell through metal ducts hanging just below the ceiling
2. To control heat gains and losses the guarded zone had the same temperature as the test cell

10.1.3 OUTPUT PARAMETERS

As the focus in this study was on the required cooling power needed to have a constant temperature in the test cell, the maximum, minimum and mean absolute difference in cooling power between the experiment and the calculations were plotted for every given hour in case of horizontally positioned blind slats and blind slats tilted 45° downward respectively. Each day was divided into hours and an average of that hour of every 20 days of the experiment represented the average cooling power. An average of 95 % of the measured results were in the case seen as a credible limit for the experiment. The plots for horizontally positioned blind slats are shown in figures 10.3 and 10.4 while plots for blind slats tilted 45° downward are shown in figures 10.5 and 10.6.

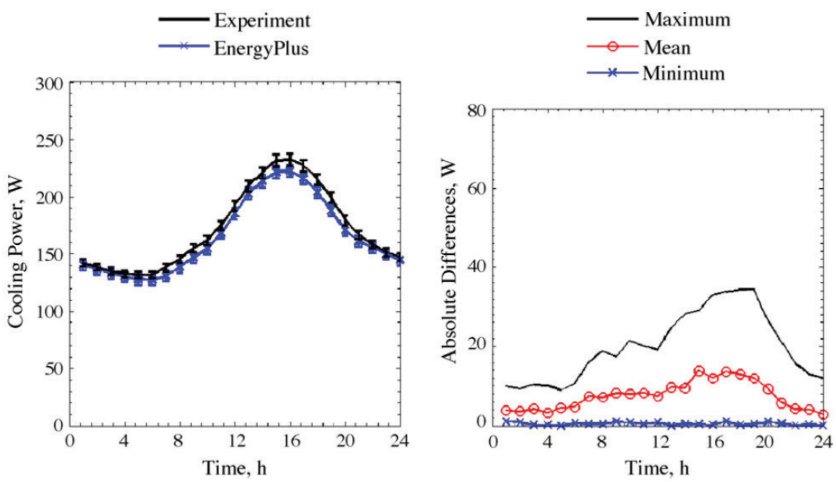

Figure 10.3: *Left: Comparison of cooling power. Right: Absolute maximum, mean and minimum difference of cooling power. In both cases with exterior Venetian blinds with slats in a horizontal position. [Loutzenhiser et al., 2007]*

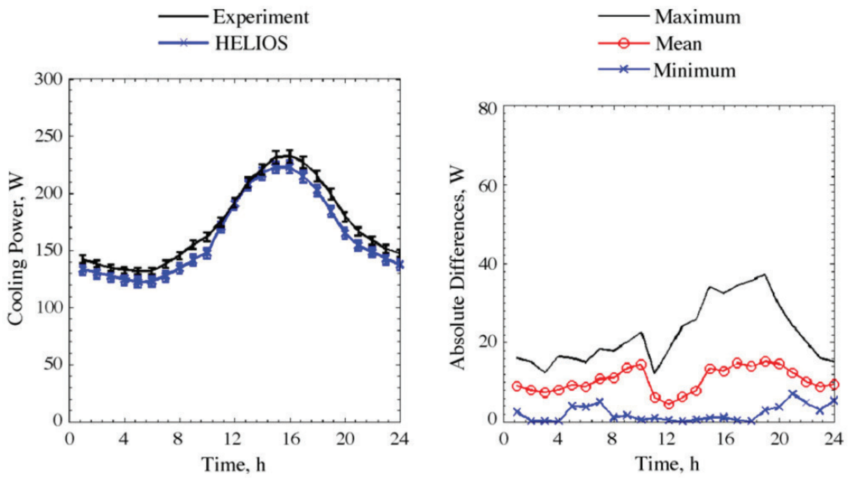

Figure 10.4: *Left: Comparison of cooling power. Right: Absolute maximum, mean and minimum difference of cooling power. In both cases with exterior Venetian blinds with slats in a horizontal position. [Loutzenhiser et al., 2007]*

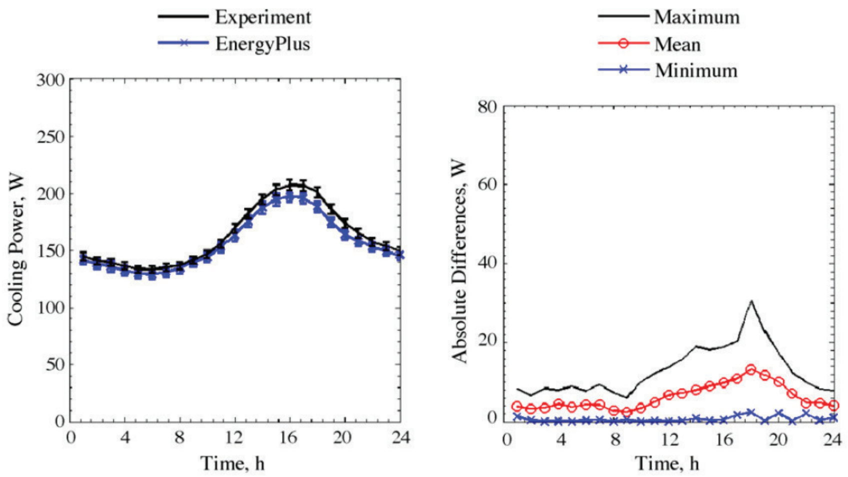

Figure 10.5: *Left: Comparison of cooling power. Right: Absolute maximum, mean and minimum difference of cooling power. In both cases with exterior Venetian blinds with slats tilted 45° downward. [Loutzenhiser et al., 2007]*

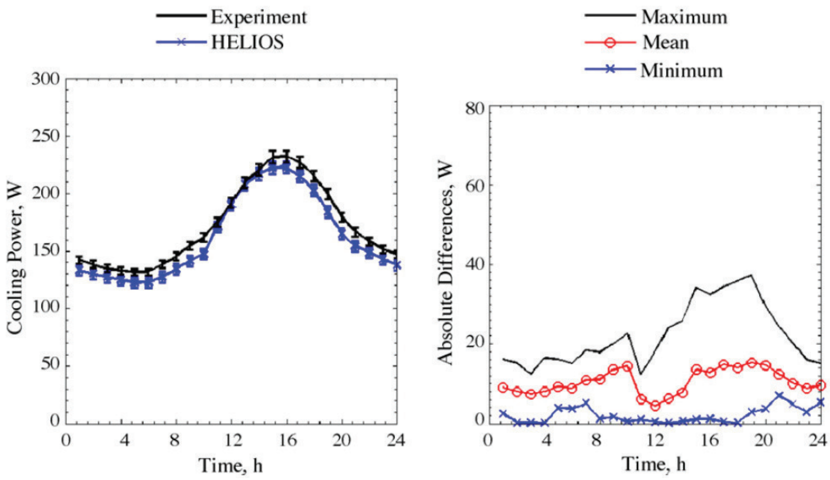

Figure 10.6: *Left: Comparison of cooling power. Right: Absolute maximum, mean and minimum difference of cooling power. In both cases with exterior Venetian blinds with slats tilted 45° downward. [Loutzenhiser et al., 2007]*

The figures above shows a difference between the experiment and simulations made in EnergyPlus and HELIOS. This means that the calculation methods should be re-evaluated to make it possible to calculate values closer to the measurements than this show. By comparing e.g. figure 10.3 with 10.5 it is clear that and increase in slat angle from 0° to 45° results in a decrease in cooling power, i.e. by increasing the slat angle the g-value of the glazing system decreases.

The temperature stratification of the air in the test cell was smaller than 0,5 K in the experiment of this study. Regarding thermal bridge losses they are in this study of modest influence since the temperature difference between the test cell and the guarded zone is small, which leads to a small heat conductance in the walls of steel. The air tightness of the test cell was measured during a blower door test at a pressure of of 50 Pa in the test cell. This gave an air exchange of 0,2 h^{-1}, which gives an air tightness assumed to be negligible in this study.

The study has also shown results about incident solar radiant flux. The solar reflectance was measured to be 44,1 ± 1,0 % and the emittance was measured to be 86,2 ± 4,3 % of the Venetian blind slats. With horizontally positioned Venetian blind slats it was possible for the beam radiation to enter directly through the glazing and into the test cell when the sun had a position which gave a incident angle smaller than 33°. This would only happen the last two hours before sunset. When the blind slats were tilted 45° downward there was no solar beam radiation transmitted into the test cell.

10.2 THERMAL RESISTANCE OF A WINDOW WITH AN ENCLOSED VENETIAN BLIND: GUARDED HEATER PLATE MEASUREMENTS [HUANG ET AL., 2006]

A window and its area, orientation, etc. affect solar gain and heat losses of buildings. Solar gain has a magnitude and a variability which makes it important. To control solar gain, shading as e.g. Venetian blinds is used. One-dimensional models to accurately predict the thermal performance of windows are already developed. The development of models for windows with solar shading is at a very early stage.

10.2.1 KNOWN PARAMETERS

In this study it was tried to develop a model for a double-glazed window with a Venetian blind installed in the glazing cavity. The Venetian blind were positioned as a vertical layer while the blind slats of the Venetian blind were positioned horizontal. This is illustrated in figure 10.7, where q" is the heat flux driven by the temperature difference across the glazing system with the enclosed Venetian blind. The other parameters mentioned in figure 10.7 is slat width w, distance between the slats s, slat angle ϕ, slat curvature r_c, and pane spacing L.

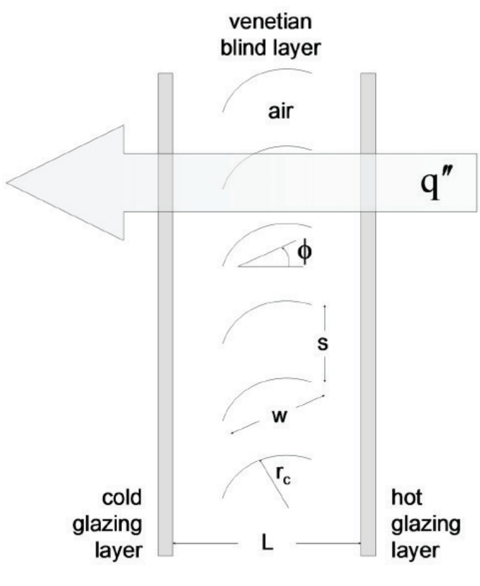

Figure 10.7: *Double-glazed window with venetian blind installed in the glass cavity. [Huang et al., 2006]*

The heat flux was investigated with the use of a guarded heater plate, GHP, apparatus. A GHP apparatus consist of two isothermal plates with the test sample placed in between, which is seen in figure 10.8. The heat flux can then be measured through the test sample. In this study the GHP apparatus measure centre-glass heat transfer rates through the double-glazed window with the enclosed Venetian blind.

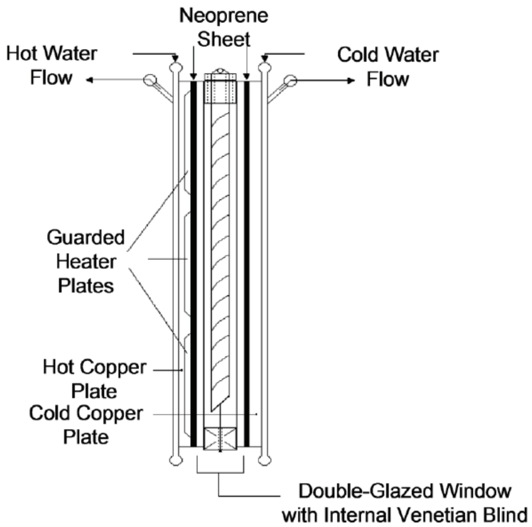

Figure 10.8: *The GHP apparatus with the test sample placed in between. [Huang et al., 2006]*

Test samples were made with different variables. Those are three different pane spacings, L, two different types of glass and two different temperature differences between cold- and hot water, ΔT_{bath}. Those are listed in table 10.2.

Pane spacing L	**Glass type**	**Temperature difference** ΔT_{bath}
1. 17,78 mm	1. Clear/clear glass	1. 20 °C
2. 25,40 mm	2. Clear/low-e glass	2. 10 °C
3. 40,01 mm		

Table 10.2: *Variables in the test samples.*

For each pane spacing, test samples were made with both glass types and both temperature differences. The smallest pane spacing was used because it was around the smallest possible pane spacing because of the Venetian blind. The middle and the largest pane spacing were used because it could give information about the influence of pane spacing.

Two different types of glass were used. The first was a normal glass while the second was a glass with a low-energy coating. The two different types of glass had different emissivities. For the uncoated glass an emissivity of ϵ_{gl} = 0,84 were used. For the coated glass an emissivity of ϵ_{le} = 0,164 was used.

The two different temperature differences between cold- and hot water, ΔT_{bath}, used in this study, appeared with a constant temperature of the hot water of 30 °C in both cases. The temperature of the cold water was set to 20 °C in case of ΔT_{bath} = 10 °C and 10 °C in case of ΔT_{bath} = 20 °C.

Regarding the Venetian blinds the same one were used in each test sample. The blind slats were made of painted aluminium. They had the following characteristics. A slat width, w, of 14,79 mm, a distance between the slats, s, of 11,84 mm and a ratio $\frac{r_c}{w}$ of 2,0. The thickness of the slats were 0,2 mm including the paint. For the painted blind slats an emissivity of ϵ_{slat} = 0,792 were used. In the experiment, the slat angle were adjusted between -75 ° and 75 °.

The edge of the test samples was insulated to avoid influence from the environment.

10.2.2 INVESTIGATIONS

Through measurements the thermal conductance of the glazing was found. As this study deals with the determination of the U-value, heat transfer coefficients, in case of the internal h_i and the external h_e was applied. These were fixed at values of 8 $^{W}/_{m^2K}$ and 23 $^{W}/_{m^2K}$ respectively.

10.2.3 OUTPUT PARAMETERS

Some of the measurements from this study were compared to measurements from another literature by [Garnet, 1999]. In the comparison the centre-glass U-value, U_{cg}, were shown as a function of the slat angle in case of a pane spacing of 17,78 mm and 25,4 mm respectively and with a ΔT_{bath} of 20 °C. There is only used normal clear/clear glass. The comparison is shown in figure 10.9.

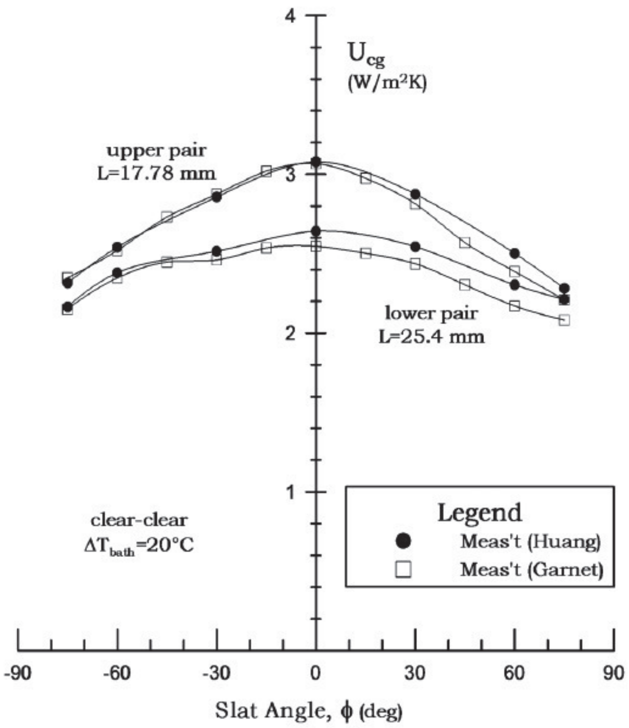

Figure 10.9: *Comparison of centre-glass U-value measurements from this study and Garnet. [Huang et al., 2006]*

With a negative slat angle the two different measurements matched within 2,5 % and with a positive slat angle the difference was as high as 8 %. A positive slat angle was obtained when the tip of the blind slat next to the hot glazing had a higher position than the tip of the blind slat next to the cold glazing.

All the measured centre-glass U-values from this study are shown in figure 10.10 as a function of the slat angle. In the figure the results are shown for the three different pane spacings, L, the two different types of glass and the two different temperature differences between cold- and hot water, ΔT_{bath}, which are listed in table 10.2.

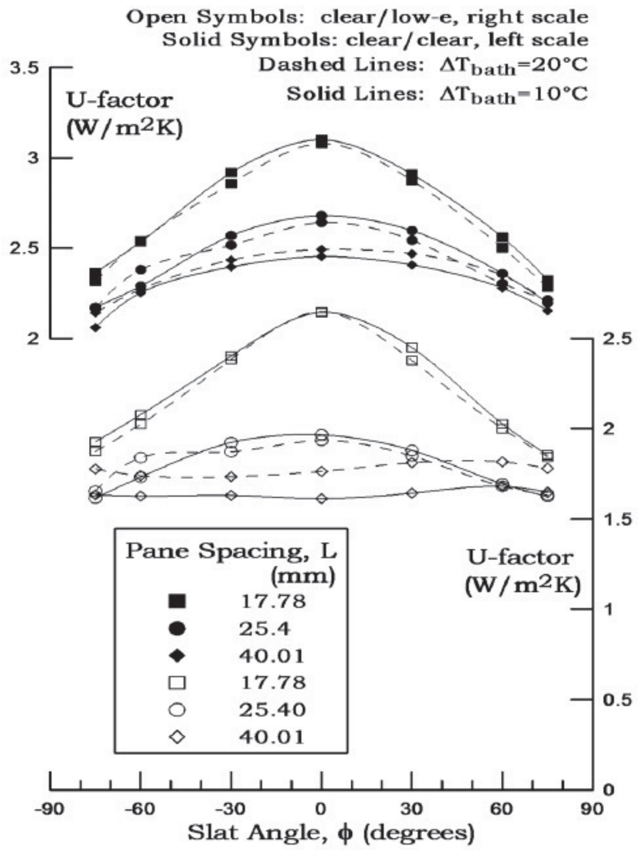

Figure 10.10: *Measured centre-glass U-values as a function of slat angle. [Huang et al., 2006]*

In figure 10.10 it is seen that the centre-glass U-value had a maximum when the blind slats were fully open, except the case with a clear/low-e glass and a pane spacing of 40,01 mm. The centre-glass U-value was seen to decrease as the blind slats closed no matter if it was a positive or a negative slat angle and the direction of the slat angle did not have a huge effect on the U-value. The bell-shaped curvature of the centre-glass U-value as a function of the slat angle occurred because the blind slats blocked the longwave radiation and thereby reduced the radiant exchange. The slat angle does also have influence on the convective heat transfer as a variation of the slat angle will cause a changed movement of the gas.

The low-energy, with low emissivity, resulted in a drop in the centre-glass U-value in all cases and is thereby a glass with a better insulating ability than the clear/clear glass.

In all cases but one, the temperature difference between cold- and hot water, ΔT_{bath}, did not have a significant influence on the U-value as a function of the slat angle.

Analysis of the width of the pane spacing showed that the centre-glass U-value decreases with increasing pane spacing length.

The results given from this study can be used as a guidance in the development of U-value and solar gain models for this type of glazing and solar shading.

CHAPTER 11

DESCRIPTION OF THE CONDUCTED EXPERIMENTS

Experiments was conducted in a laboratory under controlled conditions in order to collect data for comparison of the theoretical models used within this project. A description of the experimental setup and the conducted experiments is given in the following chapter, where the setup and a list of the experiments are followed by the description.

11.1 EXPERIMENTAL SETUP

The original idea of the experiments were to determine the g-value of the glazing system including Venetian blinds, but in lack of a hot box this was not possible. This limited the output of the experiment to the solar direct transmittance since the g-value also consists of the energy being absorbed in the inner glazing layer.

The experiments were carried out in the climate laboratory L148 at Aalborg University. The setup is shown in figure 11.1, where the main components are the window, the Venetian blind, the artificial sun and the measuring equipment.

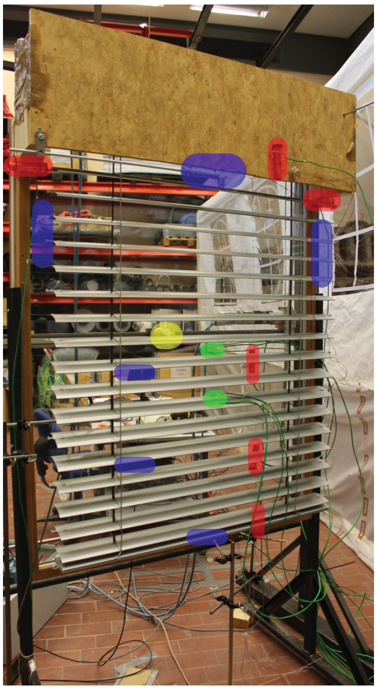

Figure 11.1: *Experimental setup with main components highlighted; Anemometers, Thermocouples, Shielded thermocouples, Pyranometer/Light meter.*

The equipment used throughout the experiments consists of:

- Artificial sun made of 56 300W OSRAM Ultra-Vitalux light bulbs
- Window containing one outer layer of 4 mm Pilkington Optifloat and one inner layer of 4 mm Pilkington Optitherm S3
- Venetian blind from Climatic
- Precision Pyranometer type CM 21 + a robot for movement of the pyranometer
- Gossen Panlux electronic 2 light meter
- Fluke 289 True RMS Multimeter
- Grant SQ1600 Data Logger for thermocouples and pyranometer
- National Instruments DAQCard-700 Data Logger for velocity transducers
- 6x Dantec 54R10 low velocity transducer
- 6x Shielded Type-K Thermocouples

- 7x Type-K Thermocouples

Both the window and the Venetian blind are described in chapters 3 and 4 respectively. In the following the artificial sun is described while the remaining measuring equipment and their calibration is briefly addressed in appendix I.

As artificial sun, a total of 56 OSRAM Ultra-Vitalux light bulbs have been used, each of 300 Watt resulting in a total of 16.800 Watts. The radiation from the artificial sun was measured by a pyranometer in order to get the exact radiation. The light bulbs are located with 20 cm in between each other, so the distribution of the radiation is as uniform as possible, this have been checked by experiments and the result showed to be acceptable [Johra, 2012]. The artificial sun is located in such a way that the radiation towards the window will have an incident angle of 0°, i.e. perpendicular to the window. A picture of the artificial sun is shown in figure 11.2.

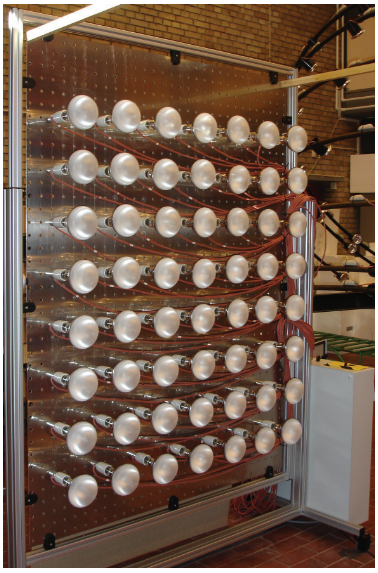

Figure 11.2: *Picture of the artificial sun.*

In order to be able to compare calculated results with measurements, it is necessary to use the correct spectral distribution of the radiation for the calculations. Even though the radiation from the OSRAM Ultra-Vitalux light bulbs are meant to reproduce the actual radiation from the sun itself [OSRAM, 2012], this is not entirely the case. This can be seen by comparing the light bulbs relative spectral distribution of radiation with the distribution of the suns radiation. This is shown in figure 11.3.

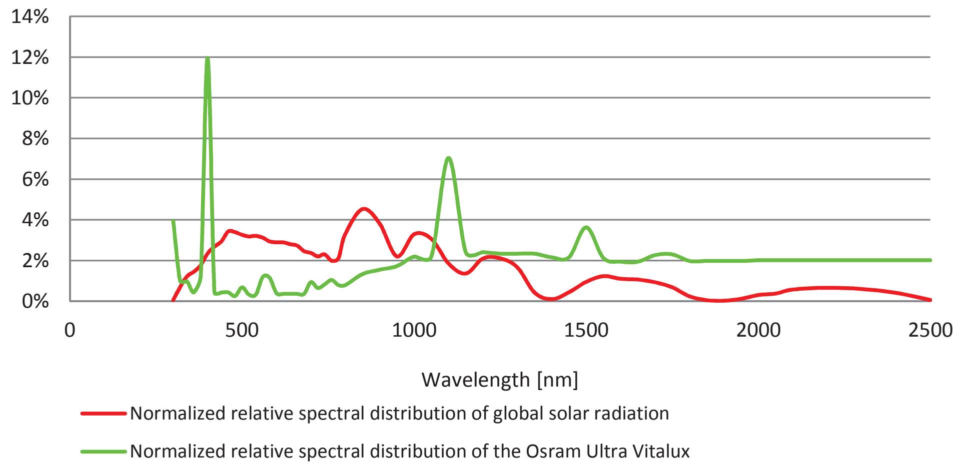

Figure 11.3: *Normalized relative spectral distributions.*

11.2 CONDUCTED EXPERIMENTS

Before doing the actual measurements, one preliminary experiment was conducted in order to determine a suitable location for doing future measurements. After the preliminary experiment was carried out, the goal of the following experiments was to gather information for determination of the following parameters, which enables the calculation of the energy characteristics of the glazing system:

1. the solar direct transmittance which is a part of the g-value of the glazing system and the solar shading factor
2. the exterior heat transfer coefficients, with and without the Venetian blind

As an extra small experiment, the shading factor was compared with the light transmittance of the glazing system with and without Venetian blinds, in order to see the shadings effect on solar direct transmittance and LT-value.

The parameters given above are measured at the same time through one experiment, but for simplicity reasons and to create an easier overview, they are described as three different experiments. The description of these are given in the following sections, while plans of the conducted experiments are given in appendix J.

As an addition to the above experiments, velocity profiles were measured in the cavity between the Venetian blind and window in order to gather information about the flow. This is used to determine whether the flow can be considered as free or forced convection, used in section 8.1.3.2. The velocity profiles are shown in appendix G.3.

11.2.1 PRELIMINARY EXPERIMENT

The goal of the preliminary experiment is to determine a good location for doing the measurements of the solar radiation. This is investigated through measurements of the distribution of the radiation as a function of distance from the artificial sun. Likewise the distribution in this distance is measured in a grid to see whether the 2D distribution is uniform or not. The idea of the preliminary experiment is sketched in figure 11.4, where the sun is seen to the left and the red dots indicates measuring points.

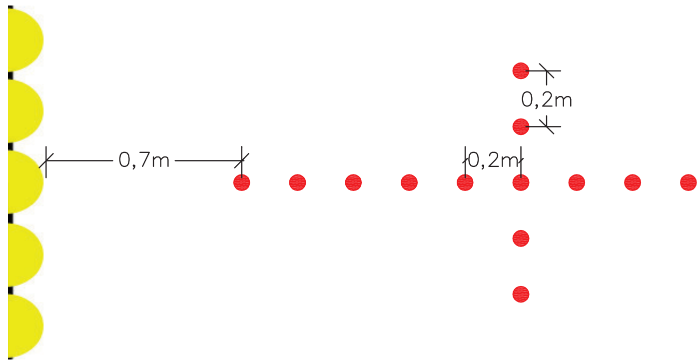

Figure 11.4: *Sketch of the preliminary experiment. Red dots are measuring points with 0,2* m *in between each.*

In case of the location with 5 red dots at one distance, this indicates a grid of 5 x 5 measuring points.

The preliminary experiment is also used later for determination of the incident radiation on the window.

11.2.2 1. TRANSMITTANCE AND SOLAR SHADING FACTOR

The purpose of this experiment is to determine the transmittance of the glazing system. Firstly for the glazing without any shading, secondly for the glazing system including external Venetian blinds, for determination of the solar shading factor of the Venetian blind. The solar direct transmittance will be measured for the following slat angles; 0°, 15°, 30°, 45°, 60°, 70°.
As the transmittance is measured at the different slat angles the shading coefficient of the Venetian blind can be determined by comparison of the transmittance with and without the Venetian blind applied.
The one part of the g-value, the solar direct transmittance, is measured with use of a pyranometer automated through a robot for movement in predefined measuring points.

The principle of the experiments are shown in figure 11.5.

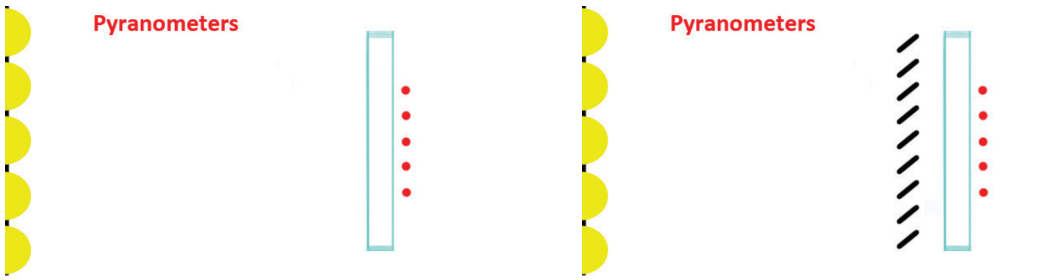

Figure 11.5: *Sketches of the first experiment without and with the Venetian blind. Red dots indicate measuring points.*

Figure 11.6 shows a close-up of the measuring points, which consists of 14 vertically aligned points.

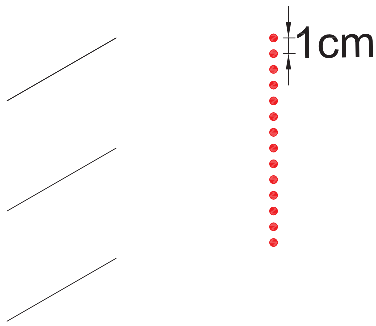

Figure 11.6: *Red dots are measuring points with 1* cm *in between each.*

The reason for doing 14 measurements on a vertical line was to get a good representation of the radiation behind the Venetian blinds and window, without having to weight the measured values based on an area which can be difficult to identify. The measurements are only located behind two sets of slat volumes and with very small distances in between each other because of the non homogeneity of the radiation found in the results of the preliminary experiment in chapter 12.1 and due to the fact that only centre values are of interest.

11.2.3 2. Determination of the exterior heat transfer coefficients

The purpose of this experiment is to gather information for calculation of the exterior heat transfer coefficient. For the outside this includes surface temperatures of the Venetian blind facing towards the window, the windows outer surface temperature and the air temperature in the cavity. The velocity of the air in between the Venetian blind and the window is determined by anemometers and used for determination of the convective heat transfer coefficient from slats to cavity, as described in section 11.2.3.1. The solar radiation on the window is found through the results of the preliminary experiment in section 12.1.

The principle of the experiment is shown in figure 11.7.

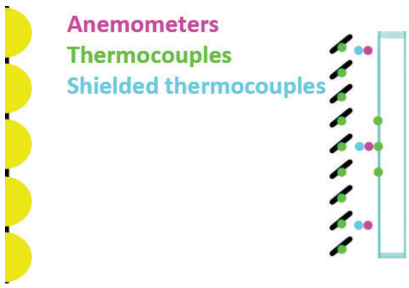

Figure 11.7: *Sketch of the second experiment with the Venetian blind.*

11.2.3.1 DETERMINATION OF THE AIR FLOW IN THE CAVITY

Velocity profiles in the cavity have been investigated in different heights for determination of the air flow in the cavity. Each velocity profile consists of measurements in 5 points as shown to the right in figure 11.8. This air flow is used for determination of the type of flow in the cavity as described in appendix G.3. The velocity profiles are measured in the following vertical distances from the bottom of the window and shading: 25 cm, 50 cm, 75 cm and 100 cm. This was done to get a good representation of the air flow. In the height of 50 cm the horizontal measurements were also made to see whether the velocity is constant over the width of the glazing system. The locations for doing measurements are illustrated to the left in figure 11.8, while a picture of the 5 anemometers used in each of these locations are shown to the right in the same figure.

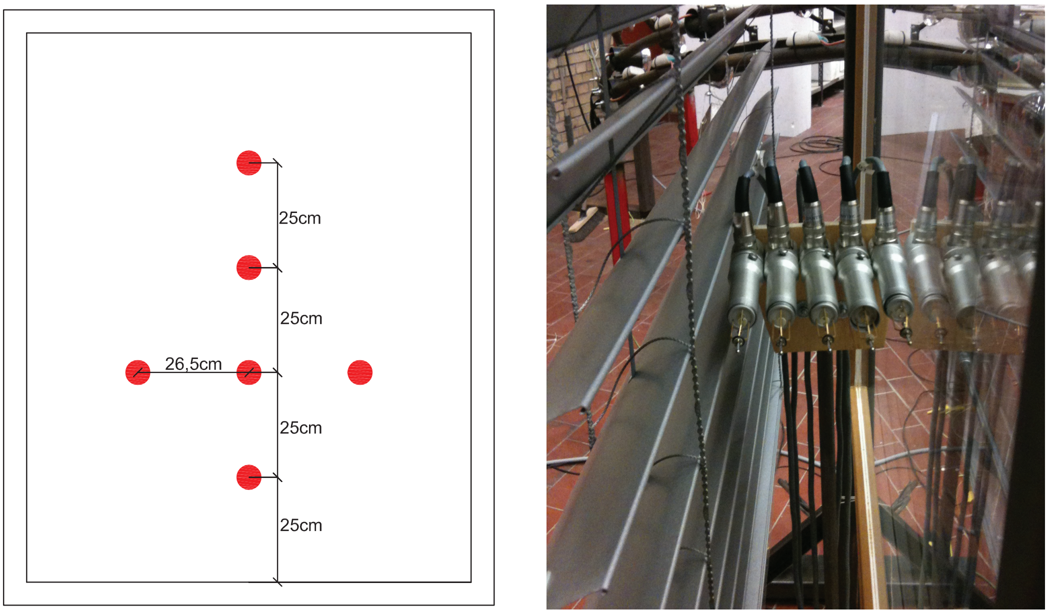

Figure 11.8: *Left: Illustration of the location of the measuring points seen from the front of the window. Right: The experimental setup for measuring the velocity profile in the cavity.*

11.2.4 3. Determination of the shadings effect on the solar direct transmittance and LT-value

Due to different wavelengths for heat and light the shading device is expected to have different effect on the solar direct transmittance and LT-value, and not for instance reduce both with 50 %. The solar direct transmittance is measured in experiment 1, while the LT-value is determined from a light meter in the same measuring points as the solar direct transmittance.

The principle of the experiments are shown in figure 11.9.

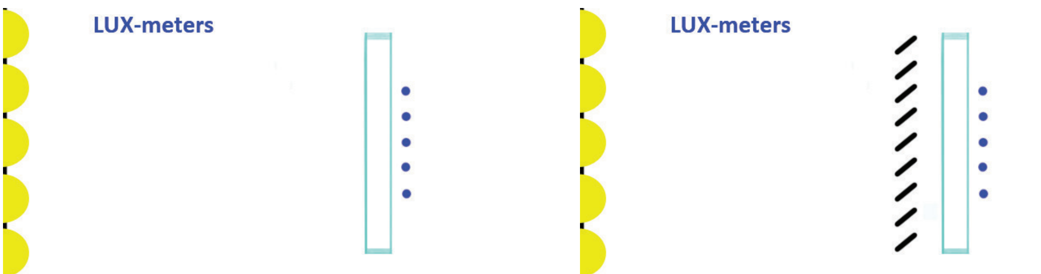

Figure 11.9: *Sketch of the third experiment without and with the Venetian blind.*

CHAPTER 12

RESULTS OF THE CONDUCTED EXPERIMENTS

In the following chapter, the results obtained from the experiments described in chapter 11 are presented. Problems which have arisen throughout the experiments and are worth mentioning are described in appendix K.

12.1 PRELIMINARY EXPERIMENT

As described in chapter 11 the goal of the preliminary experiments is to determine the radiation as a function of distance from the artificial sun through measurements and to get a picture of whether the radiation can be described as being homogenous or not. Based on these measurements an analysis is to show an ideal location for future measurements based on sufficient radiation and variation in the radiation in nearby measuring points. Furthermore, the results are used for the creation of a curve fit for determination of the radiation in the locations of the Venetian blinds and the window.

The results obtained from analysing the radiation from the artificial sun at different distances is shown in figure 12.1, where the black marks indicates measured radiations in the centre of the artificial sun while the red line connecting the measured data is a 4th degree polynomial trend line.

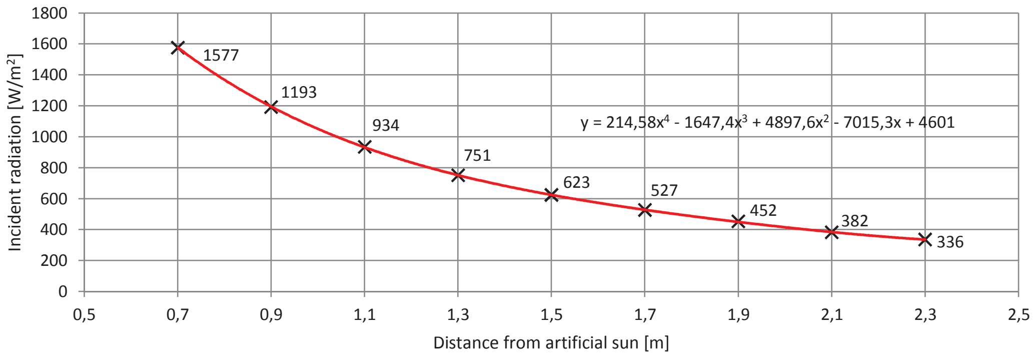

Figure 12.1: *Radiation from the artificial sun as a function of distance. The black marks indicate measured data while the red line is a trend line.*

The curve fit equation is also given in figure 12.1.

Based on the results shown in figure 12.1 the position in a distance of 1,7 m was chosen as location for future measurements, due to the small variation in radiation compared to the measured radiation in front of and behind that position.

As the position was determined to be in a distance of 1,7 m from the artificial sun the next task was to determine the homogeneity of the radiation in that location. This was done by measuring the radiation in 25 points through a 5 by 5 grid. During the experiments the measured radiation sometimes decreased or increased unreasonably. In the effort to find a reason for the uncontrolled variation in the measurements the incoming voltage to the artificial sun was controlled. The voltage was found to be more or less constant at around 227 V but at periods it could drop or increase in the interval of 222-231 V, which do not sound as much but had an obvious impact on the radiation. An example of this is shown in figure 12.2, where the voltage drops from around 229 V to 225 V. This induced a drop in the radiation of more than 5 %.

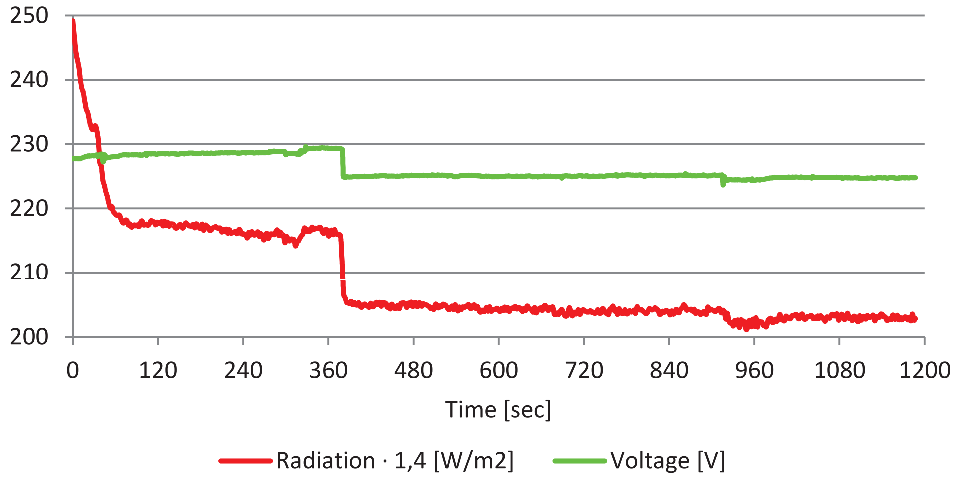

Figure 12.2: *Example of an uncontrolled drop in voltage to the artificial sun that causes an obvious decrease in measured radiation.*

The effect by averaging the results from periods with varying voltage around 227 V is looked up on in appendix K.6. It is concluded that the voltage is negligible as long as it is varying around the same voltage for all experiments.

Results of the homogeneity of the radiation from the artificial sun are illustrated in figure 12.3 as a 5 by 5 grid.

	1	2	3	4	5
1	472	496	502	496	479
2	508	522	521	524	513
3	514	526	540	536	527
4	518	537	535	530	510
5	496	514	532	509	493

Figure 12.3: *Measured averaged radiation levels in* $^{W}/_{m^2}$ *where all data are averaged.*

Looking at figure 12.3 it is seen that the radiation is not totally homogeneous but that the radiation is decreasing outwards with highest values in the centre and lowest values at the edges. Furthermore the radiation is seen to be a bit higher in the bottom of the grid than in the top. The reason for this may be that the artificial sun was tilting a bit downwards and hereby not perfectly vertical. The distribution of the radiation is important with the use of a hot box where the heat balance of the room is in focus, but as the experiments of this project was made without a hot box only the radiation near the centre of the glazing system is used. Because the radiation on the window is not homogeneous it is important to make the measurements in the same points.

The light intensity in case of LUX was measured along with the radiation. The LUX was measured from 2-3 times and based on the received data averaged. The results is seen in figure 12.4 as a 5 by 5 grid.

	1	2	3	4	5
1	27	28,5	29,5	28,5	27,5
2	29	30,5	31,5	31	29,833
3	30	31,5	32,25	32	30,75
4	30	31,75	32,5	31,5	30,5
5	28,5	30	30,25	30	28,75

Figure 12.4: *The mean measured light intensity in case of kLUX.*

As seen from figure 12.4 the measured magnitude and distribution of the LUX correspond well to figure 12.3 where the picture is much alike. Also in case of light measurements only the LUX near the centre of the glazing system is used.

12.2 1. Determination of the transmittance with and without the Venetian blind

The solar direct transmittance was measured for the glazing and the glazing including the Venetian blind. As described in chapter 11.2.2 the radiation was measured at a certain distance without window nor shading, in a total of 14 vertical point with a distance of 1 cm in between each points. The solar radiation in that certain distance was then thought of as the mean of those 14 measured values.

12.2.1 WINDOW

The radiation described above was used to find the solar direct transmittance for the glazing, by comparing the measured radiation without the window with measured radiative levels with the window in place. The measured radiation of the 14 points is given in figure 12.5, where it is seen that the radiation is constant over the 14 measuring points.

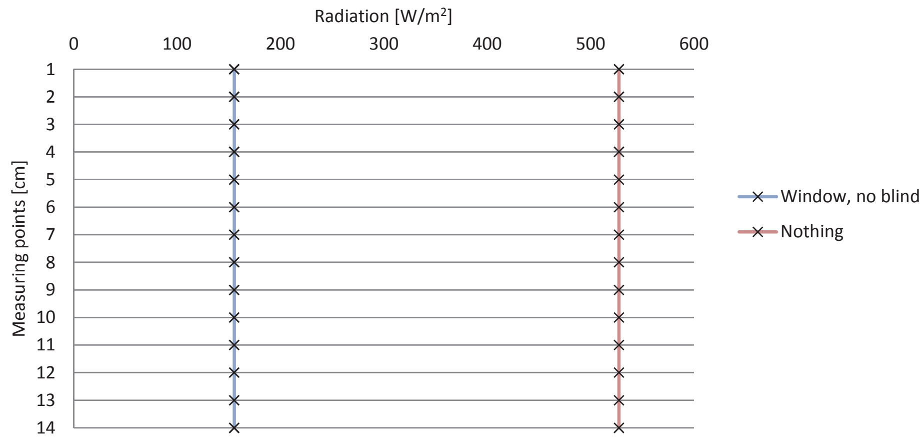

Figure 12.5: *Measured radiation at the measuring points with and without the window in place.*

This was done through the relation shown in equation 12.1.

$$\tau_e = \frac{\text{radiation including window}}{\text{radiation excluding window}} \tag{12.1}$$

By using the expression given in the above equation the results presented in table 12.1 was achieved.

Radiation without window $[{}^{W}/_{m^2}]$	Radiation with window $[{}^{W}/_{m^2}]$	τ_e [-]
527	155	0,294

Table 12.1: *Measured values of solar radiative levels with and without window, resulting in the solar direct transmittance of the window.*

12.2.2 WINDOW INCLUDING VENETIAN BLINDS

As described in chapter 11, the radiation was measured through 14 points on a vertical line. The results of these measurements are seen in figure 12.6.

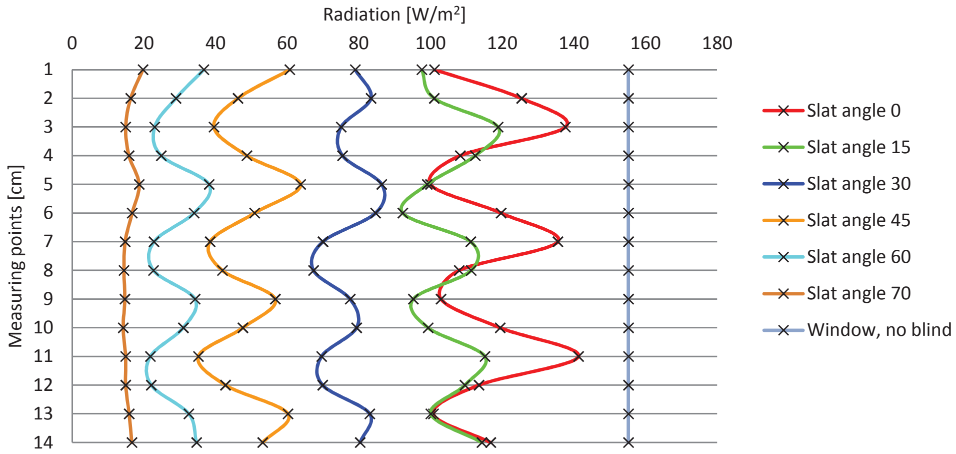

Figure 12.6: *Measured radiation of each measuring point at the various slat angles investigated. The measured radiation without slats is also illustrated.*

The solar radiation through the slats reaching the measuring points is illustrated in appendix L for the different slat angles from the experiments. From appendix L and figure 12.6 it is seen that the radiation on the window is lowest just behind slats and highest where the slats are not shading. The transmission in between the slats due to reflection from the slat surfaces is also having an effect on the measured radiation. Because of that the radiation is rising in points which are not directly irradiated.

The shading factor of the Venetian blind at the different slat angles is found through the expression given in equation 12.2 by averaging the measured radiative levels at each slat angle.

$$s_f = \frac{\text{radiation including window and Venetian blinds}}{\text{radiation including only window}} \tag{12.2}$$

Input to equation 12.2 is given in table 12.2. The input is average values of the measured radiation seen in figures 12.5 and 12.6.

Average radiation [W/m²]							
Window, with blind						Window, no blind	Nothing
ϕ [°]							
0	15	30	45	60	70		
116	105	77	49	29	16	155	528

Table 12.2: *Average values of the measured radiation without window, with and without shading.*

The shading factor for the Venetian blind and the solar direct transmittance of the glazing system including Venetian blinds are seen in table 12.3.

ϕ [°]	0	15	30	45	60	70
s_f [−]	0,75	0,68	0,50	0,32	0,19	0,10
τ_e [−]	0,22	0,2	0,147	0,094	0,056	0,0294

Table 12.3: *Measured solar shading factors of the Venetian blinds and the solar direct transmittance of the glazing system, at various slat angles and an incident angle of 0°.*

From those experiments it is seen that the Venetian blind is reducing the solar direct transmittance through the glazing system with 25 % compared to that glazing without shading at a slat angle and a incident angle of 0°. This means that the Venetian blind is shading when the incident radiation is parallel with the slats. Here it should be remembered that the slats used in the measurements are curved. The solar direct transmittance of the glazing system will be compared with theory in chapter 13.

12.3 2. Determination of the exterior heat transfer coefficients

When determining the exterior heat transfer coefficient for the outside glazing surface from measurements, an energy balance for the surface is outlined. This energy balance is given in equation 12.3 where the absorption of the glazing surface is considered. The calculation is seen in annex 8 on DVD.

$$\alpha_{glass} \cdot I_{sun,window} = \alpha_{c,3}\left(t_{glass} - t_{cavity}\right) + \alpha_r\left(t_{glass} - t_{slat}\right) + q_i \cdot I_{sun,window} \tag{12.3}$$

where:

$I_{sun,window}$	*Incident solar radiation on the glazing* $[^{W}/_{m^2}]$
t_{cavity}	*Air temperature of cavity between glazing and slats* [°C]
t_{glass}	*Surface temperature of the glazing* [°C]
t_{slat}	*Surface temperature of the slats* [°C]
q_i	*Secondary heat transfer factor of the glazing towards the inside* [−]
$\alpha_{c,3}$	*Heat transfer coefficient due to convection from the glazing to the cavity* $[^{W}/_{m^2K}]$
α_{glass}	*Absorptance of the glazing* [−]
α_r	*Heat transfer coefficient due to radiation from the glazing to the slats* $[^{W}/_{m^2K}]$

The temperatures found in the experiments are given in appendix H. The incident solar radiation, assumed to be uniformly distributed, on the glazing in case of no shading is found from figure 12.1 by curve fitting to be 584 $^{W}/_{m^2}$ as the outside of the window is in a distance of 1,58 m from the sun. This value is multiplied with the solar shading factors from table 12.3 to get the incident solar radiation on the glazing in case of different slat angles. Those values are shown in figure 12.4.

ϕ [°]	0	15	30	45	60	70
$I_{sun,window}$ $[^{W}/_{m^2}]$	438	397	292	187	111	58

Table 12.4: *Incident solar radiation on the glazing in case of different slat angles.*

The absorptance of the external glazing is found to be 0,22 and the secondary heat transfer factor of the glazing towards the inside is found to 0,06. They are calculated from the principle of equations B.12 and B.6 respectively in appendix B used in annex 2.2 on DVD. In section 7.2, the absorptance dependent on the radiation angle is described. As the absorptance of the glazing is close to constant no matter the angle of incidence the values of 0,22 and 0,06 are used even though this corresponds to an incident angle of 0°. The heat transfer coefficient due to radiation from the glazing to the slats, α_r, is found from equation 8.12 in chapter 8 and the results are seen in table 12.5.

ϕ [°]	0	15	30	45	60	70
α_r $[^{W}/_{m^2K}]$	1,25	1,25	1,27	1,28	1,3	1,34

Table 12.5: *Heat transfer coefficient due to radiation between the glazing and the slats as a function of* $\Delta t_{glass-slat}$.

It is seen that the heat transfer coefficients due to radiation in between the glazing and the slats are almost constant at different slat angles. This is due to almost equal average view factors as a high slat angle gives a high view factor from underneath the slat to the glazing while the view factor from the top side of the slat to the glazing is low compared to lower slat angles. It can also be seen that the radiative heat transfer coefficients is a bit higher at a high slat angle compared to a low slat angle. This is due to a bit higher view factor at a high slat angle than for a low slat angle.

The heat transfer coefficient due to convection from the glazing to the cavity, $\alpha_{c,3}$, is the only unknown in equation 12.3 and can thereby be solved. The results are shown in table 12.6 for the different slat angles.

ϕ [°]	0	15	30	45	60	70
$\alpha_{c,3}$ [$^{W}/_{m^2K}$]	2,53	3,03	3,31	3,45	5,11	6,65

Table 12.6: *Heat transfer coefficient due to convection from the glazing to the cavity as a function of* $\Delta t_{glass-cavity}$.

The heat transfer coefficient due to convection $\alpha_{c,3}$ and the heat transfer coefficient due to radiation α_r are in equation 12.3 found as functions of two different temperature difference, $\Delta t_{glass-slat}$ and $\Delta t_{glass-cavity}$ respectively. Due to the fact that the exterior heat transfer coefficient for the outside glazing surface, he, is a sum of $\alpha_{c,3}$ and α_r as functions of the same temperature difference, α_r is rewritten to be a function of $\Delta t_{glass-cavity}$. This heat transfer coefficient due to radiation is given the symbol $\alpha_{r,2}$ and the conversion is given in equation 12.4.

$$\alpha_{r,2} = \alpha_r \cdot \frac{\left(t_{glass} - t_{slat}\right)}{\left(t_{glass} - t_{cavity}\right)} \tag{12.4}$$

This heat transfer coefficient due to radiation is shown in table 12.7.

ϕ [°]	0	15	30	45	60	70
$\alpha_{r,2}$ [$^{W}/_{m^2K}$]	0,57	0,29	-0,22	-0,74	-2,31	-4,36

Table 12.7: *Heat transfer coefficient due to radiation in between the glazing and the slats as a function of* $\Delta t_{glass-cavity}$.

The negative radiative heat transfer coefficients in table 12.7 are due to the new temperature difference $\Delta t_{glass-cavity}$.

The exterior heat transfer coefficient for the outside glazing surface is found from equation 12.5.

$$h_e = \alpha_{c,3} + \alpha_{r,2} \tag{12.5}$$

The exterior heat transfer coefficients for the outside glazing surface calculated for the different slat angles from the measurements are given in table 12.8.

ϕ [°]	0	15	30	45	60	70
h_e [$^{W}/_{m^2K}$]	3,1	3,32	3,09	2,71	2,8	2,29

Table 12.8: *The exterior heat transfer coefficients for the outside glazing surface in case of measurements.*

The exterior heat transfer coefficient for the outside glazing surface dependent on the slat angle is also shown i figure 12.7.

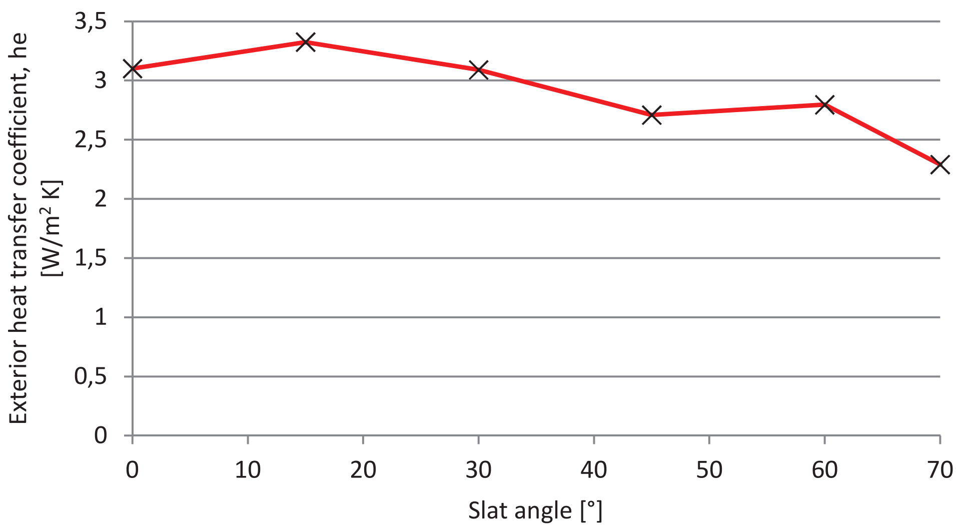

Figure 12.7: *The exterior heat transfer coefficients for the outside glazing surface illustrated in a graph.*

The exterior heat transfer coefficient for the outside glazing surface is found to be highest at a slat angle of 15° and lowest at a slat angle of 70° in case of the conducted experiments. The heat transfer coefficient is decreasing with decreasing slat angle and temperature difference between the glazing and the cavity.

12.4 3. DETERMINATION OF THE SHADINGS EFFECT ON τ_e AND LT-VALUE

The light intensity was measured for the glazing and the glazing including the Venetian blind. The light intensity was measured at a certain distance, in a total of 14 vertical point with a distance of 1 cm in between each points. The solar radiation in that certain distance was then thought of as the mean of those 14 measured values. It is the same procedure as for the calculation of the solar direct transmittance. The reason of measuring the light intensity was to find the light transmittance for the glazing with and without the Venetian blind

12.4.1 WINDOW

The measured light intensity of the 14 points without the Venetian blind is shown in figure 12.8. It can be seen that the light intensity is constant for the different measuring points.

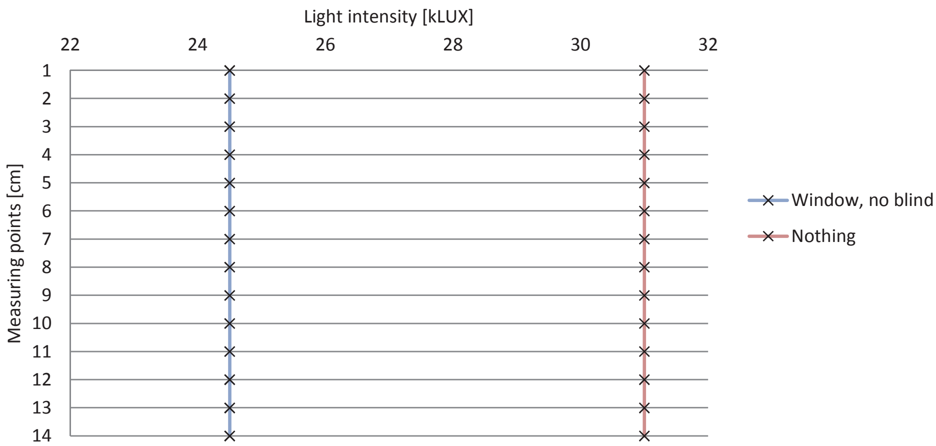

Figure 12.8: *Measured light intensity of each measuring point with and without the window in place.*

The LT-value of the glazing itself, is found by comparing measurements of the light intensity with and without the window, through equation 12.6

$$LT\text{-value} = \frac{\text{light intensity including window}}{\text{light intensity excluding window}} \tag{12.6}$$

By using the expression given in the above equation the results presented in table 12.9 was achived.

Light intensity with window [kLUX]	Light intensity without window [kLUX]	*LT* [-]
24,5	31	0,79

Table 12.9: *Measured values of light intensity levels with and without window, resulting in the LT-value of the window.*

12.4.2 WINDOW INCLUDING VENETIAN BLINDS

The measured light intensity for each measuring point with use of the window and the Venetian blind are shown in figure 12.9 as a function of slat angle.

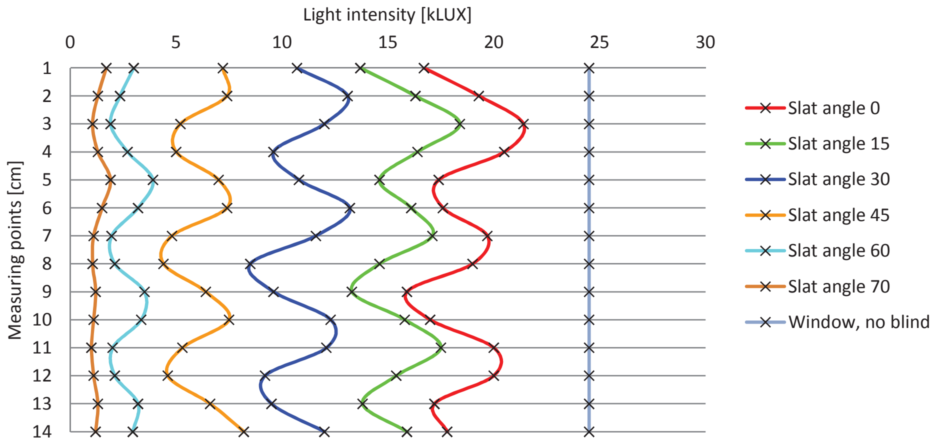

Figure 12.9: *Measured light intensity of each measuring point at the various slat angles investigated. The measured intensity without slats is also illustrated.*

The radiation through the slats reaching the measuring points is illustrated in appendix L for the different slat angles from the experiments. From appendix L and figure 12.9 it is seen that the light intensity on the window is lowest just behind slats and highest where the slats are not shading. The transmission in between the slats due to reflection from the slat surfaces is also having an effect on the measured light intensity. Because of that the light intensity is rising in points which are not directly irradiated. The tendency is the same as in case of solar radiation.

The shading factor of light for the Venetian blind at the different slat angles is found through the expression given in equation 12.7 by averaging the measured light intensities at each slat angle.

$$s_{LT} = \frac{\text{light transmittance including window and Venetian blinds}}{\text{light transmittance including only window}} \tag{12.7}$$

Input to equation 12.7 is given in table 12.10. The input is average values of the measured light intensity seen in figures 12.8 and 12.9.

Average light intensity [kLUX]							
Window, with blind ϕ [°]						**Window, no blind**	**Nothing**
0	15	30	45	60	70		
18,5	15,6	11	6,2	2,7	1,3	24,5	31

Table 12.10: *Average values of the measured light intensity without window, with and without shading.*

The shading factor of light for the Venetian blind and the light transmittance of the glazing system including Venetian blinds are seen in table 12.11.

ϕ [°]	0	15	30	45	60	70
s_{LT} [−]	0,76	0,64	0,45	0,25	0,11	0,05
LT [−]	0,6	0,5	0,36	0,2	0,08	0,04

Table 12.11: *Measured shading factor of light for the Venetian blinds and light transmittance for the glazing system, at various slat angles and an incident angle of 0°.*

The solar shading factor and the shading factor of light are compared in table 12.12. Results are from tables 12.3 and 12.11.

ϕ [°]	0	15	30	45	60	70
s_f [−]	0,75	0,68	0,50	0,32	0,19	0,10
s_{LT} [−]	0,76	0,64	0,45	0,25	0,11	0,05

Table 12.12: *Comparison of the two shading factors for heat and light.*

From table 12.12 it looks like the Venetian blind have a greater effect on the LT-value than the part of the g-value, τ_e. When looking at the accuracy of the pyranometer of 5 % and the light meter of 3,5 % described in appendix I the shading factors will be close to each other, i.e. the difference between the shading factors is within the range of the uncertainty of the measuring equipment at the highest shading factors. Because of those inaccuracies it is not possible to say anything about if the Venetian blind have a greater effect on the LT-value than on τ_e or not.

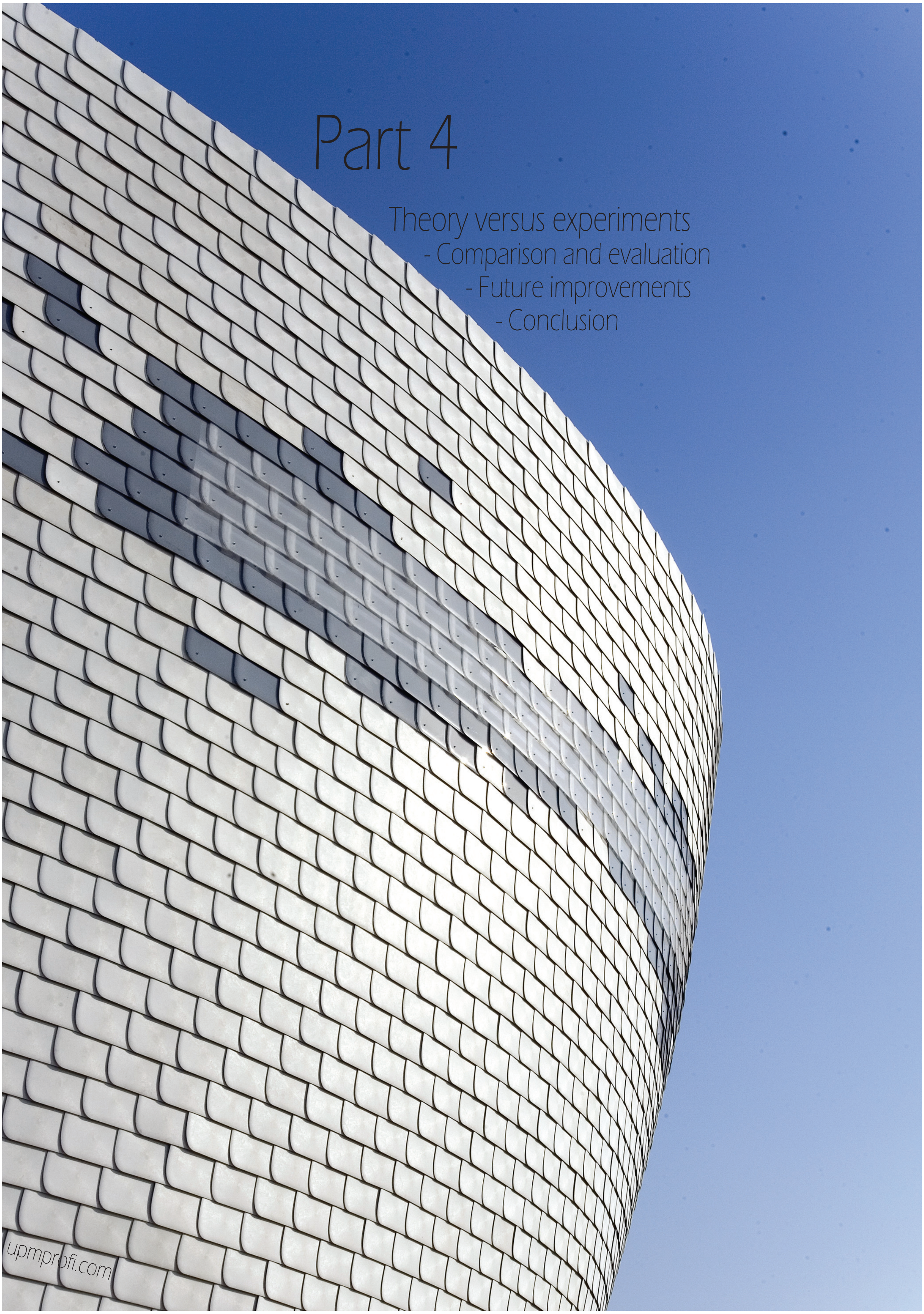

Part 4

Theory versus experiments

- Comparison and evaluation
- Future improvements
- Conclusion

CHAPTER 13

COMPARISON AND EVALUATION

In this chapter experimental results are compared with theory in order to evaluate the theoretical models of this project. For simplicity, a list of the comparisons is listed below. Each of these is described in their respective sections. For an easy overview, references are made to the sections in which the results to be compared are given.

- *Theoretical solar direct transmittance of the glazing compared with the measured solar direct transmittance of the glazing*
- *Theoretical shading factor compared to measured shading factor of the Venetian blinds at different slat angles*
- *Theoretical exterior heat transfer coefficient compared with the heat transfer coefficient found through experiments, also at different slat angles*

The deviation is given as the experimental values in proportion to theoretical values.

13.1 SOLAR DIRECT TRANSMITTANCE

The solar direct transmittance was through theory and measurements found in sections 7.4 and 12.2 respectively. The obtained results is represented in table 13.1.

Solar direct transmittance τ_e	
Theory	0,30
Experiment	0,294
Deviation	2%

Table 13.1: *Comparison of calculated and measured solar direct transmittances for the glazing of the experiment.*

The theoretical value of the solar direct transmittance is calculated with use of the relative spectral distribution matching the artificial sun. As can be seen from the comparison of the transmittances in table 13.1 the theoretical model is in good agreement with the measurements. As only the solar direct transmittance is measured a comparison in between all the solar optical properties of the glazing cannot be made. Despite of this it can be concluded that the theoretical model is able to calculate the solar direct transmittance in accordance to experiments.

13.2 SOLAR SHADING FACTOR

The solar shading factor have been calculated theoretically through the ***optimal-surface model*** in section 8.2.1. The experimental results is given in section 12.2.2. The results of these are given in table 13.2 and figure 13.1. Measurements presented in section 6.2 made by [Collins and Jiang, 2008] are also given in the figure for comparative reasons.

Solar shading factor s_f						
Slat angle	0°	15°	30°	45°	60°	70°
Theory	1	0,74	0,48	0,26	0,07	0,04
Experiment	0,75	0,68	0,50	0,32	0,19	0,10
Deviation	0,25	0,06	-0,02	-0,06	-0,12	-0,06

Table 13.2: *Comparison of calculated and measured solar direct transmittances of the glazing of the experiment.*

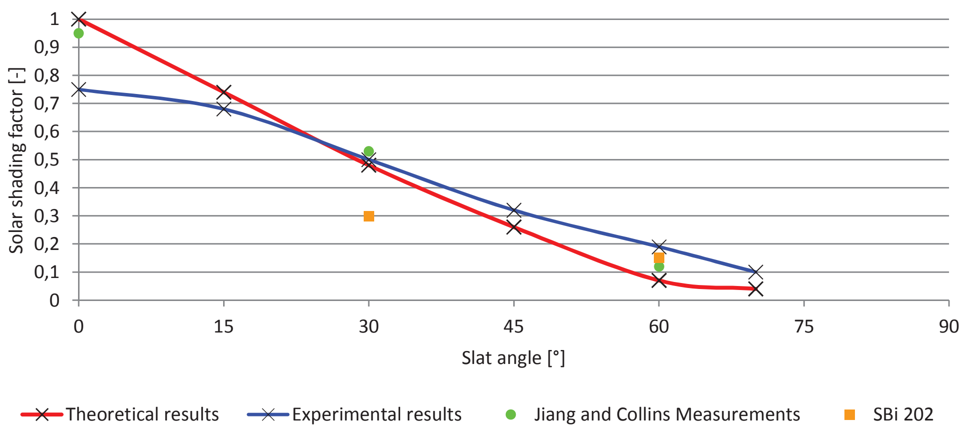

Figure 13.1: *Theoretical and experimental results of the solar shading factor.*

As can be seen in figure 13.1 the theoretical and experimental results of the shading factor are following the same trend without matching each other perfectly. Among reasons for this error may be some of the approximations made in the theoretical model, e.g. the flat slat assumption instead of a curved slat as in reality and the assumption of zero thickness of the slats which also is not entirely correct. This is illustrated in figure 13.2 where the distance in between the slats is defined as being 7 cm where in fact it should be defined as the distance of the slats subtracted with the height of the curving slats. Measurements by [Collins and Jiang, 2008] also shows better agreement with measured values from this report as can be seen in figure 13.1. The prescribed values from *SBi 202* for bright slats as presented in figure 4.2 chapter 4 shows good agreement with a slat angle of 60°, while the shading factor at 30° is far from both experiments, measurements and [Collins and Jiang, 2008].

Figure 13.2: *Illustration of the actual slats, which are curved.*

Seeing how the shading factor in table 13.2 is 1 at a slat angle of 0, is obviously not the case in reality as 1 cm of the slat distance of 7 cm is actually blocked by the curved slat as shown in figure 13.2. This means that a more reasonable theoretical shading factor would have been 0,84, as 1 over 7 equals 0,16, which also corresponds better with the experiments. This also shows that the theoretical shading factor is in the high end and should have been closer to 0,84. The measured shading factor is even lower and the reason for this may be due to inaccurate locations of the measuring points behind the glazing system. It can also be because the artificial sun probably not is totally vertical.

13.3 EXTERIOR HEAT TRANSFER COEFFICIENT

The exterior heat transfer coefficient in between the Venetian blind and the window was calculated theoretically in section 8.1.3 through application of different literature, which are valid for situations which does not match the once from the experiment. This was done in lack of literature on this subject. The calculation of the exterior heat transfer coefficient based on measurements are done through the energy balance described in

12.3. The results of the theory and measurements for the investigated slat angles are shown in table 13.3 and figure 13.3.

Exterior heat transfer coefficient h_e						
Slat angle	0°	15°	30°	45°	60°	70°
Theory						
Danvak/Glent	4,8	4,8	4,8	4,6	4,5	4,4
DS/EN 673	3,9	3,9	3,9	3,7	3,6	3,5
Experiments						
	3,1	3,3	3,1	2,7	2,8	2,3

Table 13.3: *Theoretical and experimental exterior heat transfer coefficients.*

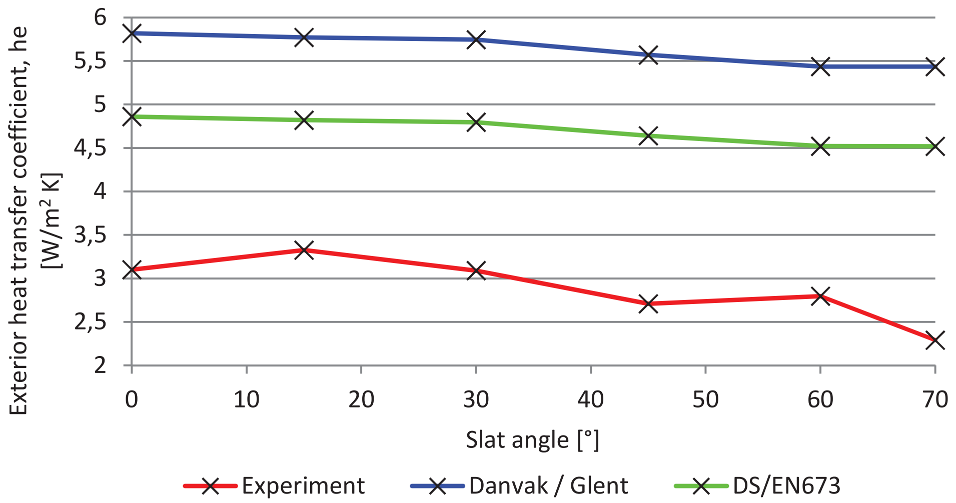

Figure 13.3: *Theoretical and experimental results of exterior heat transfer coefficient.*

Comparisons of the results shows that the experimental coefficient peaks at a slat angle of 15° while the theoretical coefficients decreases with increasing slat angle as the temperature difference in between the air in the cavity and the bounding surfaces decreases with increasing slat angle. Based on these results it is concluded that more work have to be put into this subject and the creation of empirical models valid for glazing systems including exterior Venetian blinds. This means that new values of the constant A and the exponent n used in the calculations of the exterior heat transfer coefficient in section 8.1.3.2 needs to be generated.

CHAPTER 14

FUTURE IMPROVEMENTS

Possible improvements of the models used within this project and ideas to future work is given in this chapter. For simplicity the ideas are listed individually as points.

- Modify the ***optimal-surface model*** so the curvature and thickness of slats is taken into account
- Modify the ***optimal-surface model*** so the specular radiation from the Venetian blinds towards the window is dependent on the radiation angle
- Modify the ***optimal-surface model*** so reflections from the window towards the Venetian blind layer is taken into account
- Integrate diffuse radiation into the ***optimal-surface model***, so it calculates with global radiation instead of direct radiation
- Create a model which accurately calculates the exterior heat transfer coefficient for a glazing system including Venetian blinds
  - Empirical investigation of the constant A and the exponent n in order to find new valid values. This may have to be done for every slat angle
- Emprical evaluation of the type of flow in the cavity between the window and Venetian blinds
- Investigate the extinction coefficient for panes with coating
- Enable the evaluation of the energy balance E_{ref} of a glazing system with Venetian blinds by implementing the systems control strategy in the calculations
- Use hot box in experiments so the g-value can be measured
- Set up a model to determine the air temperature in the cavity between the slats and the glazing dependent on the ambient air temperature

Chapter 15

Conclusion

The aim of this project was to create theoretical models which could describe and determine what happens when exterior Venetian blinds are applied to a window. These models have been compared with experimental results to evaluate whether the theory is representative for such a case or not.

The solar direct transmittance of a two-layer glazing was determined theoretically and compared with measured values. This showed that the model based on the theory of [Standard, 2011b], was able to calculate the solar direct transmittance within 2 %, as the normalized relative spectral distribution of the global solar radiation was changed to fit the artificial sun of the experiment. Calculations without the standardized spectral distribution was far from comparable with measurements, meaning that it is crucial to have detailed information about the artificial sun of the experiment.

The solar direct transmittance of the same glazing but including Venetian blinds was investigated at different slat angles for determination of the shading factor. The slat angles were: $0°$, $15°$, $30°$, $45°$, $60°$, $70°$. Results showed that the tendency of the shading factor was the same for both measurements and theory, without having same results. Comparison with measurements from the literature review showed to be in good agreement with the theoretical calculations, while an obvious error was produced through the flat-slat zero-thickness assumption made in the ***optimal-surface model***.

In lack of better the exterior heat transfer coefficient was through well known literature calculated based on assumptions not matching the situation of this project with Venetian blinds in front of a window. This was done for two different scenarios at the different slat angles which gave calculated values in the region of 3,5-3,9 $^{W}/_{m^2K}$ and 4,4-4,8 $^{W}/_{m^2K}$ respectively. The necessary parameters to calculate the exterior heat transfer coefficient for the experimental setup was found through measurements. This showed a coefficient in the region of 2,3-3,1 $^{W}/_{m^2K}$ which is far from the theoretical results. The coefficient showed to be decreasing with increasing slat angle for both theory and experiments. Further studies have to be done in order to create new empirical expressions for calculation of the exterior heat transfer coefficient for Venetian blinds in front of a window.

References

Aiulfi, Blay, Clancy, Collineau, Fracastoro, Heiselberg, Hibi, Inard, Kato, Kolsaker, Kondo, Koskela, Mathisen, Mierzwinski, Müller, Murakami, Nagano, Nielsen, Niemelä, Ozeki, Perino, Popiolek, Müller, Roulet, Sandberg, Schälin, Togari, Maas, Vogel, Vogl, Waters, Yamamura, and Yokoi, **February 1998**. D. Aiulfi, D. Blay, E. Clancy, S. Collineau, G.V. Fracastoro, P. Heiselberg, K. Hibi, C. Inard, S. Kato, K. Kolsaker, Y. Kondo, H. Koskela, H.M. Mathisen, S. Mierzwinski, H. Müller, S. Murakami, S. Nagano, P.V. Nielsen, R. Niemelä, Y. Ozeki, M. Perino, Z. Popiolek, D. Müller, C.A. Roulet, M. Sandberg, A. Schälin, S. Togari, J.V.D. Maas, P. Vogel, N. Vogl, R. Waters, S. Yamamura, and M. Yokoi. *Ventilation of Large Spaces in Buildings - Analysis and Prediction Techniques.* ISSN: 1395-7953 R9803, 1. edition. Kolding Trykcenter A/S, February 1998.

Baker and Steemers, **2000**. Nick Baker and Koen Steemers. *Energy and Environment in Architecture - A Technical Design Guide.* ISBN: 0-419-22770-9, 1. edition. E & FN Spon - Taylor & Francis Group, 2000.

Collins and Jiang, **2008**. Michael R. Collins and Tao Jiang. *Validation of Solar/Optical Models for Louvered Shades Using a Broad Area Illumination Integrating Sphere*, Department of Mechanical and Mechatronics Engineering - University of Waterloo and Stantec, 2008.

Duffie and Beckman, **2006**. John A. Duffie and William A. Beckman. *Solar Engineering of Thermal Processes.* ISBN: 978-0471698678, 3. edition. John Wiley & Sons, 2006.

Enterprise and Authority, **november 2011**. Danish Enterprise and Construction Authority. *Danish Building Regulation 2010*, november 2011. URL `http://www.ebst.dk/bygningsreglementet.dk`.

Ferro and Maccari. Patricia Ferro and Augusto Maccari. *Shade-Lux, Simulation model for the evaluation of energy savings in buildings provided with external non homogeneous shading devices*, CIRPS and ENEA.

Frank and Carl. Th. Frank and S. Carl. *HELIOS-XP*, Bundesamt für Energie BFE.

Garnet, **1999**. J. M. Garnet. *Thermal performance of windows with inter-pane venetian blinds*, University of Waterloo, 1999.

Glasindustrien, **September 2010**. Glasindustrien. *Kort og godt om termoruder*, September 2010.

Heiselberg, **January 2008**. Per Heiselberg. *Microclimate of Buildings*, Aalborg Universitity, January 2008.

Heiselberg, Andersen, and Aggerholm, **2002**. Per Heiselberg, Karl Terpager Andersen, and Søren Aggerholm. *SBi Anvisning 202 : Naturlig ventilation i erhhvervsbygninger*. ISBN: 87-563-1128-1, 1. edition. By og Byg Statens Byggeforskningsinstitut, 2002.

Hodapp, **november 2011**. Stefan Hodapp. *Schûco 2° System*. Presentation, november 2011.

Huang, Wright, and Collins, **2006**. Ned Y. T. Huang, John L. Wright, and Michael R. Collins. *Thermal Resistance of a Window with an Enclosed Venetian Blind: Guarded Heater Plate Measurements*, ASHRAE, 2006.

Hyldgård, **1997**. Carl Erik Hyldgård. *Måleteknik ved måling af indeklima og energiforbrug i bygninger*. ISSN: 1395-8232 U9704. Aalborg Universitet - Instituttet for Bygningsteknik, 1997.

Investment, **January 2012**. Union Investment. *Solar shading systems, protection from outside*. Internet, January 2012. URL `http://www.sustainable-realestate-investments.com/en/topics/climate-engineering/climate-control/protection-external-solar-shading-systems/`.

Jensen and Lund, **October 1995**. Jerry Møller Jensen and Hans Lund. *Design Reference Year, DRY - Et nyt dansk referenceår*, Danmarks Tekniske Universitet, October 1995.

Johra, **April 2012**. Hicham Johra. *ClimaWin Project - Experimental Investigation of the Thermal Efficiency of a Dobule Window with Ventilated Air Gap and Shading Device.*, Aalborg University - Indoor Environmental Engineering Department, April 2012.

Kotey and Wright. N. A. Kotey and J. L. Wright. *Simplified Solar Optical Calculations for Windows with Venetian Blinds*, Department of Mechanical Engineering - University of Waterloo.

Kotey, Collins, Wright, and Jiang, **May 2009**. N. A. Kotey, M. R. Collins, J. L. Wright, and T. Jiang. *A Simplified Method for Calculating the Effective Solar Optical Properties of a Venetian Blind Layer for Building Energy Simulation*, Department of Mechanical Engineering - University of Waterloo and BC Hydro, May 2009.

Kuhn, **2006**. Tilmann E. Kuhn. *Solar control: A general evaluation method for facades with venetian blinds or other solar control systems*, Fraunhofer Institute for Solar Energy Systems ISE, 2006.

Kuhn, Bühler, and Platzer, 2000. Tilmann E. Kuhn, Christopher Bühler, and Werner J. Platzer. *Evaluation of Overheating Protection with Sun-shading Systems*, Department of Thermal and Optical Systems, Fraunhofer Institute for Solar Energy Systems ISE, 2000.

Larsen, August 2010. Tine Steen Larsen. *Lavenergihuse plages af overophedning og kolde rum*, Aalborg University, August 2010. URL `http://ing.dk/artikel/111357-lavenergihuse-plages-af-overophedning-og-kolde-rum`.

Loutzenhiser, Manz, Carl, Simmler, and Maxwell, February 2007. Peter G. Loutzenhiser, Heinrich Manz, Stephan Carl, Hans Simmler, and Gregory M. Maxwell. *Empirical validation of solar gain models for a glazing unit with exterior and interior blind assemblies*, ELSEVIER, February 2007.

Manz, Loutzenhiser, Frank, Strachan, Bundi, and Maxwell, July 2005. H. Manz, P. Loutzenhiser, T. Frank, P. A. Strachan, R. Bundi, and G. Maxwell. *Series of experiments for empirical validation of solar gain modeling in building energy simulation codes - Experimental setup, test cell characterization, specifications and uncertainty analysis*, ELSEVIER, July 2005.

Materials and Sources, January 2012. Materials and Sources. *Exterior Venetian Blinds from SkyShield.* Internet, January 2012. URL `http://materialsandsources.com/exterior-venetian-blinds-from-sky-shield/`.

Mróz, December 2003. Tomasz M. Mróz. *Subtask A: Overview of retrofitting Measures*, December 2003.

Nielsen, Skistad, Mundt, Hagström, and Railio, August 2002. Peter V. Nielsen, Håkon Skistad, Elisabeth Mundt, Kim Hagström, and Jorma Railio. *Displacement Ventilation in Non-industrial Premises*, Rehva, August 2002.

Energy, june 2012. U.S. Department of Energy. *EnergyPlus Energy Simulation Software*, june 2012. URL `http://www.energyplus.gov`.

OSRAM, 2012. OSRAM. *OSRAM ULTRA-VITALUX - Powerful replacement sunlight for a wide range of applications.* Technical Data Sheet, 2012.

Parmelee and Aubele, 1952. G. V. Parmelee and W. W. Aubele. *The Shading of Sunlit Glass - An Analysis of the Effect of Uniformly Spaced Flat Opaque Slats*, Ashve Transactions, 1952.

Parmelee, Aubele, and Vild, 1953. G. V. Parmelee, W. W. Aubele, and D. J. Vild. *The Shading of Sunlit Glass - An Experimental Study of Slattype Sun Shades.*, ASHVE Transactions, 1953.

Rationel, January 2012. Rationel. *Energibalance Eref*, January 2012. URL `http://www.rationel.dk/professionelle/energi/energibegreber/energibalance-eref.`

Research, January 2012. Wolfram Research. *Index of Refraction*, January 2012. URL `http://scienceworld.wolfram.com/physics/IndexofRefraction.html.`

Rosenfeld, Breitenbach, Lart, and Langle, 2001. J. L. J. Rosenfeld, J. Breitenbach, S. Lart, and I. Langle. *Optical and Thermal Performance of Glazing with Integral Venetian Blinds*, Energy and Buildings, 2001.

Roulet, 1992. Claude-Alain Roulet. *Expérimentation in situ en relation avec les qualités thermiques et aérauliques du bâtiment*. 5.th J. Cartier Conference, Montreal, 1992.

Stampe, 1982. Ole B. Stampe. *Glent Ventilation*. Glent & Co. A/S, 1982.

Stampe, Hansen, and Kjerulf-Jensen, 2006. Ole B. Stampe, H.E. Hansen, and P. Kjerulf-Jensen. *Varme- og Klimateknik, Grundbog*. ISBN: 87-982652-8-8, 3. edition. Danvak ApS, 2006.

Standard, April 2011a. Danish Standard. *DS 418 : Calculation of heat loss from buildings*, European Committee for Standardization, April 2011a.

Standard, February 2007. European Standard. *DS/EN 13363-1 : Solar protection devices combined with glazing - Calculation of solar and light transmittance - Part 1: Simplified method*, European Committee for Standardization, February 2007.

Standard, February 2011b. European Standard. *DS/EN 410 : Glass in building - Determination of luminous and solar characteristics of glazing*, European Committee for Standardization, February 2011b.

Standard, February 2011c. European Standard. *DS/EN 673 : Glass in building - Determination of thermal transmittance (U-value) - Calculation method*, European Committee for Standardization, February 2011c.

Steinle, 2012. Dr. Helmut Steinle. *Wavelength Regions - Spectrum*. Astronomy Resources MPE, 2012. URL `http://www.mpe.mpg.de/AstR/topics.html.`

Termoruder.dk, January 2012. Termoruder.dk. *Værd at vide om termoruder og energiruder.*, January 2012. URL `http://www.termoruder.dk/vaerd-at-vide-om-termoruder.html.`

UK, 2012. Pilkington Building Products UK. *Pilkington Optitherm S3 - The latests in thermal insulation*, Pilkington, 2012.

Velfac, January 2012. Velfac. *Energibalance for vinduer - en helhedsorienteret betragtning*, January 2012. URL http://www.velfac.dk/Global/Energibalance_for_vinduer_en_helhedsorienteret_betragtning?OpenDocument.

WebEcoist, 2012. WebEcoist. *7 Ancient Wonders of Green Design & Technology*, 2012. URL http://webecoist.momtastic.com/2009/01/25/ancient-green-architecture-alternative-energy-design/.

Wright, Collins, and Huang, 2007. John L. Wright, Michael R. Collins, and Ned Y. T. Huang. *Thermal Resistance of a Window with an Enclosed Venetian Blind: A Simplified Model*, ASHRAE, 2007.

Yahoda and Wright, 2005. Darryl S. Yahoda and John L. Wright. *Methods for Calculating the Effective Solar-Optical Properties of a Venetian Blind Layer*, Department of Mechanical Engineering - University of Waterloo, 2005.

Yahoda and Wright, 2004. Darryl S. Yahoda and John L. Wright. *Methods for Calculating the Effective Longwave Radiative Properties of a Venetian Blind Layer*, Department of Mechanical Engineering - University of Waterloo, 2004.

Zonen, 2006. Kipp & Zonen. *Calibration Ceterficate - Pyranometer*, Kipp & Zonen B.V., 2006.

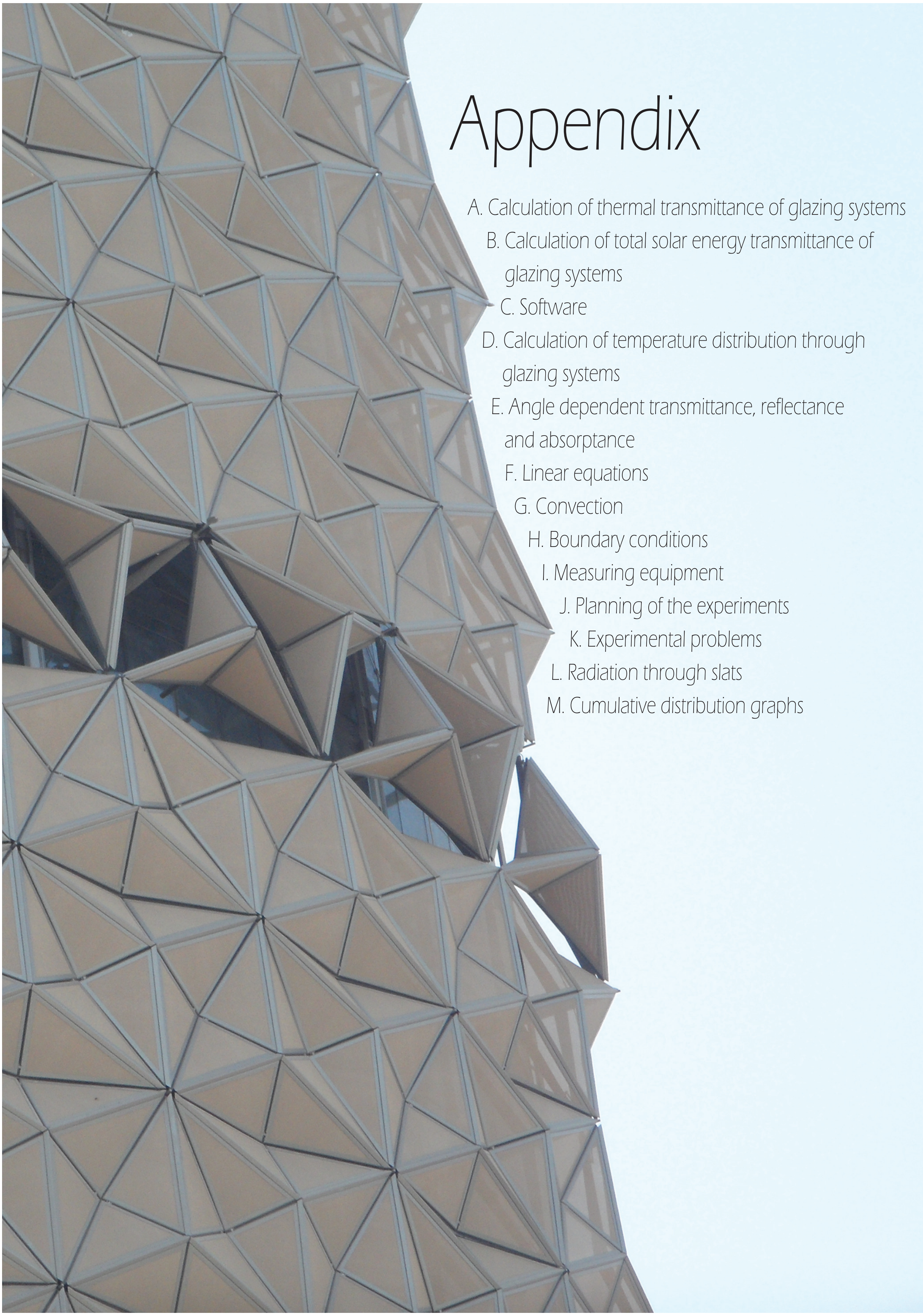

Appendix

APPENDIX A

CALCULATION OF THERMAL TRANSMITTANCE OF GLAZING SYSTEMS

The method presented in this chapter of calculating the thermal transmittance, U-value, of glazing systems is based on the European Standard: *DS/EN 673: Glass in building - Determination of thermal transmittance (U-value) - Calculation method* [Standard, 2011c].

In its pure form the U-value is given by equation A.1.

$$\frac{1}{U} = \frac{1}{h_e} + \frac{1}{h_t} + \frac{1}{h_i} \tag{A.1}$$

where:

h_e	*External heat transfer coefficient* $[^{W}/_{m^2K}]$
h_t	*Thermal conductance of the glazing* $[^{W}/_{m^2K}]$
h_i	*Internal heat transfer coefficient* $[^{W}/_{m^2K}]$

A.1 EXTERNAL AND INTERNAL HEAT TRANSFER COEFFICIENTS

The external and internal heat transfer coefficients, h_e and h_i respectively, are functions of radiation and convection as results of the outdoor and indoor climatic conditions. h_e is standardised to $25\,^{W}/_{m^2K}$. h_i is given by equation A.2.

$$h_i = h_r + h_c \tag{A.2}$$

where:

h_r	*Internal radiative heat transfer coefficient* $[^{W}/_{m^2K}]$
h_c	*Internal convective heat transfer coefficient* $[^{W}/_{m^2K}]$

For standard uncoated soda lime glass with an emissivity of 0,837, h_r is given at 4,1 $^{W}/_{m^2K}$. For glass with lower emissivity on the inner surface h_r is corrected according to the emissivity, but as coatings rarely appear on the inner surface of a window, this correction is seldom needed. h_c is given at 3,6 $^{W}/_{m^2K}$ for free convection.

A.2 THERMAL CONDUCTANCE OF THE GLAZING SYSTEM

The thermal conductance, h_t, of the glazing is determined from the entire glazing system consisting of both panes and gas spaces and is given by equation A.3.

$$\frac{1}{h_t} = \sum_1^N \frac{1}{h_s} + \sum_1^M d_j \cdot \lambda_j^{-1} \tag{A.3}$$

where:

h_s	*Thermal conductance of each gas space* [$^{W}/_{m^2K}$]
N	*Number of gas spaces* [−]
d_j	*Thickness of each material layer* [m]
λ_j^{-1}	*Thermal resistivity of each material layer* [$^{mK}/_{W}$]
M	*Number of material layers* [−]

A.2.1 THERMAL CONDUCTANCE OF THE GAS SPACE

The thermal conductance of a gas space, h_s, is given by equation A.4.

$$h_{s,k} = h_{r,k} + h_{g,k} \tag{A.4}$$

where:

$h_{r,k}$	*Radiation conductance of the k'th gas space* [$^{W}/_{m^2K}$]
$h_{g,k}$	*Conductance of the gas in the k'th space* [$^{W}/_{m^2K}$]

A.2.1.1 RADIATION CONDUCTANCE OF THE GAS SPACE

The radiation conductance, h_r, is given by equation A.5.

$$h_{r,k} = 4\sigma \left(\frac{1}{\epsilon_{1,k}} + \frac{1}{\epsilon_{2,k}} - 1 \right)^{-1} T_{m,k}^3 \tag{A.5}$$

where:

σ	*Stefan Boltzmann constant* $[\mathrm{Wm^{-2}K^{-4}}]$
$\epsilon_{x,k}$	*Emissivities of the surfaces bounding the gas spaces between the panes* $[\mathrm{W/m^2K}]$
$T_{m,k}$	*Mean absolute temperature of the gas space* $[\mathrm{K}]$

The emissivities to choose for a gas space is shown in figure A.1 for a glazing system consisting of two panes and one cavity. Each pane got two emissivities ϵ_1 and ϵ_2 for their two surfaces, which for regular non coated glass are the same for each surface. Going from outside to inside ϵ_2 is chosen for the outside pane and ϵ_1 is chosen for the inside pane.

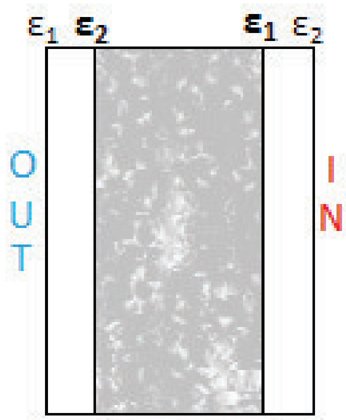

Figure A.1: *Glazing system with pane emissivities. The emissivities to use in equation A.5 are shown in bold.*

A.2.1.2 CONDUCTANCE OF THE GAS SPACE

The gas conductance, h_g, is given by equation A.6.

$$h_{g,k} = Nu \cdot \frac{\lambda_k}{s_k} \tag{A.6}$$

where:

Nu	*Nusselt's number* $[-]$
λ_k	*Thermal conductivity of the k'th gas space* $[\mathrm{W/mK}]$
s_k	*Width of the k'th gas space* $[\mathrm{m}]$

The Nusselt number is found from the Grashof and Prandtl numbers along with a constant A and exponent n describing the convection as a function of the positioning of the glazing system. Values of A and n are given for vertical glazing, horizontal glazing and glazing at an angle of 45° [Standard, 2011c]. The nusselt number is given by equation A.7.

$$Nu = A \cdot (Gr \cdot Pr)^n \tag{A.7}$$

where:

A	*Constant* [−]
Gr	*Grashof number* [−]
Pr	*Prandtl number* [−]
n	*Exponent* [−]

The Grashof number is given by equation A.8.

$$Gr = \frac{9,81 \cdot s^3 \cdot \Delta T \cdot \rho^2}{T_m \cdot \mu^2} \tag{A.8}$$

where:

ΔT	*Temperature difference between glass surfaces bounding the gas space* [K]
ρ	*Density of the gas* [$^{kg}/_{m^3}$]
T_m	*Mean temperature of the gas* [K]
μ	*Dynamic viscosity* [$^{kg}/_{ms}$]

The Prandtl number is given by equation A.9.

$$Pr = \frac{\mu \cdot c_p}{\lambda} \tag{A.9}$$

where:

c_p	*Specific heat capacity of the gas* [$^{J}/_{kgK}$]

APPENDIX B

CALCULATION OF TOTAL SOLAR ENERGY TRANSMITTANCE OF GLAZING SYSTEMS

The calculation method of the total solar energy transmittance, g-value, of glazing systems which is presented in this chapter is based on the European Standard: *DS/EN 410: Glass in building - Determination of luminous and solar characteristics of glazing* [Standard, 2011b].

The g-value is given as the fraction of the incident solar radiation transmitted through the glass. This is seen in equation B.1.

$$g = \tau_e + q_i \tag{B.1}$$

where:

τ_e	*Solar direct transmittance* $[-]$
q_i	*Secondary heat transfer factor of the glazing towards the inside* $[-]$

B.1 THE SOLAR DIRECT TRANSMITTANCE OF THE GLAZING

The solar direct transmittance is given in equation B.2.

$$\tau_e = \frac{\sum_{\lambda=300nm}^{2500nm} S_\lambda \tau(\lambda) \Delta\lambda}{\sum_{\lambda=300nm}^{2500nm} S_\lambda \Delta\lambda} \tag{B.2}$$

where:

S_λ	*Relative spectral distribution of the solar radiation* $[-]$
$\tau(\lambda)$	*Spectral transmittance of the glazing* $[-]$
$\Delta\lambda$	*Wavelength interval* $[-]$

The product $S_\lambda \Delta\lambda$ is given for different wavelengths between 300 nm and 2500 nm in table 2 in [Standard, 2011b]. The relative spectral distribution valid for the experiments can be found in appendix H.

B.1.1 THE SPECTRAL TRANSMITTANCE OF THE GLAZING

The total spectral transmittance of the glazing is dependent on whether the window consists of one pane, two panes or three panes. For windows with one pane the spectral transmittance of the glazing is given directly as a window property. For windows with two and three panes the spectral transmittance is calculated from the spectral transmittances and reflectances of the individual panes. These calculations are shown in equation B.3 and B.4 respectively.

$$\tau(\lambda) = \frac{\tau_1(\lambda)\tau_2(\lambda)}{1-\rho_1'(\lambda)\rho_2(\lambda)} \tag{B.3}$$

where:

$\tau_1(\lambda)$	*Spectral transmittance of the 1st (outer) pane* [−]
$\tau_2(\lambda)$	*Spectral transmittance of the 2nd pane* [−]
$\rho_1'(\lambda)$	*Spectral reflectance of the 1st pane, measured in direction opposite to radiation* [−]
$\rho_2(\lambda)$	*Spectral reflectance of the 2nd pane, measured in direction of radiation* [−]

$$\tau(\lambda) = \frac{\tau_1(\lambda)\tau_2(\lambda)\tau_3(\lambda)}{\left[1-\rho_1'(\lambda)\rho_2(\lambda)\right]\left[1-\rho_2'(\lambda)\rho_3(\lambda)\right]-\tau_2{}^2(\lambda)\rho_1'(\lambda)\rho_3(\lambda)} \tag{B.4}$$

where:

$\tau_3(\lambda)$	*Spectral transmittance of the 3rd pane* [−]
$\rho_2'(\lambda)$	*Spectral reflectance of the 2nd pane, measured in direction opposite to radiation* [−]
$\rho_3(\lambda)$	*Spectral reflectance of the 3rd pane, measured in direction of radiation* [−]

The individual spectral transmittances and reflectances of the each panes are given as pane properties. They are illustrated in figure B.1 for one pane, two panes and three panes.

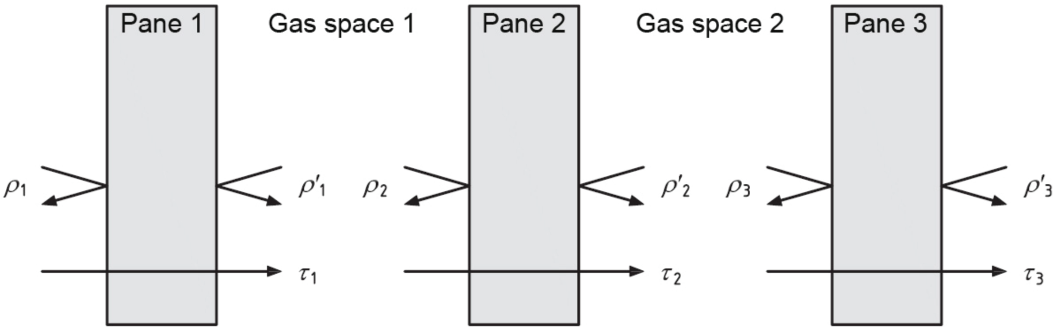

Figure B.1: *Transmittance and reflectance of the one pane, two panes and three panes [Standard, 2011b], edited.*

B.2 THE SECONDARY HEAT TRANSFER FACTOR OF THE GLAZING TOWARDS THE INSIDE

The secondary heat transfer factor of the glazing towards the inside is dependent on the number of panes in the glazing system. The calculations for one, two and three panes are shown in equation B.5, B.6 and B.7 respectively.

$$q_i = \alpha_e \frac{h_i}{h_e + h_i} \tag{B.5}$$

where:

α_e	*Absorptance* [−]
h_e	*External heat transfer coefficient* [W/m²K]
h_i	*Internal heat transfer coefficient* [W/m²K]

$$q_i = \frac{\left[\frac{\alpha_{e1}+\alpha_{e2}}{h_e} + \frac{\alpha_{e2}}{\Lambda}\right]}{\left[\frac{1}{h_i} + \frac{1}{h_e} + \frac{1}{\Lambda}\right]} \tag{B.6}$$

where:

α_{e1}	*Absorptance of the 1st (outer) pane* [−]
α_{e2}	*Absorptance of the 2nd pane* [−]
$\Lambda = h_t$	*Thermal conductance between the outer surface and the innermost surface* [W/m²K]

$$q_i = \frac{\left[\frac{\alpha_{e3}}{\Lambda_{23}} + \frac{\alpha_{e3}+\alpha_{e2}}{\Lambda_{12}} + \frac{\alpha_{e3}+\alpha_{e2}+\alpha_{e1}}{h_e}\right]}{\left[\frac{1}{h_i} + \frac{1}{h_e} + \frac{1}{\Lambda_{12}} + \frac{1}{\Lambda_{23}}\right]} \tag{B.7}$$

where:

α_{e3}	*Absorptance of the third pane* $[-]$
Λ_{12}	*Thermal conductance between outer surface of 1st pane and center of 2nd pane* $[^{W}/_{m^2K}]$
Λ_{23}	*Thermal conductance between center of 2nd pane and innermost surface of 3rd pane* $[^{W}/_{m^2K}]$

The thermal conductance for two panes and the internal- and external heat transfer coefficient are described in appendix A.

B.2.1 THERMAL CONDUCTION IN CASE OF THREE PANES

The division of the thermal conduction in case of three panes is illustrated in figure B.2.

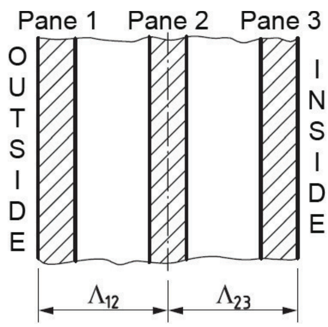

Figure B.2: *The division af the thermal conduction [Standard, 2011b], edited.*

B.2.2 ABSORPTANCE

The absorptance is calculated different dependent on whether the window is with one pane, two panes or three panes.

B.2.2.1 ABSORPTANCE FOR ONE PANE

The solar direct absorptance, α_e is calculated from equation B.8.

$$\tau_e + \rho_e + \alpha_e = 1 \tag{B.8}$$

where:

ρ_e	*Reflectance* $[-]$

The only unknown is the reflectance which is calculated from equation B.9.

$$\rho_e = \frac{\sum_{\lambda=300nm}^{2500nm} S_\lambda \rho(\lambda) \Delta\lambda}{\sum_{\lambda=300nm}^{2500nm} S_\lambda \Delta\lambda} \tag{B.9}$$

where:

$\rho(\lambda)$	*Spectral reflectance of the glazing* $[-]$

The total spectral reflectance of the glazing is dependent on whether the window contains of one pane, two panes or three panes. For windows with one pane the spectral reflectance of the glazing is given directly as a window property. For windows with two and three panes the spectral reflectance is calculated from the spectral transmittances and reflectances of the individual panes. These calculations are shown in equation B.10 and B.11 respectively.

$$\rho(\lambda) = \rho_1(\lambda) + \frac{\tau_1^2(\lambda)\rho_2(\lambda)}{1-\rho_1'(\lambda)\rho_2(\lambda)} \tag{B.10}$$

where:

$\rho_1(\lambda)$	*Spectral reflectance of the 1st (outer) pane, measured in direction of radiation* $[-]$

$$\rho(\lambda) = \rho_1(\lambda) + \frac{\tau_1^2(\lambda)\rho_2(\lambda)\left[1-\rho_2'(\lambda)\rho_3(\lambda)\right] + \tau_1^2(\lambda)\tau_2^2(\lambda)\rho_3(\lambda)}{\left[1-\rho_1'(\lambda)\rho_2(\lambda)\right]\left[1-\rho_2'(\lambda)\rho_3(\lambda)\right] - \tau_2{}^2(\lambda)\rho_1'(\lambda)\rho_3(\lambda)} \tag{B.11}$$

Those mentioned transmittances and reflectances of the individual panes are given as window properties.

B.2.2.2 ABSORPTANCE FOR TWO PANES

The absorptances of the individual panes are different for two and three panes. For two panes α_{e1} and α_{e2} are calculated as shown in equations B.12 and B.13.

$$\alpha_{e1} = \frac{\sum_{\lambda=300nm}^{2500nm} S_\lambda \left(\alpha_1(\lambda) + \frac{\alpha_1'(\lambda)\tau_1(\lambda)\rho_2(\lambda)}{1-\rho_1'(\lambda)\rho_2(\lambda)}\right) \Delta\lambda}{\sum_{\lambda=300nm}^{2500nm} S_\lambda \Delta\lambda} \tag{B.12}$$

$$\alpha_{e2} = \frac{\sum_{\lambda=300nm}^{2500nm} S_\lambda \left(\frac{\alpha_2(\lambda)\tau_1(\lambda)}{1-\rho_1'(\lambda)\rho_2(\lambda)} \right) \Delta\lambda}{\sum_{\lambda=300nm}^{2500nm} S_\lambda \Delta\lambda} \tag{B.13}$$

where:

$\alpha_1(\lambda)$	*Spectral direct absorptance of outer pane, measured in direction ofradiation* [−]
$\alpha_1'(\lambda)$	*Spectral direct absorptance of outer pane, measured in opposite direction to radiation* [−]
$\alpha_2(\lambda)$	*Spectral direct absorptance of the 2nd pane, measured in direction of radiation* [−]

These spectral direct absorptances for the panes are calculated from the following equations B.14 to B.16.

$$\alpha_1(\lambda) = 1 - \tau_1(\lambda) - \rho_1(\lambda) \tag{B.14}$$

$$\alpha_1'(\lambda) = 1 - \tau_1(\lambda) - \rho_1'(\lambda) \tag{B.15}$$

$$\alpha_2(\lambda) = 1 - \tau_2(\lambda) - \rho_2(\lambda) \tag{B.16}$$

B.2.2.3 ABSORPTANCE FOR THREE PANES

For three panes α_{e1}, α_{e2} and α_{e3} are calculated from the following equations B.17 to B.19.

$$\alpha_{e1} = \frac{\sum_{\lambda=300nm}^{2500nm} S_\lambda \left(\alpha_1(\lambda) + \frac{\tau_1(\lambda)\alpha_1'(\lambda)\rho_2(\lambda)[1-\rho_2'(\lambda)\rho_3(\lambda)]+\tau_1(\lambda)\tau_2^2(\lambda)\alpha_1'(\lambda)\rho_3(\lambda)}{[1-\rho_1'(\lambda)\rho_2(\lambda)]\cdot[1-\rho_2'(\lambda)\rho_3(\lambda)]-\tau_2^2(\lambda)\rho_1'(\lambda)\rho_3(\lambda)} \right) \Delta\lambda}{\sum_{\lambda=300nm}^{2500nm} S_\lambda \Delta\lambda} \tag{B.17}$$

$$\alpha_{e2} = \frac{\sum_{\lambda=300nm}^{2500nm} S_\lambda \left(\frac{\tau_1(\lambda)\alpha_2(\lambda)[1-\rho_2'(\lambda)\rho_3(\lambda)]+\tau_1(\lambda)\tau_2(\lambda)\alpha_2'(\lambda)\rho_3(\lambda)}{[1-\rho_1'(\lambda)\rho_2(\lambda)]\cdot[1-\rho_2'(\lambda)\rho_3(\lambda)]-\tau_2^2(\lambda)\rho_1'(\lambda)\rho_3(\lambda)} \right) \Delta\lambda}{\sum_{\lambda=300nm}^{2500nm} S_\lambda \Delta\lambda} \tag{B.18}$$

$$\alpha_{e3} = \frac{\sum_{\lambda=300nm}^{2500nm} S_\lambda \left(\frac{\tau_1(\lambda)\tau_2(\lambda)\alpha_3(\lambda)}{[1-\rho_1'(\lambda)\rho_2(\lambda)]\cdot[1-\rho_2'(\lambda)\rho_3(\lambda)]-\tau_2^2(\lambda)\rho_1'(\lambda)\rho_3(\lambda)} \right) \Delta\lambda}{\sum_{\lambda=300nm}^{2500nm} S_\lambda \Delta\lambda} \tag{B.19}$$

where:

$\alpha_2'(\lambda)$	*Spectral direct absorptance of 2nd pane, measured in opposite direction to radiation* [−]
$\alpha_3(\lambda)$	*Spectral direct absorptance of 3rd pane, measured in direction of radiation* [−]

These spectral direct absorptances for the panes are calculated as shown in equations B.20 and B.21

$$\alpha_2'(\lambda) = 1 - \tau_2(\lambda) - \rho_2'(\lambda) \tag{B.20}$$

$$\alpha_3(\lambda) = 1 - \tau_3(\lambda) - \rho_3(\lambda) \tag{B.21}$$

APPENDIX C

SOFTWARE

This appendix contains a brief description of the solar energy related software used within this project. The software consists of:

- ParaSol 6.6
- WINDOW 7

The main purpose of the programs have been the calculation of the U-value and g-value of the glazings without solar shading, solely for comparative reasons and validation of own calculations. The results obtained within the softwares are only comparable with theoretical calculations with use of standardised boundary conditions

In addition to the programs used, WIS, EnergyPlus and HELIOS are briefly described due to the mentioning of the software in the theoretical and experimental literature surveys chapter 6 section 6.4.2 and chapter 10 section 10.1.3.

C.1 PARASOL 6.6

A picture of the software interface is shown in C.1.

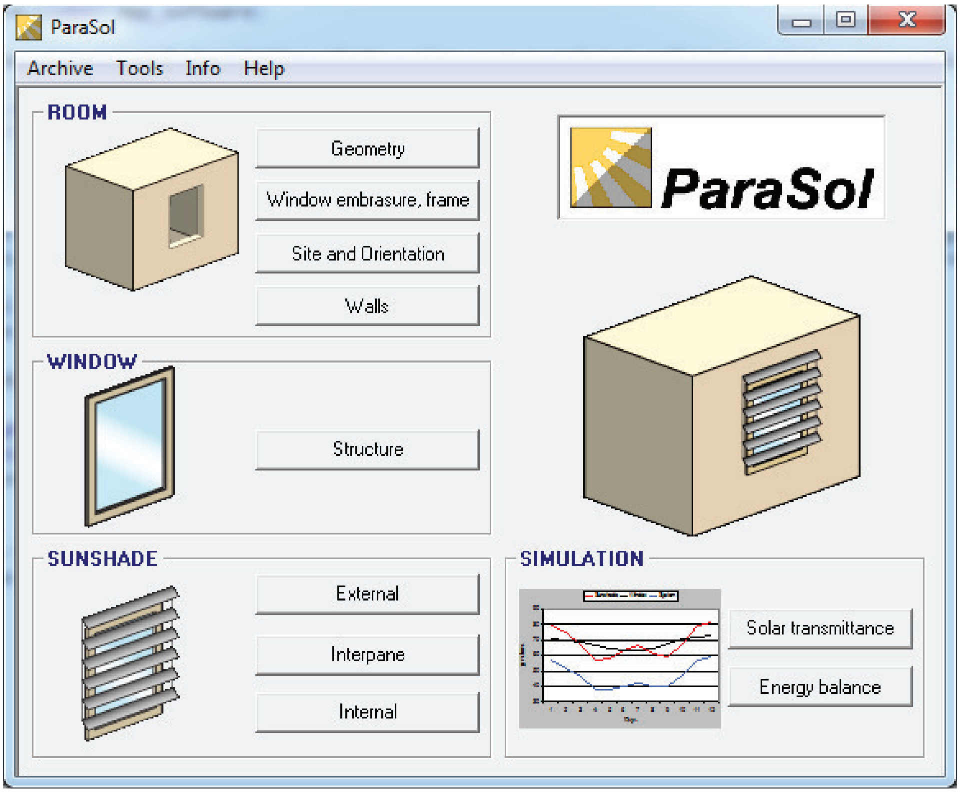

Figure C.1: *Parasol interface.*

In ParaSol the boundary conditions can be changed when doing calculations of the U-value and g-value. This was done so they corresponded to the once given in appendix H. Furthermore the convection model can be changed so it calculates according to *DS/EN 673* [Standard, 2011c], which is the standard used within this project.

C.2 WINDOW 7

A picture of the software interface is shown in C.2.

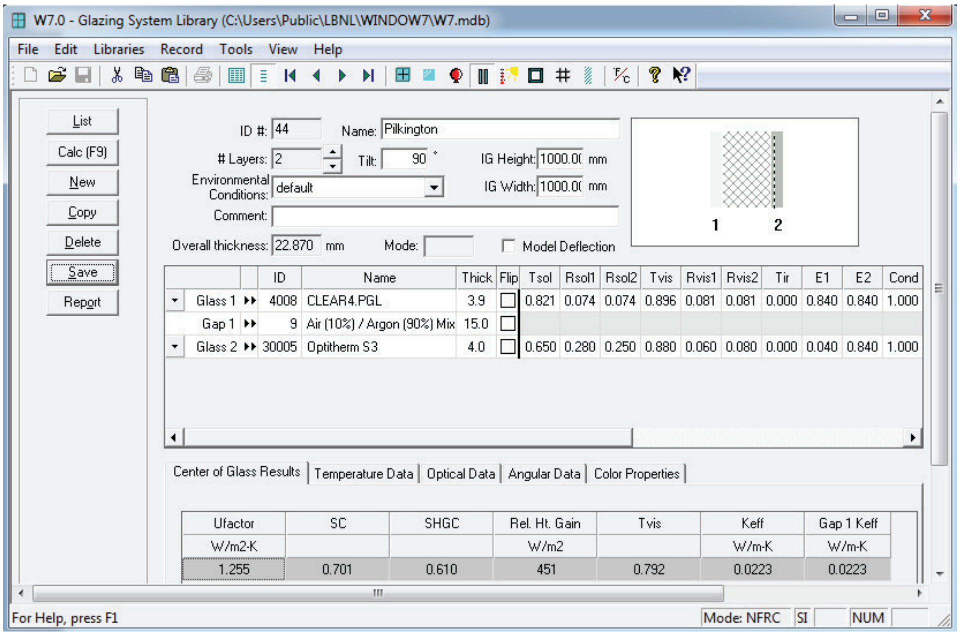

Figure C.2: *Window interface.*

As for ParaSol, the boundary conditions can be changed according to desires in WINDOW 7, but the convection model cannot be changed to *DS/EN 673* [Standard, 2011c] which may be the reason for the higher calculated U-value in chapter 7.4 compared to own calculations and ParaSol.

WINDOW 7 is also used for determination of angle dependent solar optical properties in case of solar direct transmittance, reflectance and absorptance in section 7.2. The g-value og the glazing is also found as a function of incident angle.

C.3 WIS

A picture of the software interface is shown in C.3.

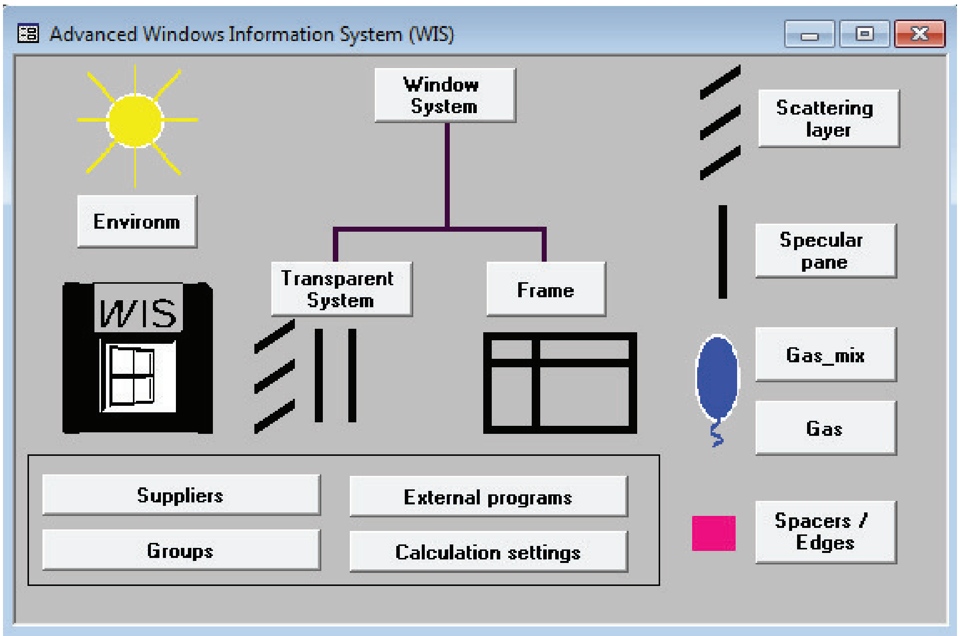

Figure C.3: *WIS interface.*

WIS is able to calculate U-value, g-value, LT-value and the components included in these parameters for glazing systems with various amounts of panes and including solar shading, in case of for instance Venetian blinds. Both exterior and interior boundary conditions can be adjusted.

C.4 ENERGYPLUS

EnergyPlus is a simulation program based on a user's description of a building. From this user description EnergyPlus is for instance able to calculate heating and cooling loads based on energy balances. Simulations in EnergyPlus perform as if it was a real building, with boundary conditions in case of weather data. [of Energy, 2012]

C.5 HELIOS

HELIOS is a building energy simulation program which is based on single zone modelling. The part of interest to this project is HELIOS' ability to do detailed calculations of the total heat transfer through a glazing system with blinds and the possibility to define user boundary conditions for temperatures. [Frank and Carl]

APPENDIX D

CALCULATION OF TEMPERATURE DISTRIBUTION THROUGH GLAZING SYSTEMS

The transmission loss, ϕ_t, through a window is calculated from equation D.1 according to [Standard, 2011a].

$$\phi_t = \frac{1}{R} \cdot A \cdot (t_i - t_e) \tag{D.1}$$

where:

R	*Thermal resistance* $[^{\mathrm{m^2K}}/_{\mathrm{W}}]$
A	*Transmission area* $[\mathrm{m}^2]$
T_i	*Temperature on the inside of the layer* [K]
T_e	*Temperature on the outside of the layer* [K]

In addition to the conduction through the window, longwave radiation will occur in between the surfaces bounding the cavity in the glazing. This longwave radiation is determined from the temperature of the bounding surfaces. The fraction of the energy leaving surface i which is intercepted by surface j is calculated from equation D.2.

$$\Phi_{ij} = \Psi_{ij} \cdot \epsilon_i \cdot \epsilon_j \cdot \sigma \cdot A_i \cdot 4T_{ref}^3 \left(t_i - t_j\right) \tag{D.2}$$

where:

Φ	*Heat transfer* [W]
Ψ	*View factor* [−]
ϵ	*Emissivity* [−]
σ	*Stefan-Boltzmann constant* [$^{W}/_{m^2K^4}$]
A	*Area* [m^2]
T_{ref}	*Absolute mean temperature* [K]
t	*Surface temperature* [°C]

The investigation of the temperature distribution through the window system can be seen as a 1D problem, because the temperature is assumed to be evenly distributed on the surfaces facing inside and outside. To solve the problem the finite element method is used. The method is shown in figure D.1, where the red numbers are the element numbers and the green numbers are the point numbers. The known temperatures in the ends, in point j and point n where n is the amount of points, are the outdoor air temperature and indoor air temperature respectively. The temperature distribution is found in the remaining points on behalf of those known temperatures.

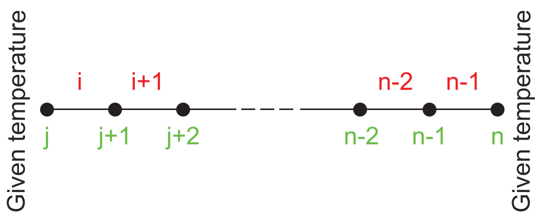

Figure D.1: *1D problem solved by FEM.*

The method of how to calculate the temperature in a point where no longwave radiation is occurring, is shown in equation D.3.

$$0 = \frac{1}{R_i} \cdot A \cdot \left(t_j - t_{j+1}\right) + \frac{1}{R_{i+1}} \cdot A \cdot \left(t_{j+2} - t_{j+1}\right) \tag{D.3}$$

When the equation for each point through the window is found a number of equations with a number of unknowns are obtained. Those equations are solved and the temperatures through the window are found. This is illustrated in an example in the following.

D.1 EXAMPLE

The procedure for calculating the temperature distribution through a window is as follows:

1. Divide the window into points seperated by elements
2. The transmission loss is written for each element, equation D.1
3. Longwave radiation is added between the two points on the surfaces bounding the cavity, equation D.2
4. The energy balance is written for each point, equation D.3
5. Each energy balance is rewritten and assembled in a matrix for calculation of the temperature at each point

D.1.1 POINTS AND ELEMENTS

The components of the window; two glass panes and one gas layer, is divided into an amount of elements with each element surrounded by two points. In the case of this report each component is divided into two elements, resulting in six elements and seven points, as seen in figure D.2.

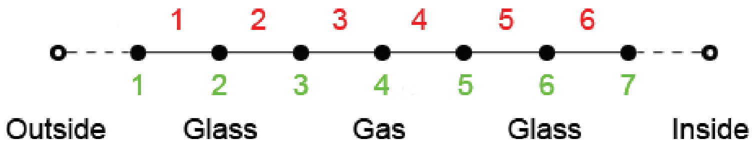

Figure D.2: *Window divided into points and elements including outdoor and indoor points.*

The convection within the gas layer is not taken into consideration and the temperature in the gas layer is assumed to be linear, even though that is not necessarily the case in reality.

D.1.2 TRANSMISSION LOSS

With the window divided into six elements, a total of six equations concerning the transmission loss is needed. These six equations are found using equation D.1 and with $^1/_R = U$, they can be written as the following:

$$\phi_1 = U_1 \cdot A \cdot (t_1 - t_2)$$

$$\phi_2 = U_2 \cdot A \cdot (t_2 - t_3)$$

$$\phi_3 = U_3 \cdot A \cdot (t_3 - t_4)$$

$$\phi_4 = U_4 \cdot A \cdot (t_4 - t_5)$$

$$\phi_5 = U_5 \cdot A \cdot (t_5 - t_6)$$

$$\phi_6 = U_6 \cdot A \cdot (t_6 - t_7)$$

D.1.3 ENERGY BALANCE

With the transmission loss equations given, the energy balance can be written. Due to steady state, each point must be in balance, i.e. in = out. With a higher indoor temperature than outdoors, the flow of energy will go from point 7 towards point 1. This means that point $j+1$ will receive energy from point $j+2$ and loose energy towards point j. Knowing that the points must be in balance energy wise, the transmission losses in the two surrounding elements, here element i and $i+1$, must be equal to each other since in = out. This yields the expression given in equation D.4, which can be rewritten as equation D.5.

$$\phi_i = \phi_{i+1} \tag{D.4}$$

$$U_i \cdot A \cdot \left(t_j - t_{j+1}\right) = U_{i+1} \cdot A \cdot \left(t_{j+1} - t_{j+2}\right) \tag{D.5}$$

By isolating the expression so it equals zero, the energy balance of point j+1 is achieved shown in equation D.6.

$$0 = U_i \cdot A \cdot \left(t_j - t_{j+1}\right) + U_{i+1} \cdot A \cdot \left(t_{j+2} - t_{j+1}\right) \tag{D.6}$$

The energy balance for each points of the window can be written as follows:

$$0 = h_e \cdot A \cdot (t_{out} - t_1) + U_1 \cdot A \cdot (t_2 - t_1)$$

$$0 = U_1 \cdot A \cdot (t_1 - t_2) + U_2 \cdot A \cdot (t_3 - t_2)$$

$$0 = U_2 \cdot A \cdot (t_2 - t_3) + U_3 \cdot A \cdot (t_4 - t_3) + \psi_{3-5} \cdot \epsilon_3 \cdot \epsilon_5 \cdot \sigma \cdot A_3 \cdot 4T_{ref}^3 \cdot (t_3 - t_5)$$

$$0 = U_3 \cdot A \cdot (t_3 - t_4) + U_4 \cdot A \cdot (t_5 - t_4)$$

$$0 = U_4 \cdot A \cdot (t_4 - t_5) + U_5 \cdot A \cdot (t_6 - t_5) + \psi_{5-3} \cdot \epsilon_5 \cdot \epsilon_3 \cdot \sigma \cdot A_5 \cdot 4T_{ref}^3 \cdot (t_5 - t_3)$$

$$0 = U_5 \cdot A \cdot (t_5 - t_6) + U_6 \cdot A \cdot (t_7 - t_6)$$

$$0 = U_6 \cdot A \cdot (t_6 - t_7) + h_i \cdot A \cdot (t_{inside} - t_7)$$

D.1.4 MATRIX AND CALCULATION

These equation can be written as a matrix shown in equation D.7.

$$Bx = b \tag{D.7}$$

Where B corresponds to $U \cdot A$ and x are the temperature of the points t_j. An example will be made for the general expression shown in equation D.6, which can be rewritten into equation D.8.

$$0 = \overbrace{U_i \cdot A}^{B_i} \cdot t_j + \overbrace{U_{i+1} \cdot A}^{B_{i+2}} \cdot t_{j+2} - \overbrace{(U_i \cdot A + U_{i+2} \cdot A)}^{B_{i+1}} \cdot t_{j+1} \tag{D.8}$$

By rewriting the energy balance equations from the previous section in the form of equation D.8 and setting them up in a matrix in the form of equation D.7, it would look like the matrix given below containing 7 equations with 7 unknowns.

$$\begin{bmatrix} B_2 & B_3 & 0 & 0 & 0 & 0 & 0 \\ B_3 & B_4 & B_5 & 0 & 0 & 0 & 0 \\ 0 & B_5 & B_6 & B_7 & LW & 0 & 0 \\ 0 & 0 & B_7 & B_8 & B_9 & 0 & 0 \\ 0 & 0 & LW & B_9 & B_{10} & B_{11} & 0 \\ 0 & 0 & 0 & 0 & B_{11} & B_{12} & B_{13} \\ 0 & 0 & 0 & 0 & 0 & B_{13} & B_{14} \end{bmatrix} \begin{bmatrix} t_1 \\ t_2 \\ t_3 \\ t_4 \\ t_5 \\ t_6 \\ t_7 \end{bmatrix} = \begin{bmatrix} -B_1 \cdot t_{out} \\ 0 \\ 0 \\ 0 \\ 0 \\ 0 \\ -B_{15} \cdot t_{in} \end{bmatrix}$$

In order to find the temperatures of the points 1-7, the above matrix is solved with respect to the temperatures, by taking the inverse of B.

The temperature distribution was calculated throughout the window described in chapter 3, with a temperature difference in between the inside and outside of 15° and a mean temperature of 10° of the gas-layer which are the standardized boundary conditions [Standard, 2011c]. These boundary conditions are achieved in the case of an outdoor temperature of 3° and an indoor temperature of 18°. The temperature distribution is shown in figure D.3.

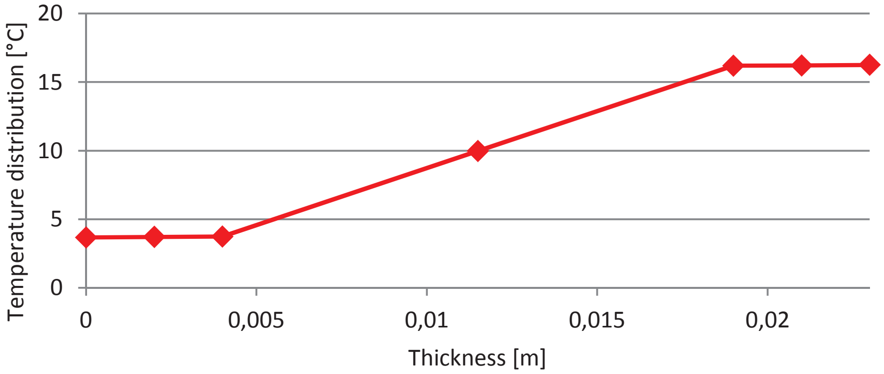

Figure D.3: *Temperature distribution through the window.*

ANGLE DEPENDENT TRANSMITTANCE, REFLECTANCE AND ABSORPTANCE

An incident angle of 0° occurs during sunrise or sunset for windows with a vertical position depending on their orientation. Otherwise the angle of incidence is different from 0°. To emphasize this a sun chart for the location of Copenhagen is shown in figure E.1 given for the 21st in every month of the year, the same sun chart as shown in chapter 2. In this case an east oriented vertical window will only have an angle of incidence of 0° at sunrise, where the solar altitude angle is just above 0°. The same goes for a west oriented vertical window at sunset.

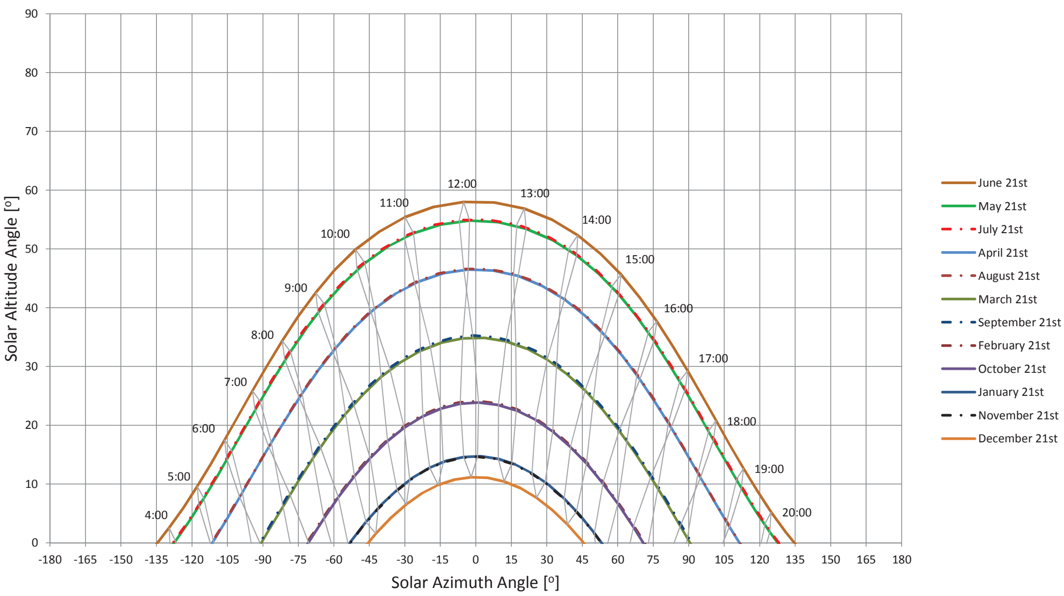

Figure E.1: *Sun chart at the location of Copenhagen.*

Due to this it is important to be able to evaluate the properties of glazing systems at different angles of incidence. A model calculating the transmittance τ, the reflectance ρ and the absorptance α, depending on the incident angle, has been made by combining the knowledge from different well-established literature. [Duffie and Beckman, 2006] [Standard, 2011b]

In order to determine the relation between τ, ρ and α as a function of the angle of incidence, certain properties of the panes in a glazing system needs to be known. Among these are the following three; the thickness of the glass, the refractive index and the extinction coefficient. The last two are functions of the radiations wavelength; though assuming wavelength independence has shown to be an excellent assumption [Duffie and Beckman, 2006].

The refractive index, n, of glass can be expressed as the ratio of the speed of light in vacuum relative to that in glass [Research, 2012]. For glass the refractive index is given at 1,526 meaning that the speed of light is 1,526 times faster in vacuum than in glass. For air the refractive index can be assumed to be unity since the speed of light in air is very close to the speed of light in vacuum. Since the refractive indices of air and glass are different from each other, the refraction angle will be different from the incident angle on the window, i.e. the radiation is deflected. Knowing that the speed of light is different in various mediums, Snell's law can be used to determine the refraction angle as a function of the refractive indices of the mediums, here air and glass, and the angle of incident. The situation is sketched in figure E.2.

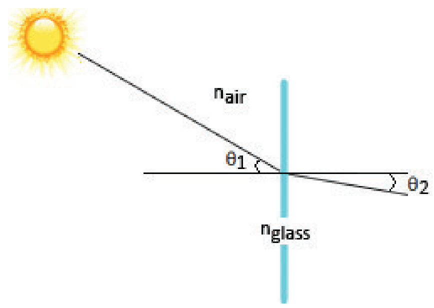

Figure E.2: *Incident angle θ_1 and refraction angle θ_2 as a function of different refractive indices in medium 1, air, afbøjetand medium 2, glass.*

The refraction angle shown in figure E.2 is calculated by use of Snell's law:

$$\frac{n_{air}}{n_{glass}} = \frac{sin(\theta_2)}{sin(\theta_1)} \tag{E.1}$$

The extinction coefficient, K, varies from $4\,m^{-1}$ for "water white" glass to approximately $32\,m^{-1}$ for greenish glass [Duffie and Beckman, 2006]. For a glazing with coating, this value could be even higher, but actual values have not been found. This will be estimated.

E.1 MODEL

The glazing system used in the experiment contains two different glass panes. Both panes are with a thickness of 0,004 m and a refractive index of 1,526. The outer pane has an extinction coefficient of 16,1 m^{-1} while it for the inner pane is found to be 85 m^{-1} to fit as best as possible to calculations in annex 4.1 on DVD. The calculations are based on these values.

As stated earlier in equation 3.2, the sum of the transmittance, τ, the reflectance, ρ, and the absorptance α is 1. With this in mind α is determined on behalf of τ and ρ. The principle of calculating the angular dependence of τ, ρ and α are based on a ray-tracing technique given in *"Solar Engineering of Thermal Processes"* [Duffie and Beckman, 2006].

E.1.1 TRANSMITTANCE, REFLECTANCE AND ABSORPTANCE

The transmittance of a glazing system containing two glass panes is calculated as a mean of the perpendicular and parallel components of the transmittance, as given in equation E.2. The same is the case for the reflectance as seen in equation E.3. These equations are based on the derived expressions by Fresnel [Duffie and Beckman, 2006].

$$\tau = \frac{1}{2}\left[\left(\frac{\tau_1\tau_2}{1-\rho_1\rho_2}\right)_\perp + \left(\frac{\tau_1\tau_2}{1-\rho_1\rho_2}\right)_\parallel\right] \tag{E.2}$$

$$\rho = \frac{1}{2}\left[\left(\rho_1 + \frac{\tau_1^2\rho_2}{1-\rho_1\rho_2}\right)_\perp + \left(\rho_1 + \frac{\tau_1^2\rho_2}{1-\rho_1\rho_2}\right)_\parallel\right] \tag{E.3}$$

where:

$\perp$	*Perpendicular components* [−]
$\parallel$	*Parallel components* [−]
τ_1	*Transmittance of the first (outer) pane* [−]
τ_2	*Transmittance of the second pane* [−]
ρ_1	*Reflectance of the first pane* [−]
ρ_2	*Reflectance of the second pane* [−]

The perpendicular components of the transmittance, $\tau_\perp$, and the reflection, $\rho_\perp$, is determined from equations E.4 and E.5.

$$\tau_\perp = \tau_\alpha \frac{1-r_\perp}{1+r_\perp}\left(\frac{1-r_\perp^2}{1-(r_\perp\tau_\alpha)^2}\right) \tag{E.4}$$

$$\rho_{\perp} = r_{\perp}(1 + \tau_{\alpha}\tau_{\perp}) \tag{E.5}$$

where:

r	*Reflection of radiation* [−]
τ_{α}	*Transmittance with only absorption losses considered* [−]

The parallel components are determined in a similar manner as shown in equations E.4 and E.5.

The reflection of radiation passing from medium 1, in this case air, to medium 2, glass, is covered by expressions derived by Fresnel containing a perpendicular and a parallel component, given by equations E.6 and E.7 [Duffie and Beckman, 2006].

$$r_{\perp} = \frac{sin^2(\theta_2 - \theta_1)}{sin^2(\theta_2 + \theta_1)} \tag{E.6}$$

$$r_{\parallel} = \frac{tan^2(\theta_2 - \theta_1)}{tan^2(\theta_2 + \theta_1)} \tag{E.7}$$

θ_1 and θ_2 are illustrated in figure E.2.

The transmittance of a glass pane, when only taking absorption losses into account and here by neglecting reflection losses, is described by Bouguer's law which can be rewritten into equation E.8.

$$\tau_{\alpha} = exp\left(-\frac{KL}{cos(\theta_2)}\right) \tag{E.8}$$

where:

K	*Extinction coefficient* [m^{-1}]
L	*Thickness of glass pane* [m]

E.2 RESULTS

Having presented the way of calculating the angular dependent transmittance, τ, the reflectance, ρ, and the absorptance, α, in section E.1, the results will now be presented. As mentioned earlier the results are given for a window comparable to the one used for the experiments, corresponding to a 2-layer glazing system with different glass panes. The angular dependent parameters are given in figure E.3, for two glass panes.

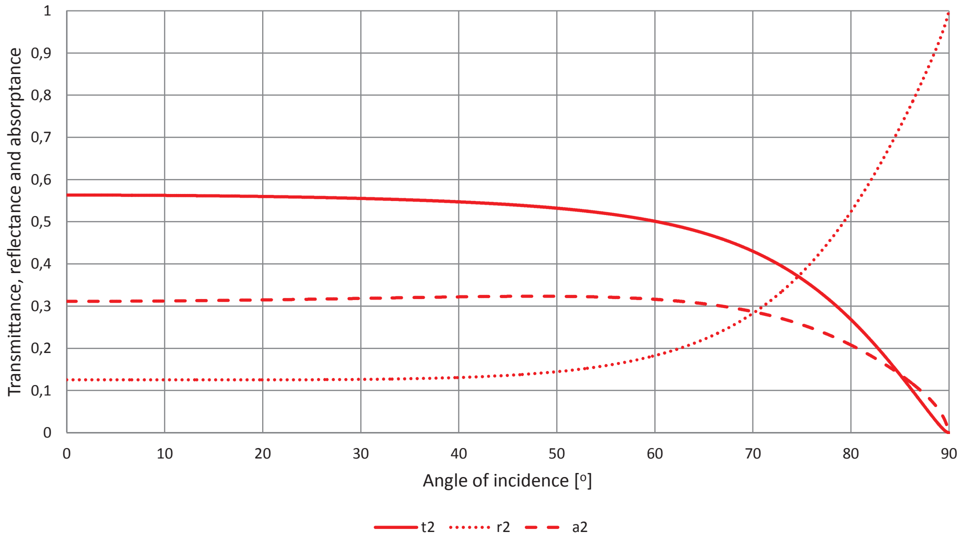

Figure E.3: *The transmittance, reflectance and absorptance for the glazing system used for the experiments as a function of incident angle.*

As seen from the graphs the closer the angle of incidence is to 0° the higher transmittance, and as the incident angle approaches 90° the reflectance is increasing. The absorption is more or less independent of the angle of incidence but is dropping to 0 at an angle of 90°.

APPENDIX F

LINEAR EQUATIONS

This appendix deals with the description of the basic linear equations used within this project, along with an example of how to calculate the specular and diffuse radiation.

F.1 FUNDAMENTALS

To express the line a and b values are found. The slope of the line a and the intersection with the y-axis b are calculated from equations F.1 and F.2 respectively.

$$a = tan(\angle) \tag{F.1}$$

where:

$\angle$	*Angle to the x-axis* [°]

$$b = y - ax \tag{F.2}$$

In equation F.2 x and y coefficients are the coordinates for a known point on the line. If no points are known, the intersection between two known lines, intersecting with the unknown line, are calculated from equations F.3 and F.4, to get a known point.

$$x = \frac{b_2 - b_1}{a_1 - a_2} \tag{F.3}$$

$$y = ax + b = a_1 \cdot \frac{b_2 - b_1}{a_1 - a_2} + b_1 \tag{F.4}$$

To find distances e.g. for the surfaces on the slats numbered in figure 8.5, Pythagoras' theorem is used. The distances are calculated from equation F.5.

$$|AB| = \sqrt{(x_2 - x_1)^2 + \left(y_2 - y_1\right)^2} \tag{F.5}$$

The coordinate system of the slat volume is illustrated in figure F.1.

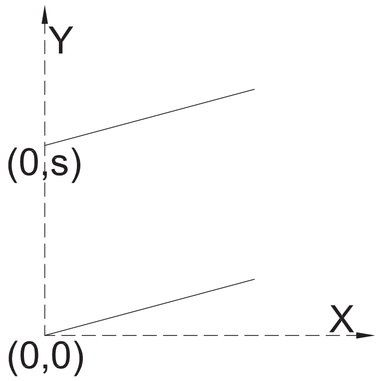

Figure F.1: *Coordinate system of the slat volume.*

F.2 EXAMPLE

This example describes the procedure of calculating the specular and diffuse radiation through the ray tracing technique based on linear equations. In the example the following parameters are known:

- Angle of radiation: $\Omega = 45^\circ$
- Slat angle: $\phi = 15^\circ$
- Vertical distance in between slats: $s = 7\,\text{cm}$
- Width of the slats: $v = 7\,\text{cm}$
- Distance from end of slat to the window at $\phi = 0^\circ$: 15,4 cm

The distances are shown in figure F.2 along with numbers describing the start and end coordinates of the slats $l1$ and $l2$. The angles are defined in figure F.3.

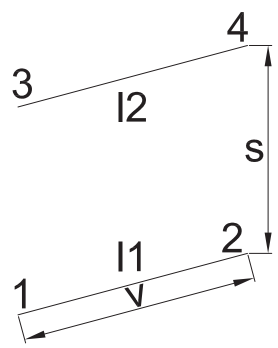

Figure F.2: *Definition of distances and points.*

The coordinates (x;y) of the points 1, 2, 3 and 4 shown in figure F.2 are calculated through the following:

$$
\begin{aligned}
1 &= (0;0) \\
2 &= \left(cos(\phi)\cdot v; sin(\phi)\cdot v\right) \\
3 &= (0;s) \\
4 &= \left(cos(\phi)\cdot v; sin(\phi)\cdot v + s\right)
\end{aligned}
$$

F.2.1 LENGTHS

The lines corresponding to the radiations and reflections are seen in figure F.3.

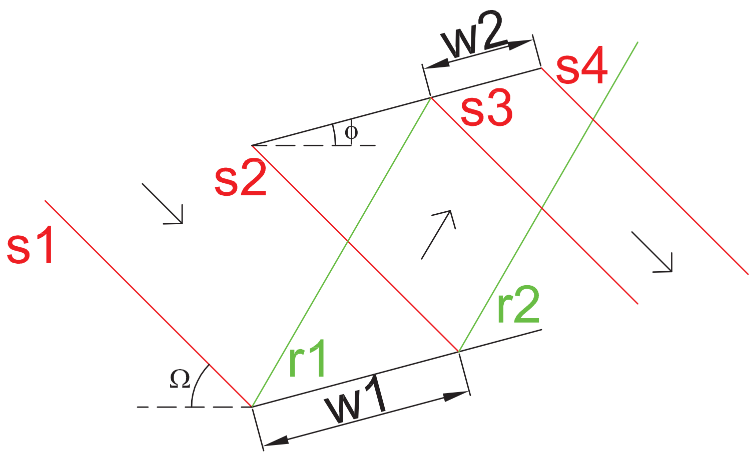

Figure F.3: *Radiation and reflectances through the slat volume.*

The linear equations for these lines are given in the following.

$$
\begin{aligned}
&s1: y = -tan(\Omega)\cdot x\\
&s2: y = -tan(\Omega)\cdot x + s\\
&s3: y = -tan(\Omega)\cdot x + \begin{cases} y_{r1l2} + tan(\Omega)\cdot x_{r1l2} \text{ if } x_{r1l2} \leq cos(\phi)\cdot v \text{ and } x_{r1l2} \geq 0\\ sin(\phi)\cdot v + s + tan(\Omega)\cdot cos(\phi)\cdot v \text{ if } x_{r1l2} > cos(\phi)\cdot v\\ s \text{ if } x_{r1l2} < 0\end{cases}\\
&s4: y = -tan(\Omega)\cdot x + \begin{cases} y_{r2l2} + tan(\Omega)\cdot x_{r2l2} \text{ if } x_{r2l2} \leq cos(\phi)\cdot v \text{ and } x_{r2l2} \geq 0\\ sin(\phi)\cdot v + s + tan(\Omega)\cdot cos(\phi)\cdot v \text{ if } x_{r2l2} > cos(\phi)\cdot v\\ s \text{ if } x_{r2l2} < 0\end{cases}\\
&r1: y = tan(\Omega + 2\phi)\cdot x\\
&r2: y = tan(\Omega + 2\phi)\cdot x \begin{cases} y_{s2l1} - tan(\Omega+2\phi)\cdot x_{s2l1} \text{ if } x_{s2l1} \leq cos(\phi)\cdot v\\ sin(\phi)\cdot v - tan(\Omega+2\phi)\cdot cos(\phi)\cdot v \text{ if } x_{s2l1} > cos(\phi)\cdot v\end{cases}
\end{aligned}
$$

As seen from the expressions, $s3$ and $s4$ are similar, with the intersections x and y as an exception. This will also be the case if the situation contains more reflections and here by more s-lines. As for lines above $s3$, lines of $r2$ and above are the same with x and y as exceptions. The term x_{r2l2} defines the x-coordinate for the intersection between the lines $r2$ and $l2$ etc.

The expressions for the slats $l1$ and $l2$ are given in the following:

$$
\begin{aligned}
&l1: y = tan(\phi)\cdot x\\
&l2: y = tan(\phi)\cdot x + s
\end{aligned}
$$

The way of calculating the lengths of the directly irradiated surface $w1$ and the surface irradiated by specularly reflection $w2$ is given in the following:

$$
w1 = \begin{cases} v & \text{if } \phi \text{ and } \Omega = 0\\ 0 & \text{if } \Omega = 0\\ \sqrt{(x_{s2l1}-0)^2 + (y_{s2l1}-0)^2} & \text{if } x_{s2l1} \leq cos(\phi)\cdot v\\ \sqrt{(cos(\phi)\cdot v - 0)^2 + (sin(\phi)\cdot v - 0)^2} & \text{if } x_{s2l1} > cos(\phi)\cdot v\end{cases}
$$

$$w2 = \begin{cases} v & \text{if } \phi \text{ and } \Omega = 0 \\ 0 & \text{if } \Omega = 0 \\ 0 & \text{if } \Omega + \phi \geq = 0 \\ 0 & \text{if } x_{r1l2} > \text{ and } x_{r2l2} > cos(\phi) \cdot v \\ w1 & \text{if } \Omega + 2 \cdot \phi = 90 \\ \sqrt{(x_{r2l2} - x_{r1l2})^2 + \left(y_{r2l2} - y_{r1l2}\right)^2} & \text{if } x_{r1l2} \geq 0 \text{ and } x_{r2l2} \leq cos(\phi) \cdot v \\ \sqrt{(x_{r2l2} - 0)^2 + \left(y_{r2l2} - s\right)^2} & \text{if } x_{r1l2} < 0 \\ \sqrt{\left(cos(\phi) \cdot v - x_{r1l2}\right)^2 + \left(sin(\phi) \cdot v + s - y_{r1l2}\right)^2} & \text{if } x_{r1l2} < \text{ and } x_{r2l2} > cos(\phi) \cdot v \end{cases}$$

F.2.2 TRANSMITTANCE

Illustrations to this section is seen in figure 8.2 chapter 8.
As the transmittance is calculated as the ratio in between the slat height s, and the irradiated height on the window W the line of the window needs to be known. This is given in the following:

$$V : x = \left(\frac{v}{2} + d\right) + cos(\phi)\frac{v}{2}$$

As for the lines of the radiations only the lower helping line $S1$ (capital) is unknown at this moment as $s2$ is given above. $S1$ is given as the following:

$$S1 : y = -tan(\Omega) \cdot x + \left(sin(\phi) \cdot v + tan(\Omega) \cdot cos(\phi) \cdot v\right)$$

The irradiated height of the window W is found through the following expression:

$$W = \begin{cases} 0 & \text{if } x_{s2l1} \leq cos(\phi) \cdot v \\ y_{s2V1} - y_{S1V1} & \text{if } x_{s2l1} > cos(\phi) \cdot v \end{cases}$$

APPENDIX G

CONVECTION

To calculate the exterior heat transfer coefficient, h_e, when dealing with a window installed with a solar shading, the type of flow in between the shading and the glazing system needs to be determined. The flow will either occur by forced convection or by free convection. Forced and free convection have something to do with how the boundary layer of the glazing is created. In case of free convection the flow is driven by internal forces, which are temperature differences in between the surfaces bounding the cavity and the cavity.

In free convection the air velocity is increasing with the height of the window, meaning that the velocity will be lowest at the bottom of the window and highest at the top of the window. In some situations this means that the flow will be laminar at the bottom of the window, after some while it will be mixed and at the top the flow will be turbulent. If the window is not high enough the flow will never be turbulent. In case of forced convection the height of laminar flow will probably be less than in case of free convection and the turbulent flow will occur earlier. This is because of the influence of external forces which will dominate the flow.

G.1 FORCED CONVECTION

Forced convection is when external forces, e.g. the wind is dominating the flow. The expected velocity profile of forced convection is shown in figure G.1, where the velocity is constant away from the window and drop to zero at the glazing.

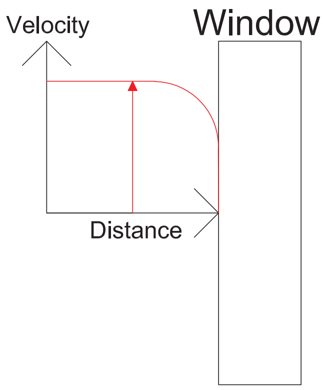

Figure G.1: *Sketch of the expected velocity profile in case of forced convective flow.*

The area of validity for laminar and turbulent flow is for forced convection along a surface determined on behalf of the Reynolds' number. Laminar flow occurs at a Reynolds' number below 100.000 while turbulent flow is defined at a Reynolds' number above 500.000.

G.2 FREE CONVECTION

Free convection is when internal boundary conditions are dominating. In this case the velocity profile is expected to show a velocity of zero far away from the window and the shading, and in between the two a velocity gradient will arise and give a free stream peak value before it will drop down to zero at the glazing. A rough illustration of the velocity profile is seen in figure G.2.

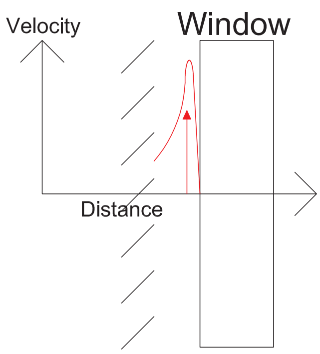

Figure G.2: *Sketch of the velocity profile in case of free convective flow.*

The area of validity for laminar and turbulent flow is for free convection determined on behalf of Rayleigh's number. Laminar flow occur at a Rayleigh's number in the region $10^4 - 10^8$ while turbulent flow is defined in a region of $10^8 - 10^{12}$.

In this report where a window installed with a solar shading is investigated the flow is expected to occur by free convection since the experimental setup is located indoors, hence no external forces will be acting on the glazing system. In order to determine the flow of the cavity velocity profiles needs to be measured at different heights of the window in order to get a mean value. This is done in the following.

G.3 AIR FLOW OF THE EXPERIMENT

The air flow in the cavity was investigated through experiments in which velocity profiles, each consisting of 5 measurements, was generated at different locations in the cavity. Based on these velocity profiles an overall air flow rate will be determined. The velocity profile was measured at four different heights as illustrated in figure 11.8 along with three different locations on a horizontal line at the height of 50 cm. The results are seen in figures G.3 and G.4 for vertical and horizontal measurements respectively.

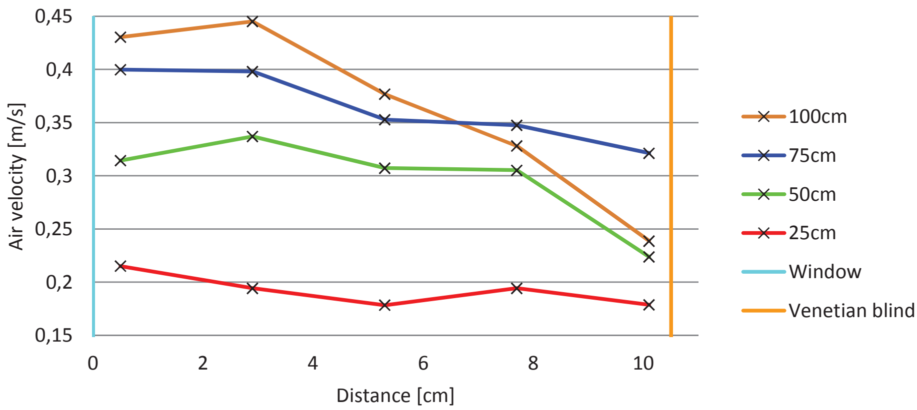

Figure G.3: *Velocity profiles measured across the cavity at four different heights.*

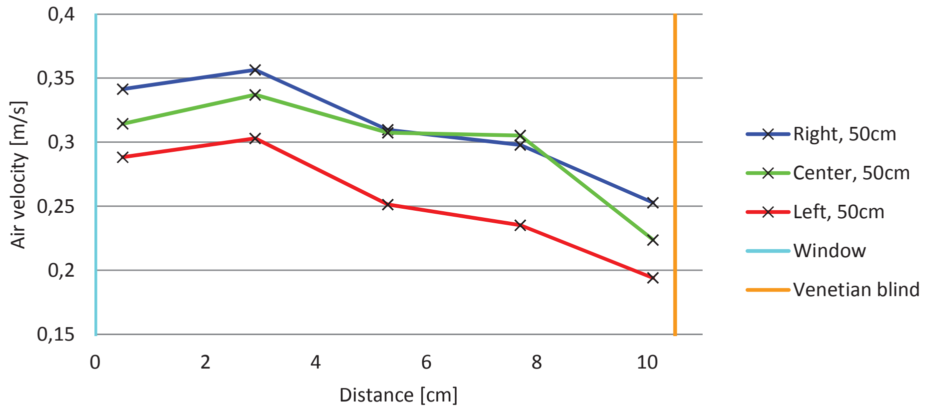

Figure G.4: *Velocity profiles measured across the cavity at three different horizontal locations.*

As can be seen from figure G.3 the velocity in the cavity is increasing with the height, while figure G.4 reveals that the velocity is more or less constant over the width of the window. The fact that the velocity is increasing with height, is in agreement with the behauvior of free convection flows as described in section G.2

By averaging all the measurements shown in figure G.3 an average velocity of the cavity is achieved. The average velocity is found to be 0,3 $^{m}/_{s}$. Having the velocity of the air, the air flow rate can be found with knowledge of the horizontal area of the cavity by multiplication of the two. The average air flow rate of the cavity is found to be 0,035 $^{m^3}/_{s}$. Measurements and calculations are seen in annex 9.1 on DVD.

For comparison reasons the theoretical peak velocity and the air flow rate was calculated with use of equations valid for free convection in case of rising flow along warm surface. These are shown in equation G.1 and G.2 respectively. [Nielsen et al., 2002]

$$v = 0,1 \cdot \left(|\Delta t| \cdot y\right)^{0,5} \tag{G.1}$$

$$q \approx 2,75 \cdot 10^{-3} \cdot (|\Delta t|)^{0,4} \cdot y^{1,2} \cdot w_{window} \tag{G.2}$$

where:

v	*Peak velocity in the flow* [$^{m}/_{s}$]
q	*Air flow rate* [$^{m^3}/_{s}$]
y	*Distance from the bottom of the glazing system* [m]
w_{window}	*Width of the window* [m]

The temperature difference Δt defines the temperature difference in between the bounding surfaces and the air temperature entering the cavity. This is outlined in equation G.3.

$$\Delta t = \left(\frac{t_{slats} + t_{glass}}{2} - t_{cavity,in} \right) \tag{G.3}$$

The theoretical peak velocity calculated through equation G.1 is compared with the measured peak velocity in table G.1. The measured peak velocity is seen as the maximum measured velocity from each velocity profile given in figure G.4.

Peak velocity [m/s]				
y [m]	0,25	0,5	0,75	1
Measurements	0,22	0,34	0,4	0,45
Calculations	0,2	0,28	0,34	0,39
Air flow rate [m³/s]				
Measurements	0,022	0,034	0,042	0,042
Calculations	0,0018	0,0042	0,0068	0,0095

Table G.1: *Comparison of peak velocities and air flow rates calculated with measurements for different heights at a slat angle of 45°.*

As can be seen from table G.1, the measured values do not match the calculated once. But as can be seen from the velocity profiles in figure G.3 the velocity of the flow is increasing with height which is characteristic for free convection. The calculations do not imply free convection but the measured velocity profiles does. The conclusion to this is that the flow does not entirely consist of free convection but must be a mix of both free and forced convection. Due to this, the equations used for the calculations assume a velocity profile different from the measurements which is the reason for the big error in between calculations and measurements. This is not investigated further within this project.

APPENDIX H

BOUNDARY CONDITIONS

Throughout the calculations and experiments two sets of boundary conditions have been used dependent on the given situation. This appendix deals with the description of these two sets of boundary conditions, which are the following:

- Standardised boundary conditions [Standard, 2011a], [Standard, 2011b], [Standard, 2011c]
- Boundary conditions matching the ones from the experiments

The boundary conditions consist of the following parameters:

- External heat transfer coefficient, h_e
- Internal heat transfer coefficient, h_i
- Temperature difference between bounding glass surfaces (theory only), Δ_T
- Mean temperature of gas space in glazings (theory only), T_m
- Surface and air temperatures (experiment only)
- Radiation levels (experiment only)

These are given in the following sections.

H.1 STANDARDISED BOUNDARY CONDITIONS

The boundary conditions of the standards, which are used for the calculation of the U-value and g-value are shown in table H.1.

h_e	$25\,{}^{\mathrm{W}}/_{\mathrm{m^2K}}$
h_i	$7{,}7\,{}^{\mathrm{W}}/_{\mathrm{m^2K}}$
Δ_T	$15\,\mathrm{K}$
T_m	$283\,\mathrm{K}$

Table H.1: *Standardised boundary conditions. [Standard, 2011c]*

The standardized relative spectral distribution is shown in figure H.1.

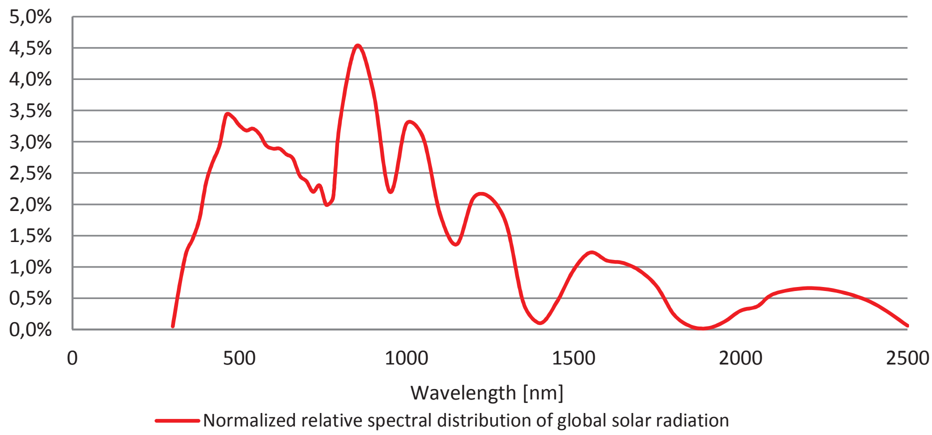

Figure H.1: *Normalized relative spectral distribution of global solar radiation.*

H.2 EXPERIMENTAL BOUNDARY CONDITIONS

The experimental boundary conditions do not consist of an external heat transfer coefficient, as this needs to be calculated. Due to the fact that no literature deals with the specific case of theory on heat transfer coefficient for a glazing system with external Venetian blinds, this value is found based on an energy balance for the system. This energy balance requires a set of temperatures why these are listed instead of the heat transfer coefficient, as these vary with the slat angle. The internal heat transfer coefficient is assumed to be the same as for the standard. The required temperatures for determination of the external heat transfer coefficient is given in table H.2 as a function of slat angle.

ϕ [°]	0	15	30	45	60	70
$t_{cavity,in}$	25,7	26	26,9	27,4	26,1	25,5
$t_{cavity,out}$	36,9	36,8	36,5	37,3	38,2	39
t_{cavity}	31,3	31,4	31,7	32,3	32,1	32,2
t_{glass}	53,9	50,5	46,8	43,4	38,5	36,3
t_{slat}	43,6	46	49,4	49,8	49,8	49,6

Table H.2: *Temperatures of the experiment, given in degrees celcius.*

The radiative levels as a function of distance from the sun, used for determining the amount of radiation on the Venetian blind and the window, is calculated from a curve fit on the preliminary experiment. This is already shown in chapter 12 but is regiven in figure H.2.

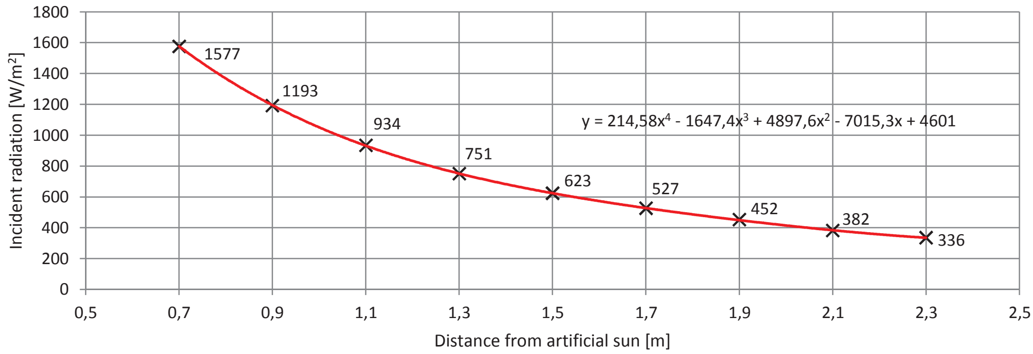

Figure H.2: *Radiation from the artificial sun as a function of distance. The black marks indicate measured data while the red line is a trend line.*

The experimental relative spectral distribution is shown in figure H.3.

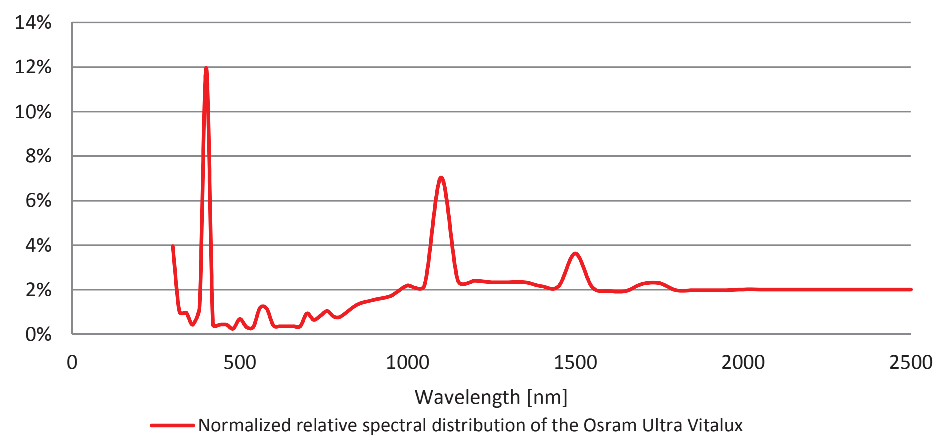

Figure H.3: *Experimental relative spectral distribution of global solar radiation.*

Data required through experiments, which are used for determination of the experimental boundary conditions, are given in annex 9.2 on DVD.

H.3 BOUNDARY CONDITIONS FOR THE CURTAIN

With the use of a curtain the temperatures of both the cavity and the surfaces are approximated based on the tendency of the measured temperatures for the experiments with the Venetian blind. This is because the curtain is assumed to correspond to the Venetian blind layer with a slat angle of 90°. The experimental temperatures are shown in figure H.4 together with their tendency lines, which are extended to 90°. This is done in annex 6 on DVD.

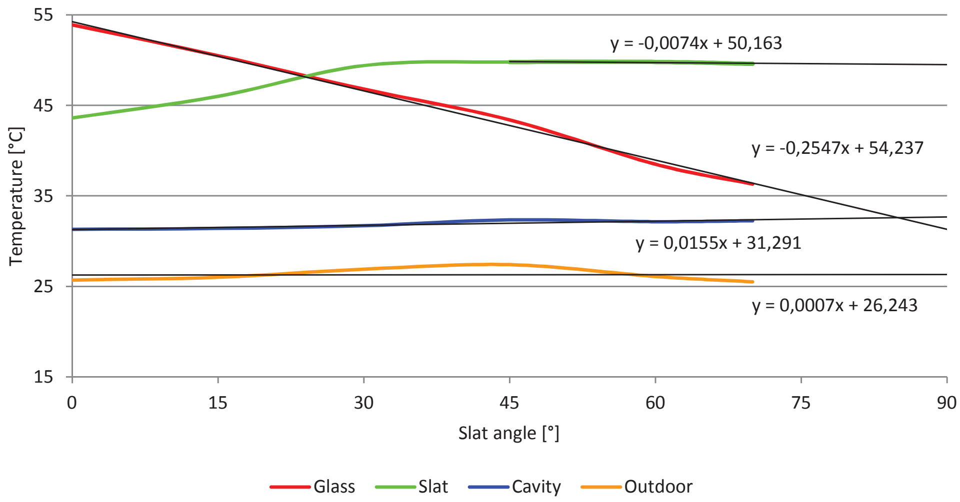

Figure H.4: *Experimental temperatures together with their extended tendency lines.*

From this the temperatures used in the calculations of the curtain is approximated to the ones given in table H.3. The slat is in this case seen as the curtain. Because the tendency line for the temperature in the cavity gives a lower value than the outdoor temperature at a slat angle of 90 °C it is set to the 26 ° which is higher than outdoor.

t_{glass} [°C]	31,3
$t_{curtain}$ [°C]	49,5
t_{cavity} [°C]	33,7

Table H.3: *Temperatures used in case of a curtain.*

APPENDIX I

MEASURING EQUIPMENT

This appendix contains a brief description of the measuring equipment used in the experiments and the calibration of the thermocouples and anemometers. The equipment consists of:

- Precision Pyranometer type CM 21
- Gossen Panlux electronic 2 light meter
- Fluke 289 True RMS Multimeter
- Grant SQ1600 Data Logger for thermocouples and pyranometer
  - 6x Shielded Type-K Thermocouples
  - 7x Type-K Thermocouples
- National Instruments DAQCard-700 Data Logger for velocity transducers
  - 6x Dantec 54R10 low velocity transducer

I.1 PRECISION PYRANOMETER TYPE CM 21

A picture of the equipment is shown in figure I.1.

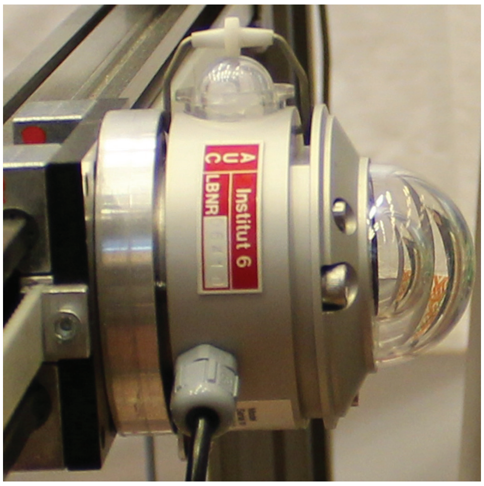

Figure I.1: *Picture of the Precision Pyranometer type CM 21.*

The pyranometer is measuring the global radiation, i.e. both the direct and diffuse radiation. The measured value is given in volts and the corresponding radiation is given through the following relation:

$$10,88\mu V/W/m^2$$

The measured voltage is divided by the expression above, independent of the measured value, i.e. the correlation is linear. The maximum error due to temperature is 0.38 % at a device temperature of 50 °C [Zonen, 2006]. This small possible error is considered negligible.

The device itself is said to have a level of confidence of 95 %.

I.2 GOSSEN PANLUX ELECTRONIC 2 LIGHT METER

A picture of the equipment is shown in figure I.2.

Figure I.2: *Picture of the Gossen Panlux electronic 2 light meter.*

The light meter is used in the experiments for measurements of the light intensity. Opposite to the other equipment the light meter is analogue. The accuracy of the light meter is ± 3,5 %.

I.3 FLUKE 289 TRUE RMS MULTIMETER

A picture of the equipment is shown in figure I.3.

Figure I.3: *Picture of the Fluke 289 True RMS Multimeter.*

The voltage to the artificial sun is measured with use of the multimeter to control the voltage of the various experiments.

I.4 GRANT SQ1600 DATA LOGGER

A picture of the equipment is shown in figure I.4.

Figure I.4: *Picture of the Grant SQ1600 Data Logger.*

The Grant data logger logs the voltages measured with the thermocouples and pyranometer. These are calculated into corresponding temperatures and radiation.

I.4.1 TYPE-K THERMOCOUPLES

A picture of the equipment, unshielded and shielded, is shown in figure I.5.

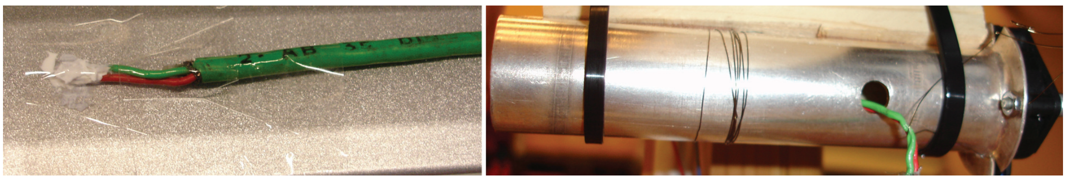

Figure I.5: *Picture of the Type-K Thermocouples. Left: unshielded. Right: shielded.*

The temperature of surfaces are measured with unshielded thermocouples, while air temperatures are measured with use of a shielded thermocouple equipped with a fan in the end of the highly reflective pipe to ensure that the measured temperature is only the air temperature and not the operative temperature which is also a function of radiation.

I.5 NATIONAL INSTRUMENTS DAQCARD-700 DATA LOGGER

A picture of the equipment is shown in figure I.6.

Figure I.6: *Picture of the National Instruments DAQCard-700 Data Logger.*

The air velocities measured with use of the velocity transducers are logged with use of this device.

I.5.1 DANTEC 54R10 LOW VELOCITY TRANSDUCER

A picture of the equipment is shown in figure I.7.

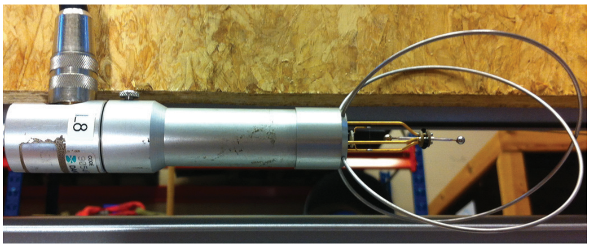

Figure I.7: *Picture of the Dantec 54R10 low velocity transducer.*

This device also measures a voltage which can be translated into the velocity of the air. The precision of the device is said to be ± 0,05 $^{m}/_{s}$, i.e. around 10-15 % for the conducted experiments, as the air velocity was in the region of approximately 0,3-0,5 $^{m}/_{s}$ [Hyldgård, 1997].

I.6 CALIBRATION

For the conducted measurements both thermocouples and anemometers were calibrated before actual measurements. This section deals with the procedure for calibrating this equipment.

I.6.1 THERMOCOUPLES

For the calibration of the thermocouples a device able to keep a constant temperature was used along with a reference thermometer. The thermocouples response to temperature is linear and the output from the thermocouples was investigated at the temperatures 10°, 30°, 50° and 70°. A calibration curve was made based on what voltage the thermocouple was measuring compared to the actual temperature measured by the reference thermometer. An example of a calibration curve along with an expression on how to calculate the temperature based on the measured volts is given in figure I.8.

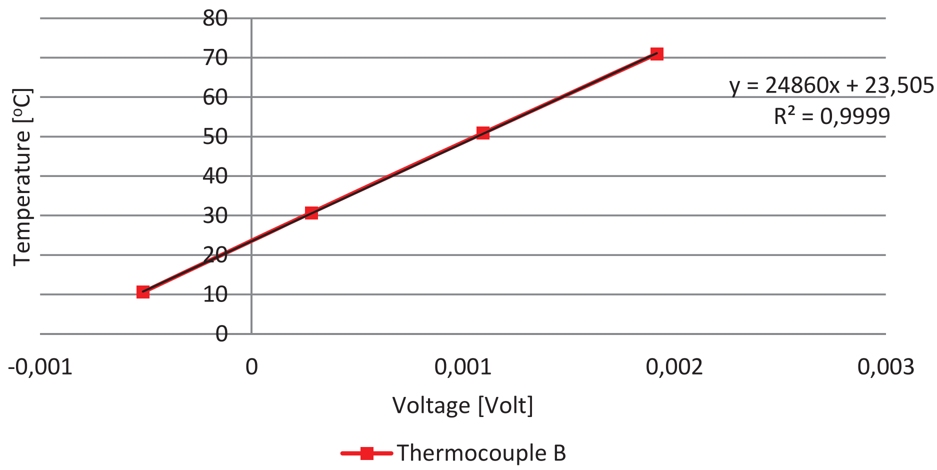

Figure I.8: *Calibration curve and expression for a thermocouple.*

The calibration curves for the remaining thermocouples can be found in annex 10.1 on DVD.

I.6.2 ANEMOMETERS

The anemometers were calibrated in a wind tunnel where the actual air velocity was known. This was done at enough different velocities within 0-1 $^{m}/_{s}$ in order to get an expression valid for the entire span. As for the thermocouples the measured voltage of the anemometers was translated into an air speed based on the actual air velocity at the moment of the measured voltage from the anemometers. An example of a the measurements is seen in figure I.9.

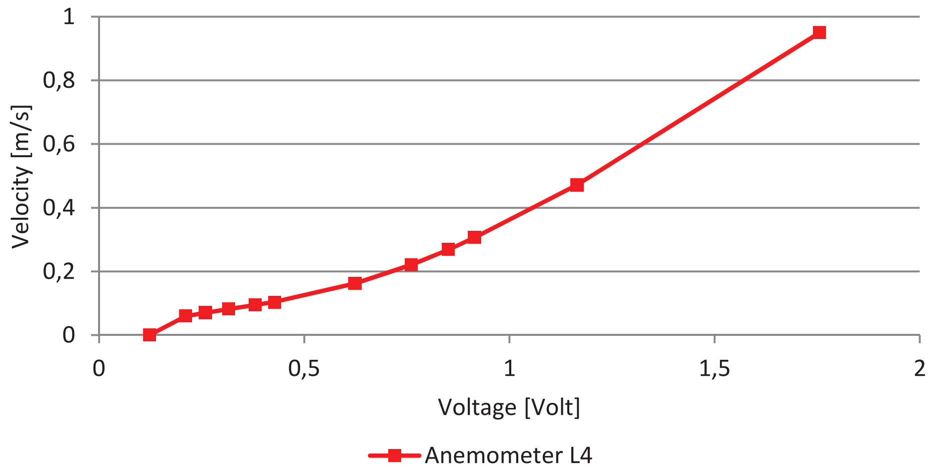

Figure I.9: *Measured air velocities as a function of voltage.*

The input to the computer in case of calibration curves is given through calibration files and not a tendency line as for the thermocouples. For the anemometers interpolation is made in between measuring point's conversion of voltages to air velocity. The calibration files can be seen in annex 10.2 on DVD.

APPENDIX J

PLANNING OF THE EXPERIMENTS

This appendix presents the procedure used in the planning of the experiments conducted through this project, followed by the actual plan and description of the 5 experiments and the preliminary one.

Due to the costs of and time needed to conduct experiments, careful planning of the experiments is essential [Aiulfi et al., 1998]. The procedure followed to ensure this is presented below [Roulet, 1992].

1. Define the problem to be solved. If there is no problem, no measurement need be performed!
2. List the questions to be answered to solve the problem.
3. List the measurements required, if any, to answer these questions.
4. Define the method which will be used to interpret the measurements in order to get the required information with the required accuracy (and not better, accuracy is expensive!). Perform preliminary error analysis.
5. Define the conditions in which the measurements will be performed; in particular define the best location of measurement points.
6. Choose the appropriate instruments.

The following sections describing each of the 5 experiments are based on this guideline. 3 different experiments with shading and 2 without shading, leading to 5 experiments in total plus the preliminary experiment.

J.1 PRELIMINARY EXPERIMENT - PLAN AND DESCRIPTION

1. The goal of this preliminary experiment is to determine the best location for doing the measurements of the solar radiation.

2. What is the radiation distribution as a function of the distance from the artificial sun. Is the distribution of the radiation uniform, i.e. will the amount of radiation hitting the window be the same throughout the surface of the window?

3. In order to answer the questions given, the radiation is measured in different distances from the sun, and in one of these distances the radiation is measured in 25 points to verify whether it is uniform or not.

4. Based on the measurements in different distances, the radiation distribution will be drawn as a function of the distance from the artificial sun. Based on this graph the most suitable position for further measurements and location of the glazing system will be decided. In the most suitable location the radiation will be measured in more than one point and it is verified, based on these grid measurements, whether the distribution is uniform or not.

5. Measurements are done in multiple locations in order to gain knowledge about most suitable locations for the further experiments.

6. The main components used for the experimental setup includes; artificial sun. The instrument used for measuring is the following; pyranometer.

J.2 EXPERIMENT 1 - PLAN AND DESCRIPTION

1. The goal of this experiment is to measure the transmittance, τ_e, of the window which is one of the two parameters of a windows g-value. This is done without shading applied.

2. What is the solar radiation in a given distance, behind the window, both with and without the window in place.

3. Measurements of the solar radiation from the artificial sun needs to be done behind the window.

4. In the distance from the artificial sun where the radiations are measured, the measuremenets are carried out in not only one point but in a line with 14 points. The results are given as a mean of these 14 points. The difference in between the radiations measured in front of and behind the window is used to calculated the transmittance, τ_e.

5. On behalf of the preliminary experiment, the distance from the artificial sun to the measurement points have been chosen to 1,7 m, since this ensures good conditions for the experiment in case of sufficient solar radiation.

6. The main components used for the experimental setup includes; artificial sun and window. The instrument used for measuring is the following; pyranometer.

J.3 EXPERIMENT 2 - PLAN AND DESCRIPTION

1. The goal of this experiment is to measure the transmittance, τ_e, of the glazing system including the Venetian blind which is one of the two parameters of a windows systems g-value. This is done while applying solar shading in case of a Venetian blind with slats at the following angles; 0°, 15°, 30°, 45°, 60° and 70°.

2. What is the solar radiation in a given distance, behind the window and the shading, both with the window and the shading in place and without the shading but with the window in place. With shading the measurements needs to be done for each of the given slat angles.

3. Measurements of the solar radiation from the artificial sun needs to be done behind the glazing system.

4. In the distance from the artificial sun where the radiations are measured, the measuremenets are carried out in not only one point but in a line with 14 points. The results are given as a mean of these 14 points. The difference in between the radiations measured in front of and behind the window is used to calculated the transmittance, τ_e.

5. On behalf of the preliminary experiment, the distance from the artificial sun to the measurement points have been chosen to 1,7 meter, since this ensures good conditions for the experiment in case of sufficient solar radiation.

6. The main components used for the experimental setup includes; artificial sun, window and the Venetian blind. The instrument used for measuring is the following; pyranometer.

J.4 EXPERIMENT 3 - PLAN AND DESCRIPTION

1. The goal of this experiment is to determine the exterior heat transfer coefficient. This is done while applying solar shading in case of Venetian blind with slats at the following angles; 0°, 15°, 30°, 45°, 60° and 70°.

2. What is the mean temperature of the air in between the Venetian blind and the window? What is the mean surface temperature of the windows exterior surface, i.e. the surface closest to the artificial sun? What is the temperature of the slat surface facing towards the window? What is the mean velocity of this air?

3. Measurements of the air temperature in between the Venetian blind and the window. Measurements of the temperature on the surface of the slats facing towards the window. Measurements of the temperature on the exterior surface of the window. Measurements of the air velocity in the cavity between the blinds and the window.

4. The measured data in case of temperatures and velocity are used to calculate the heat transfer coefficient by use of the equations valid for this.

5. The measurements of the air temperature and velocity in the cavity will be done in three vertical points in the middle of the cavity. The temperature on the slats will be measured in two upper points and one lower point on a centralised slat. The outer surface temperature of the window will be done in two points at the center of the window.

6. The main components used for the experimental setup includes; artificial sun, window and the Venetian blind. The instruments used for measuring are the following; shielded thermocouples for measuring air temperature, thermocouples for surface temperature and anemometers.

J.5 EXPERIMENT 4 - PLAN AND DESCRIPTION

1. The goal of this experiment is to measure the light transmittance of the window and compare this with the solar direct transmittance found in experiment 1 to see whether there is a difference between the two values or not. This is done without shading applied.

2. What is the light intensity in a given distance, behind the window, both with and without the window in place.

3. Measurements of the light intensity received from the artificial sun, needs to be done behind the window.

4. In the distance from the artificial sun where the light intensity are measured, the measurements are carried out in not only one point but in a line with 14 points. The results are given as a mean of these 14 points. The difference in between the light intensity measured in front of and behind the window is used to calculated the LT-value of the window.

5. The measurements are carried out in the same points as the solar direct transmittance in experiment 1 and 2 which is in a distance of 1,7 m.

6. The main components used for the experimental setup includes; artificial sun and window. The instrument used for measuring is the following; Light meter.

J.6 EXPERIMENT 5 - PLAN AND DESCRIPTION

1. The goal of this experiment is to measure the light transmittance of the window and compare this with the transmittance found in experiment 2 to see whether there is a difference between the two values or not. This is done while applying solar shading in case of a Venetian blind with slats at the following angles; 0°, 15°, 30°, 45°, 60° and 70°.

2. What is the light intensity in a given distance, behind the window and the shading, both with the window and the shading in place and without the shading but with the window in place. With shading the measurements needs to be done for each of the given slat angles.

3. Measurements of the light intensity received from the artificial sun needs to be done behind the glazing system.

4. In the distance from the artificial sun where the light intensity are measured, the measurements are carried out in not only one point but in a line with 14 points. The results are given as a mean of these 14 points. The difference in between the light intensity measured in front of and behind the window is used to calculated the LT-value of the window.

5. The measurement are carried out in the same points as the solar direct transmittance in experiment 1 and 2 which is in a distance of 1,7 m.

6. The main components used for the experimental setup includes; artificial sun, window and the Venetian blind. The instrument used for measuring is the following; Light meter.

APPENDIX K

EXPERIMENTAL PROBLEMS

This appendix deals with the description of some of the problems which have arisen through the experiments and may have led to errors.

K.1 ANEMOMETERS

Before using the anemometers they have to be calibrated, which can be done for two scenarios:

- vertical flow
- horizontal flow

As can be seen in figure 11.1 section 11 a total of six anemometers where used located in different positions. Based on smoke the four anemometers in the middle of the experimental setup was assumed to be positioned in a vertical air flow stream, while the two on the sides was assumed to be positioned in a horizontal air flow stream. Even though the smoke measurements showed flow like this most of the times, the flow direction was very unsteady in some of the points, hence hard to determine. This means that there may be some uncertainties in the results of the measurements.

K.2 DATA LOGGER WITHOUT ICE POINT REFERENCE

The measuring of temperatures was done with a data logger, as described in appendix I, which does not use an Ice Point Reference. As this is not the case the ambient temperature can influence the results, as the thermocouples are calibrated at one ambient temperature and the measurements may have been done with a different ambient temperature. This can produce errors in the measurements as the thermocouples measures a difference in voltage from the temperature it measures to the temperature of the data logger.

K.3 EXPERIMENTAL SETUP

An error of the experimental setup was discovered as the artificial sun was not totally vertical, due to the heavy weight and the poor possibility to secure the artificial sun in a straight vertical line. This meant that it was tilted a bit downwards which led to a higher solar radiation at the bottom of the window than at the top.

K.4 INACCURATE SLAT ANGLES

The Venetian blind used throughout the experiments showed to be inaccurate in case of adjusting the angle of the slats. The slat angle was adjusted by setting the correct angle on the slats in the middle of the Venetian blind but this did not give the exact same slat angle at the top and bottom of the Venetian blind, which may have affected the measurements.

K.5 INTERFERENCE IN MEASUREMENTS

The pyranometer used in the experiments is measuring a voltage which is translated into a solar radiation. The robot used for moving around the pyranometer showed to produce a constant interference in the readings of the solar radiation meaning that the measured solar radiative levels had to be subtracted $16{,}5\,{}^{W}/_{m^2}$.

K.6 VARYING VOLTAGE

To see if the effect of averaging the results from periods with varying voltage around 227 V is negligible or not, the results were analysed in the following two ways. After steadiness in the measurements have occurred...

1. all data is averaged
2. only data measured when the voltage was close to 227 V is averaged

The results of option 1 and 2 are illustrated in figure K.1 as a 5 by 5 grid, with option 1 to the left and option 2 to the right.

	1	2	3	4	5
1	472	496	502	496	479
2	508	522	521	524	513
3	514	526	540	536	527
4	518	537	535	530	510
5	496	514	532	509	493

	1	2	3	4	5
1	472	492	502	496	480
2	505	519	523	524	513
3	514	529	540	536	525
4	517	536	537	531	509
5	496	512	528	518	488

Figure K.1: *Measured averaged radiation levels in* $^{W}/_{m^2}$ *based on two different ways of data processing. Left: All data averaged. Right: Data averaged for periods where voltage to the sun has been around 227*V*.*

As seen from the results shown in figure K.1 the variation in between the two distribution graphs are close to zero and averaging the graphs results in an average radiation of 514 $^{W}/_{m^2}$ for both option 1 and 2 meaning that the voltage is negligible as long as it is varying around the same voltage for all experiments. The cumulative distribution of the voltage recorded when running the experiments are seen in appendix M. The voltages are the ones used to generate the two sets of results in figure K.1.

As mentioned, tests have been made where the voltage was as low as 222 V which gave noticeable lower radiation levels. Based on this, it is recommended that all future experiments are to be run at voltages in the same region.

APPENDIX L

RADIATION THROUGH SLATS

The radiation through the slats determined from experiments is shown in figures L.1, L.2 and L.3 for a slat angle of 0°, 15°, 30°, 45°, 60° and 70°. The measuring points are shown to illustrate how the radiation is at the different points. All the situations is valid for an incident angle of 0°.

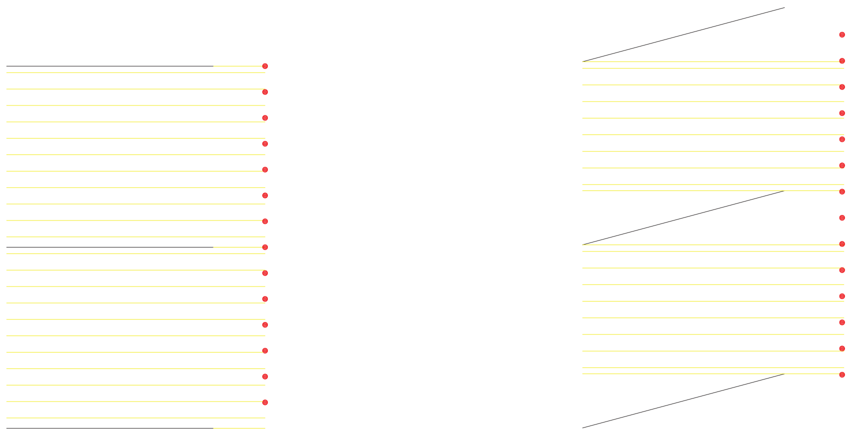

Figure L.1: *Illustration of radiation through slats and measuring points. Left: Slat angle of 0°. Right: Slat angle of 15°.*

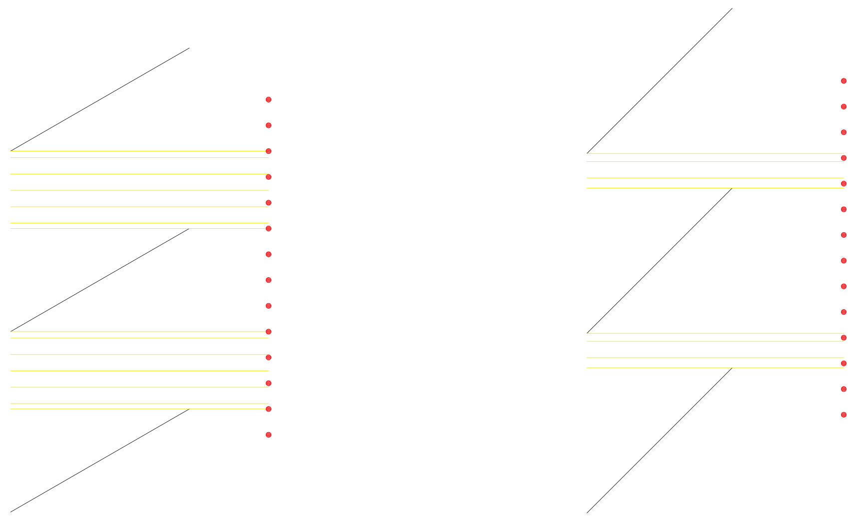

Figure L.2: *Illustration of radiation through slats and measuring points. Left: Slat angle of 30°. Right: Slat angle of 45°.*

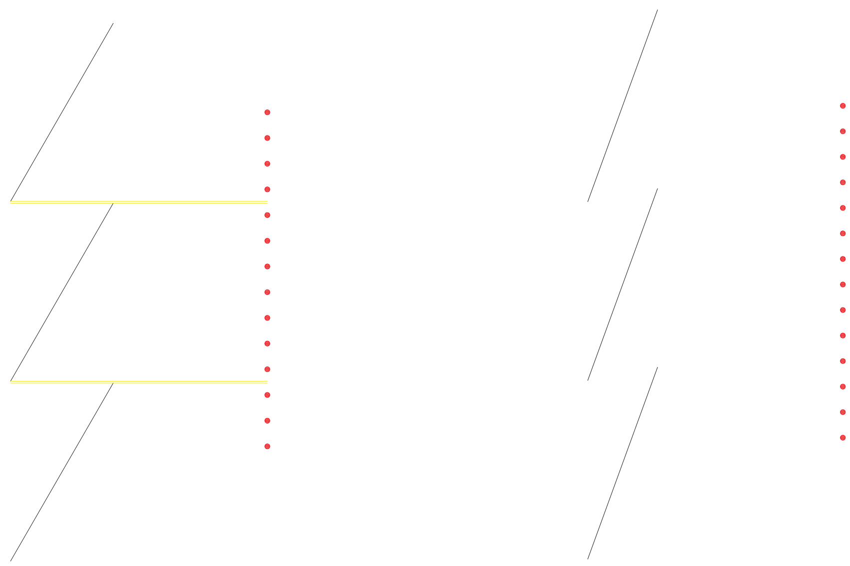

Figure L.3: *Illustration of radiation through slats and measuring points. Left: Slat angle of 60°. Right: Slat angle of 70°.*

APPENDIX M

CUMULATIVE DISTRIBUTION GRAPHS

This appendix contains cumulative distribution graphs of recorded voltages during the preliminary experiments described in chapter 12. The measurements are given in annex 11 on DVD.

Two sets of graphs are shown for each row of the 5x5 measuring grid:

1. where all data are averaged
2. where only data around a voltage of 227 V are averaged

M.1 ROW 1

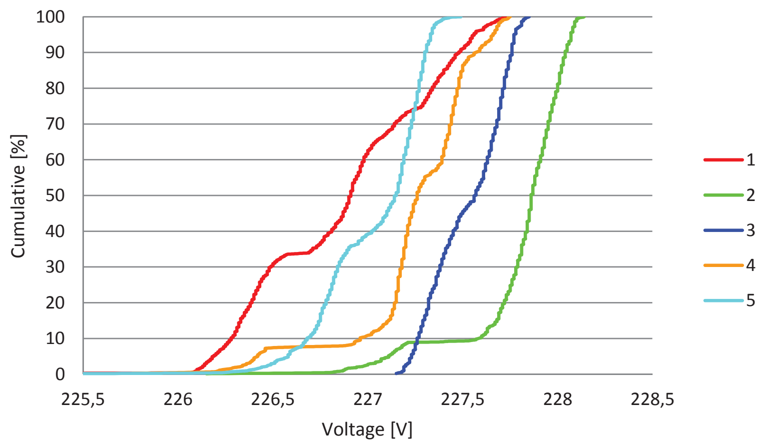

Figure M.1: *Cumulative distribution of recorded voltage; 1. option.*

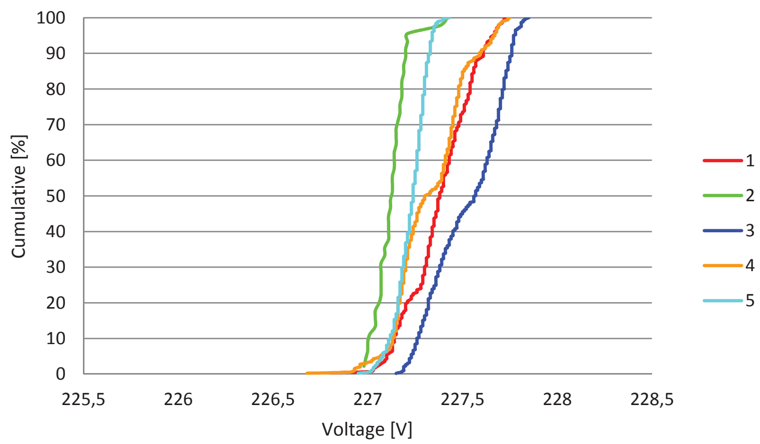

Figure M.2: *Cumulative distribution of recorded voltage; 2. option.*

M.2 ROW 2

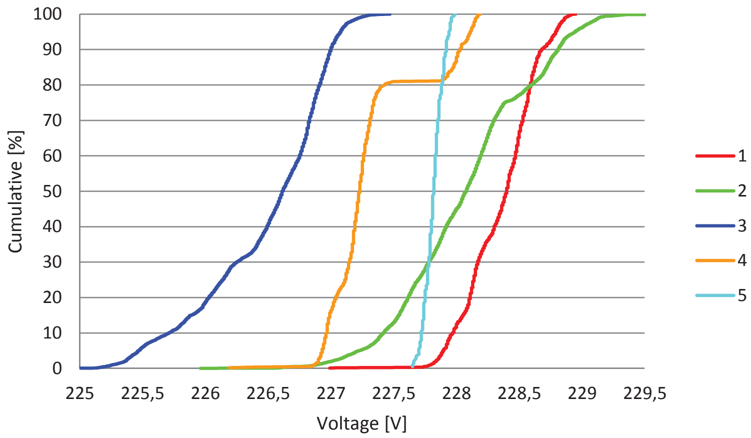

Figure M.3: *Cumulative distribution of recorded voltage; 1. option.*

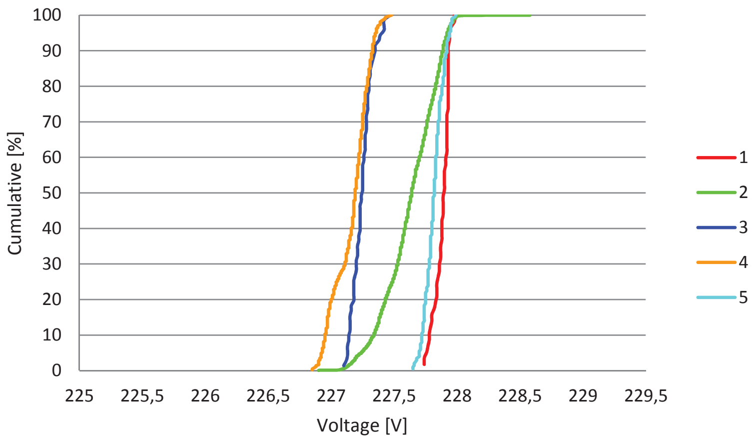

Figure M.4: *Cumulative distribution of recorded voltage; 2. option.*

M.3 ROW 3

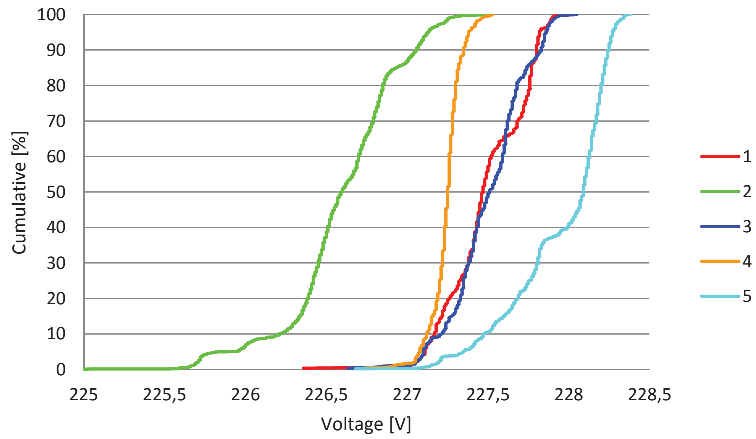

Figure M.5: *Cumulative distribution of recorded voltage; 1. option.*

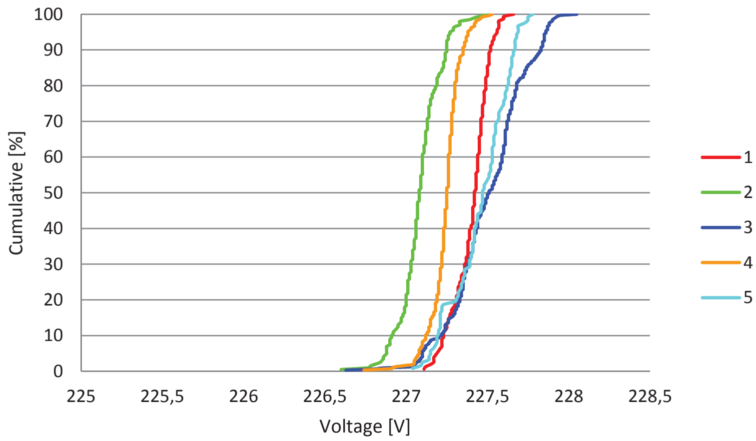

Figure M.6: *Cumulative distribution of recorded voltage; 2. option.*

M.4 ROW 4

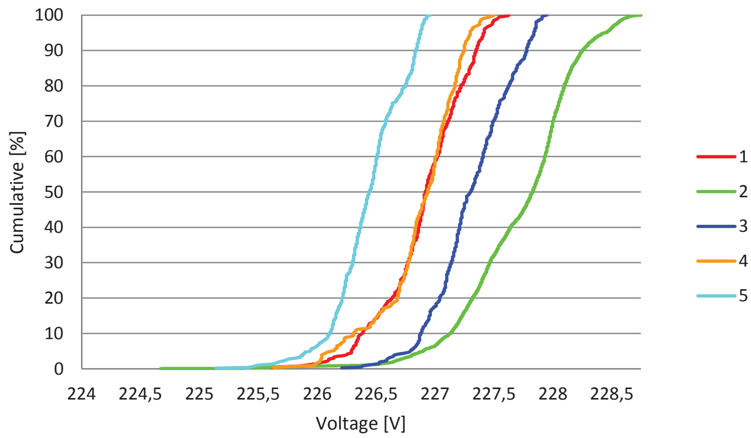

Figure M.7: *Cumulative distribution of recorded voltage; 1. option.*

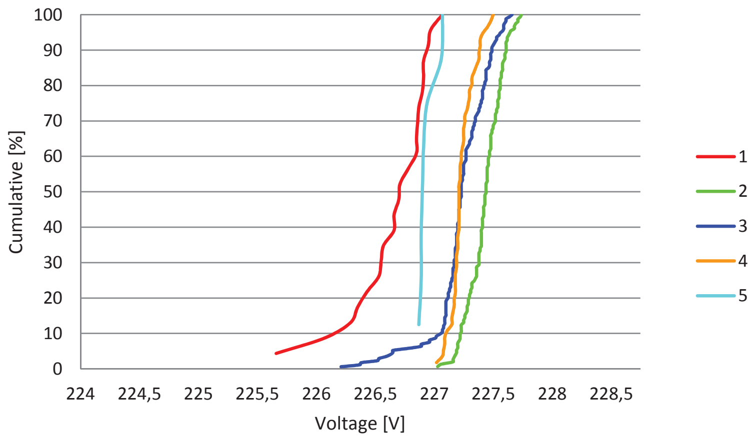

Figure M.8: *Cumulative distribution of recorded voltage; 2. option.*

M.5 ROW 5

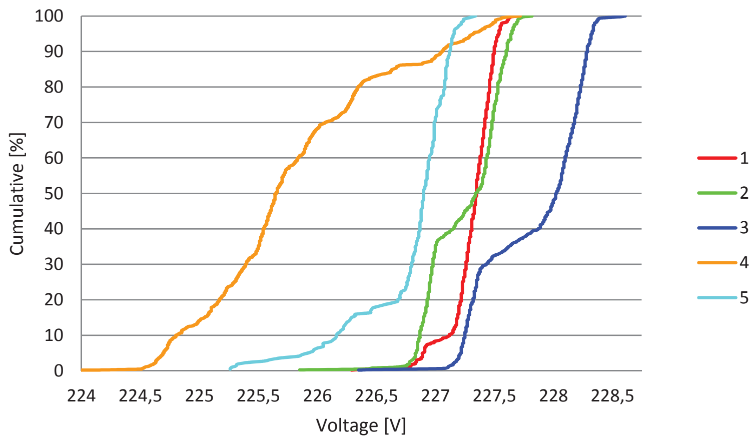

Figure M.9: *Cumulative distribution of recorded voltage; 1. option.*

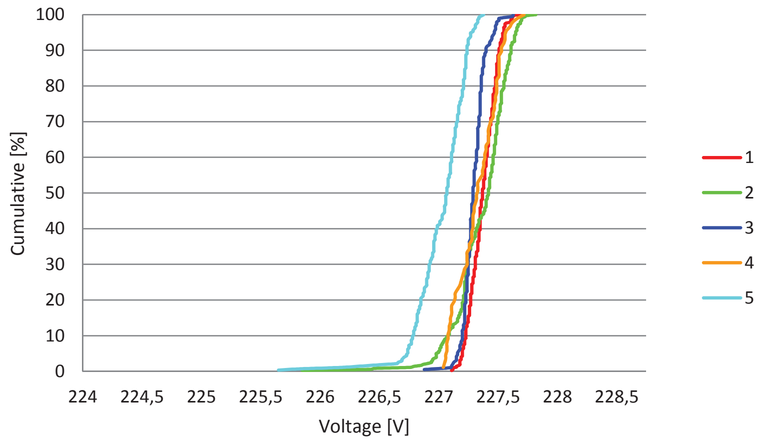

Figure M.10: *Cumulative distribution of recorded voltage; 2. option.*

The scope of the project is to develop a model for calculation of the g-value of a glazing system including Venetian blinds. This is done through present available literature and experiments.

Two main parameters are investigated. This includes the shading factor of the Venetian blinds and the exterior heat transfer coefficient on the outside of the glazing due to a change in airflow compared to glazings with no use of shading. Through experiments only the slat angle is varying while the theoretical models are varying dependent on both radiation angle and slat angle.

The velocity profile in the cavity is measured to study the type of air flow. The solar radiation through the window, both with and without shading, is measured for calculation of the shading factor of the Venetian blind.

The theoretical models are evaluated and compared with measurements done in a laboratory.